1998

Creep-fatigue behaviour and life prediction

Tarun Goswami
University of Wollongong

Recommended Citation

CREEP-FATIGUE
BEHAVIOUR AND LIFE PREDICTION

A thesis submitted in fulfilment of the requirements
for the award of the degree
Master of Engineering (Honours)

From

THE UNIVERSITY OF WOLLONGONG

By

Tarun Goswami (M.E.)

Department of Materials Engineering
University of Wollongong
Australia.

ABSTRACT

This thesis describes an investigation into the creep-fatigue behaviour and life prediction for high temperature materials. The methodology adapted in this research was not experimental, but, analytical using data compiled from several sources. High temperature low cycle fatigue (HTLCF) data generated internationally on 0.5Cr-Mo-V, 1Cr-Mo-V, 1.25Cr-Mo, 2.25Cr-1Mo, 2.25Cr-1Mo-V and 9Cr-1Mo low alloy steels were compiled and analysed to identify trends in creep-fatigue behaviour and life prediction for those steels. Effects of alloying elements such as chromium and vanadium were investigated and it was shown that with increase in chromium content the life improved, but with vanadium addition to a 2.25Cr-Mo steel the life was lowered. For the annealed condition, in which the material tensile properties were nearly half the value for the normalized and tempered condition, the 2.25Cr-1Mo steel had higher life.

Phenomenological methods of life prediction such as the damage summation approach (DSA), the frequency modified approach (FMA), the strain range partitioning (SRP), the damage rate approach (DRA), the hysteresis energy approach (HEA), the damage parameter approach (DPA) and the assessment procedure R-5 are all in the developmental stage when examined with the data bank compiled no one method was found to be better than other. The phenomenological methods require a number of material and test parameters determined from complex tests, as a result, alternate methods in the creep-fatigue life prediction are explored. A statistical method, known as Diercks equation has been proposed in the literature as a better method that was modified and its applicability was extended and assessed with the creep-fatigue data for low alloy steels compiled in this investigation. The reliability of modified Diercks equation was found to be higher than other methods.

Microstructural damage produced under HTLCF was documented optically for a titanium alloy IMI 829 and a nickel based superalloy MAR M 002 under different test conditions. The alloy IMI 829 contained interfacial cracks, cavitation and oxide banding resulting into intrusions and multiple cracking at 600°C. However, wedge type of cracking and oxidation damage by depletion of γ' phase were observed for MAR M 002. The HTLCF damage documented is described by a five stage model developed in this investigation and an empirical oxidation life prediction method is developed for MAR M 002. A reasonable prediction was observed at all the temperatures only under unaged condition, however, data were over-predicted under ageing heat treatment which produced material microstructure amenable to cracking. Further work is needed to apply this method in the creep-fatigue life prediction of high temperature materials.

LIST OF PUBLICATIONS

The following chapters from this thesis became individual papers in International Journals as follows:

Chapters 4 and 5   Goswami, T. (1995) Creep - Fatigue : Paper I Compilation of data and trends in the behavior of low alloy steels, High Temperature Materials and Processes, Vol. 14, No. 1, pp 1-20.

Chapter 6   Goswami, T. (1995) Creep - Fatigue : Paper II Life prediction - methods and trends, High Temperature Materials and Processes, Vol. 14, No. 1, pp. 21-33.

Chapter 7   Goswami, T. (1995) Damage development under creep-fatigue in a titanium and a superalloy, High Temperature Materials and Processes, Vol. 14, No. 2, pp. 47-55.

Chapter 8   Goswami, T. (1995) Creep-Fatigue : Paper III Diercks equation : modification and applicability, High Temperature Materials and Processes, Vol. 14, No. 1, pp. 35-45.

Following publication of these papers, National Research Institute for Metals, Tokyo, Japan, provided creep-fatigue data for further analysis which are published as follows:

Paper 1   Goswami, T. (1995) Applicability of modified Diercks equation with NRIM data, High Temperature Materials and Processes, Vol. 14, No. 2, pp. 81-90.

Paper 2   Goswami, T. (1996) Prediction of low cycle fatigue lives of low alloy steels, Iron and Steel Institute of Japan, ISIJ International, Vol. 36, No. 3, pp. 354-360.

Paper 3   Goswami, T. and Plumbridge, W. J. (1996) Applicability of new creep-fatigue life prediction models with low alloy steels, Paper No. C494/095/96. I. Mech. E. London, pp. 175-192.

PREFACE

This thesis submitted for the degree of Master of Engineering (Hons.) of the University of Wollongong is an account of research carried out at the Materials Engineering Department and at the Materials Discipline of the Open University (U.K.). The Work reported in this thesis is original and has not been submitted elsewhere for any other degree. Works of others used for data compilation have been duly referenced.

Tarun Goswami.

TABLE OF CONTENTS

1. INTRODUCTION

Engineering materials are selected for particular applications based upon their mechanical and other relevant properties. An ideal material is expected to perform satisfactorily under severe loading and environmental conditions where the service loads and the environment change with respect to time. Materials used to perform at room temperature can not be used at high temperature because their mechanical properties degrade with rise in temperature. Fatigue may be one of the candidate failure mechanisms of components operating at room temperature, however, at high temperature, in addition to fatigue, creep and interactions of creep-fatigue becomes an important failure mode. Hence, study of creep-fatigue interactions of high temperature materials is a topic of recent research.

The service requirements of candidate materials in applications such as power generation and jet propulsion are very demanding. Components for these applications are not only loaded very severely, but also, are required to operate at high temperatures. The failure mechanisms of the components operating at high temperature are by creep, fatigue and creep-fatigue interactions. Creep is a time dependent damage mechanism which occurs mainly under sustained loading conditions, whereas, fatigue is a cyclic event and results from cyclic action of loading. When loading of a component is such that there is a component of cyclic and sustained condition, interaction between creep and fatigue occurs. In practise, study of creep-fatigue interaction becomes important for high temperature applications such as components of power plants and gas turbines. Engineering artefacts are designed to experience the cyclic action of loading and probability that loading will be steady at high temperature is quite small due mainly to flow fluctuations, pressure difference and plant operating conditions which depart from ideal conditions. Hence, the study of failure mechanisms under creep-fatigue interactions of high temperature materials is very important.

The creep-fatigue interactions in high temperature materials are not yet fully understood due probably to the utilization of various materials for numerous high temperature

applications such as power generation and gas turbines. In addition, there is very little interaction among research workers in the two fields identified above. The materials of power equipment are mainly stainless steels and low alloy steels containing chromium, molybdenum and vanadium whereas, gas turbine materials are titanium alloys and superalloys. The metallurgy and physical and mechanical properties of low alloy steels, titanium alloys and superalloys are very different. To provide some unification, this investigation seeks to establish a link between the two groups of research (power generation and gas turbines) by studying the creep-fatigue behaviour and life prediction of low alloy steels, a titanium alloy and a superalloy.

Since 1960's there have been many instances of premature failures in the power industry and also in commercial aircraft engines. Components in these applications operate under high mechanical loading at high temperatures and their failure mechanisms are due mainly to creep-fatigue interactions. There is a growing interest to develop reliable life prediction methods that will be useful to predict life of components operating at high temperature. The attention of the research community has been attracted to investigate high temperature low cycle fatigue (HTLCF) behaviour, creep-fatigue interaction failure mechanisms and life prediction for such components.

To determine the conservative life of power equipment and gas turbine components and to utilize fully their useful life, creep-fatigue life prediction models are very important. There are economic as well as safety reasons for this endeavour. The methods of life prediction, are still in the developmental stage and no single method is recommended as a "code" in the design of power generation and gas turbine components. Methods have been developed from the results of a selected set of laboratory creep-fatigue experiments. As a result, not all the test and material variables were represented in the parametric model developed from fitting a type of data, where such models were suitable only for particular test conditions. Validation of models with test data is a feature of current publications. Since a limited number of tests are conducted in HTLCF from 5 to 15 tests, the life

prediction models are assessed with fewer data. Hence, more knowledge needs to be gained in the development of a life prediction method and assessment of its applicability with a large data base.

Elaborate experimental programs need to be undertaken to account for all the test (e.g., hold times, strain rates, frequency, temperature and waveform) and material (e.g., microstructure, heat treatment and product form) variables. Since, creep-fatigue tests are very precise and expensive and test specimens must represent the actual component, the number of tests that can be made for a specific application is often limited. For this reason, it was more useful in the present work to compile the available creep-fatigue data into a data bank and then to assess the applicability of a life prediction method against that data bank. It was anticipated that this process would account for various test and material variables.

Manufacturers of power equipment and gas turbines use company proprietary and classified life prediction technologies. Since the development of these technologies is based upon service experiences, the methodologies are different among the manufacturers and are empirical in nature. Components of power equipment and gas turbines often perform random types of operating cycles and consequently, the life predicted by the manufacture often is over or under predicted. Additionally, very high confidence level is required in the safe operation of power equipment and gas turbines. In the case of an accident, liability issues also impose an additional requirement on the classification of life prediction methodologies. Hence, there are economical as well as safety interests in the reliable determination of lives of the components of power generation and gas turbines.

The present research was undertaken to address some of the complex issues related to material behaviour and development of reliable life prediction methodology for high temperature materials. Generation of original creep-fatigue data was difficult since there was a lack of critical equipment, support and materials. Hence, an alternative approach to the problem was formulated in terms of compiling the published and unpublished data bank for low alloy steels. The metallography of a titanium alloy and a superalloy, previously tested

under creep-fatigue, was investigated in an attempt to bridge the gap between the two research areas of gas turbines and power research. The research comprised six separate components as follows.

(1) The research programme was directed towards understanding "creep-fatigue behaviour and life prediction" and in so doing it expanded the knowledge on creep-fatigue behaviour and life prediction for a range of materials including low alloy steels, a titanium alloy and a superalloy.

(2) A compilation of existing published and unpublished creep-fatigue data was made, and as no such compilation was known to exist for low alloy steels, was an original effort. An empirical creep-fatigue life prediction method was modified and assessed with the compiled 250 creep-fatigue data points from various published and unpublished sources for the 0.5Cr-Mo-V, 1Cr-Mo-V, 1.25Cr-Mo, 2.25Cr-Mo, 2.25Cr-Mo-V and 9Cr-1Mo steels in annealed, normalized and tempered and quenched and tempered conditions respectively.

(3) The methods of creep-fatigue life prediction were not understood fully and, in fact, were the subject of a recent international symposium to review the methods of life prediction and their applicability. The major emphasis of this research was focused on to the compilation of a data bank, development and, or, modification of existing life prediction methods. Parallel to the present investigation, Nuclear Electric Plc. Inc., U.K., developed a data base on fatigue, creep and creep-fatigue for high temperature materials in several of its laboratories and established a team of large number of distinguished scientists to develop a code known as R-5, for the reliable life prediction of power equipment. This code is "in confidence of Nuclear Electric Plc. Inc." and remains classified. Common features of the two studies were:

   (a) data collection,

   (b) review of methods of life prediction, and

   (c) develop a more reliable method of life prediction.

During the course of this research, there also was a parallel effort jointly from European Communities through European Commission, with its 17 laboratories and the low cycle fatigue committee of Japan with its 10 laboratories, participated in a round robin test programme to address some of the major issues related to standardisation of test procedure and life prediction for low alloy steels. Details such as creep-fatigue test types, data and life prediction methodology employed by them are not yet published and remain confidential.

(4) The creep-fatigue behaviour of a range of low alloy steels including the 0.5Cr-Mo, 1Cr-Mo-V, 1.25Cr-Mo, 2.25Cr-Mo, 2.25Cr-Mo-V and 9Cr-1Mo steels were investigated to widen the scope of the knowledge. Trends in creep-fatigue behaviour with respect to various material conditions were analysed to determine the effects of composition and heat treatment.

(5) The metallography, under creep-fatigue test conditions for a titanium alloy and a superalloy was studied. A large number of specimens, tested under a range of creep-fatigue test conditions were available, so that the metallographic features developed under creep-fatigue test conditions were determined and are very important to the knowledge of creep-fatigue deformation mechanisms. High temperature oxidation in these samples was also observed qualitatively. Based upon these observations, a damage model was developed to contribute to the existing knowledge about the role of oxidation in failure criteria under creep-fatigue.

(6) Since the available creep-fatigue data for the superalloy were inadequate for application of a phenomenological life prediction method, an empirical life prediction method was developed using some material parameters used for other superalloys available in the published literature. This was an original analysis and contributes to existing knowledge.

1.1. FRAMEWORKS OF LIFE PREDICTION

Components of power generating equipment and of gas turbine engines operate under a complex combination of stresses and temperature which change with respect to time. Failure mechanisms under such conditions are by creep-fatigue interactions. These components experience a periodic start up - shut down schedule. Hence deformation in a material accrues, not by fatigue alone, but also, by accumulation of inelastic strain, or creep, during hold times. Currently, study of creep-fatigue interactions of high temperature materials is an important topic of research.

Conventional fatigue designs of engineering components use Goodman diagrams, which relate alternating and mean stress combinations for a particular life for the determination of safe life that is derived mainly from the relationship between stress range and cycle number, known as S-N diagrams. Recently, damage tolerance design concepts that separate total life into two stages, namely crack initiation and crack propagation to a critical size, have been used in the design of critical components. In the laboratory, high temperature low cycle fatigue (HTLCF) data are generated by controlling the total strain range. From the begin of a HTLCF test, the load decreases gradually with respect to number of cycles. When a specific percentage (e.g., 5 to 40%) load drop was achieved, the tests are terminated and considered as life at the employed strain range. These data are also known as cycles to crack initiation. The crack initiation criterion is applied in the design of power generation and gas turbine components.

It is not yet possible to define the crack initiation life of critical components which necessarily contains a period of microscopic crack growth. A crack below detection limit, or engineering size (of approximately 1 mm), is the critical crack length to cause failure in the case of a gas turbine discs and blades. Hence, creep-fatigue tests are conducted in a laboratory where specimen failure is considered as the crack initiation life of the components.

The HTLCF is a failure mechanism of engineering components usually caused by cyclic thermal stresses. However, in the laboratory, high temperature material behaviour is

often evaluated under isothermal conditions by controlling total strain and continuous strain cycles are often intercepted by a hold time at the peak tensile loading direction to simulate the service situation of a real component. Inclusion of a hold time at the peak tensile loading direction reduces the cyclic life of several engineering materials (1). Laboratory simulation of hold times range from one day to a week for the fossil and nuclear power plant components respectively, (2), but only a few minutes for gas turbine components (3-4). The design life of power equipment components varies from a few hundred thousand hours to a few hundred hours for the gas turbine blades since they operate at higher stresses and temperatures. Thus, from an engineering view point, it is of great importance to evaluate creep-fatigue behaviour and to develop a rational life prediction approach to be used in the design of such critical components.

Life prediction techniques that are proposed to correlate the laboratory strain versus life data are in the developmental stage. These methods are; American Society of Mechanical Engineers (ASME) code case 1597 N47 or Damage Summation Technique (5), Frequency Modified Approach (6), Strain Range Partitioning Technique (7), Damage Parameter Approach (8), Damage Rate Approach (9), Hysteresis Energy Approach (10) and Code R-5 (11). In addition to these methods, a few empirical methods has been developed to extrapolate creep-fatigue life for stainless steel type SS 304 by Diercks and Raskey (12) and in a modified version by Kitagawa et al, (13) were recently proposed. These models have been developed from test parameters and some form of damage such as a crack and its growth.

The objectives of the present investigation were:

1   to compile a creep-fatigue data base for low alloy steels and identify salient features of the data,

2   to determine the sources of variability in material and test parameters, to identify trends in the creep-fatigue behaviour of low alloy steels, to investigate effects of composition

of low alloy steels in creep-fatigue performance and to determine the effect of vanadium additions on the creep-fatigue behaviour of a 2.25Cr-Mo alloy,

3   to review methods for life prediction, to determine trends in the applicability of life prediction methods to the collected data, as observed by various workers and to determine the effect of material conditions and test parameters on the applicability of life prediction methods,

4   to modify Diercks equation and assess its applicability to the compiled creep-fatigue data for low alloy steels,

5   to investigate the creep-fatigue behaviour and damage mechanistic features of a titanium and a nickel based superalloy and to develop a damage mechanistic model of HTLCF for a titanium alloy and a superalloy, and

6   since the available creep-fatigue data for MAR M 002 was not assessed with any method of life prediction, a new empirical life prediction method was developed.

These objectives were pursued using the following methodologies.

(a)   A review of pertinent literature on the creep-fatigue interactions was conducted and the effect of test parameters, specimen geometry and strain control methods on the creep-fatigue life was explored. Data correlation methods using total strain range, plastic strain range and stress-strain relations were reviewed. An extensive compilation of creep-fatigue data for low alloy steels was conducted in that the complete details of test and material parameters were not revealed in the open literature. Data on three material conditions were collected to study the effect of heat treatment on the creep-fatigue behaviour. Identification of the data was made which data sets were directly comparable (Chapters 2 through 4).

(b)   From the compiled data, trends in the creep-fatigue behaviour of low alloy steels were identified (in Chapter 5).

(c)   Methods of life prediction were extensively reviewed. Test requirements, equations and number of material constants needed to apply a particular method of life prediction were

discussed. Capability of methods of life prediction as applied by various workers to their data were analyzed and aggregated to identify the trends in the applicability of methods of life prediction (in Chapter 6).

(d) An elaborate metallography of samples for 1Cr-Mo-V, a titanium alloy and a superalloy was undertaken to investigate the damage features under creep-fatigue conditions. From these features a damage development model was proposed. An empirical life prediction method was developed for the creep-fatigue life prediction of a superalloy (Chapter 7).

(e) Diercks equation was modified and its applicability was extended for a range of low alloy steels. This modified equation was assessed with the compiled creep-fatigue data for low alloy steels. The reliability of modified Diercks equation was compared with other methods of life prediction (Chapter 8-9). Finally, conclusions drawn from this investigation were summarized (Chapter 10).

2. METHODOLOGY

In Chapter 1, the scopes, objectives and goals of this investigation were discussed. In the past, very limited creep-fatigue data were assessed with the methods of life prediction. No attempts were made to compile creep-fatigue data on low alloy steels or on other high temperature materials, that can be analysed to identify trends in the creep-fatigue behaviour and life prediction methods. Hence, in this investigation a creep-fatigue data bank for low alloy steels used in the power generating equipment was compiled. Subsequently, the compiled data bank on low alloy steels was assessed with Diercks equation, a statistical method, modified in this investigation and the reliability analyses in the predicted life for the compiled data were performed. Metallography of two gas turbine materials, a titanium alloy IMI 829 and a superalloy MAR M 002 were investigated, by so doing, efforts were made to unite the two isolated groups of researchers in the power generation and gas turbines in this research.

From the compiled data, trends in the creep-fatigue behaviour for low alloy steels were identified. Methods of creep-fatigue life prediction were reviewed and trends in the prediction capability of different methods assessed with the compiled data were determined. Metallographic studies were conducted for the two gas turbine materials IMI 829 and MAR M 002 to document the damage features that developed in creep-fatigue testing. From the documented observations, a five stage damage model and a new empirical life prediction method for MAR M 002 were developed.

Thus, this thesis consists of a data bank for low alloy steels and the analysis of the data to identify trends in the creep-fatigue behaviour and life prediction. Applicability of modified Diercks equation and other methods developed in this investigation were determined. Hence, methodology in this thesis is different from other conventional theses. This chapter discusses methodology adapted in carrying out the compilation of the data, analysis of the data and life prediction of the compiled data in following stages:

1 compilation and analyses of creep-fatigue data,

2 review of creep-fatigue life prediction methods,

3 trends in the life prediction methods,

4 investigation of damage features for a IMI 829 and a MAR M 002,

5 development of an empirical life prediction model for MAR M 002,

6 modification and applicability of Diercks equation, and

7 reliability analyses

2.1. COMPILATION AND ANALYSES OF CREEP-FATIGUE DATA

No attempts have been made in the past to compile creep-fatigue data for low alloy steels, hence, a data bank was compiled as a part of this investigation. Various published and unpublished data were assembled from the literature and by requesting data from research workers around the world. In most cases, complete details of the creep-fatigue data were classified and were not available in the open literature. Hence, the data compiled in this thesis, consists only of those data which are available in the public domain.

Creep-fatigue data for following materials and conditions were compiled:

1 0.5Cr-Mo steel in normalized and tempered condition (N&T),

2 1Cr-Mo-V steel in N&T,

3 1.25Cr-Mo Steel in N&T,

4 2.25Cr-Mo steel in annealed (A), N&T and quenched and tempered (Q&T),

5 2.25Cr-Mo-V steel in N&T, and

6 9Cr-1Mo steel in N&T.

In total, eighteen (18) research laboratories around the world were requested for the creep-fatigue data. Data on six low alloy steels, under three conditions namely A, N&T and Q&T were made available by different laboratories. Heat treatment details such as heating and cooling temperature ranges, rates of heating and cooling and method of cooling employed in N&T, A and Q&T conditions were not described in the open literature. Since components

of power generating equipment and gas turbine operate under very high stresses, design requirements are placed upon higher strength of materials that result from N&T and Q&T heat treatments. Creep-fatigue test temperatures ranged from 483°C to 600°C. In excess of 250 test combinations were compiled and examined for unspecified features in the material and testing parameters. Since every test is statistically different, variations in the materials and in the creep-fatigue test parameters were identified in Chapters 4 and 5.

2.1.1. Analysis of the compiled data

The data compiled in this investigation are presented in terms of "batches". A "batch" thus denotes a particular low alloy steel, its test conditions and the source, which laboratory provided the data. Hence, there are several batches in one particular low alloy steel. Batches of a particular low alloy steel are compared with other batches to identify the trends in the creep-fatigue behaviour for that steel and also compared collectively with six steels to determine the trends in the creep-fatigue performance.

The effects of following were analyzed:

1   waveform on the creep-fatigue performance of low alloy steels,

2   product form on the creep-fatigue performance of low alloy steels, and

3   chemical composition on the creep-fatigue performance of low alloy steels.

Batches of a particular low alloy steel were first analyzed to derive a trend in the creep-fatigue behaviour in the waveform, product form and composition frameworks. Six low alloy steels namely the 0.5Cr-Mo, 1Cr-Mo-V, 1.25Cr-Mo, 2.25Cr-Mo, 2.25Cr-Mo-V and 9Cr-1Mo were investigated in the three frameworks. Hence, the analyses on the creep-fatigue behaviour contained combinations of six low alloy steels, three heat treatment conditions and the three frameworks for the effects of waveform, product form and composition.

2.2. REVIEW OF CREEP-FATIGUE LIFE PREDICTION METHODS

The following life prediction methods were reviewed:

1   damage summation approach (5),

2   frequency modified or separation approach (6),

3   strain range partitioning technique (7),

4   damage parameter approach (8),

5   damage rate approach (9),

6   hysteresis energy approach (10),

7   assessment procedure R-5 (11),

8   Diercks empirical equation (12, 13), and

9   oxidation model (14).

All these methods (5-14) are in the developmental stage where damage under creep-fatigue condition is modelled depending upon the test parameters and how the damage developed phenomenologically. The damage accrues under high temperature low cycle fatigue by transgranular or intergranular cracks. However, at the temperature when creep occurs cavitation along the grain boundaries is observed. Hence, a life prediction model apply only under certain combinations of test parameters and materials and for this reason such models are called parametric methods. When the test and material parameters are changed outside the range of parametric methods prediction of life also changed. No single method of life prediction is universally applicable to all types of creep-fatigue test data.

The oxidation model (14) for life prediction was useful in this investigation, as oxidation was observed during creep-fatigue tests conducted at 850°C and 1000°C on a superalloy, MAR M 002. Since, the available data were too limited to determine various material and test parameters, as a result, no life prediction method was assessed with the data. Hence, a new empirical life prediction method was developed accounting for the role of oxidation in decreasing the life for a superalloy MAR M 002 by assuming several material parameters that were available in the published literature (12).

2.2.1. Derivation of material parameters for life prediction methods

The mathematical equations for life prediction methods (5-13) required numerous test and material parameters where every parameter was determined from a particular type of test. Each method was developed to predict different types of creep-fatigue test conditions. The material and test parameters were derived generally from a linear logarithmic best fit extrapolation equation which provided an exponent and a slope. Material parameters (exponents and slopes) changed when the data e.g., total strain range changed to plastic strain range with cycles to failure. These material parameters were different when strain rate, stress range and frequency were plotted with cyclic life. Hence, a large number of material parameters for various life prediction methods were possible. These parameters were inputs to develop methods of life prediction where every method required several combinations of tests and material parameters. Since the data compiled in this investigation were total strain range and cycles to failure, derivation of only one set of material parameter (total strain range with life) was possible. Total strain range with life extrapolation equations were determined for nearly 50 combinations of tests. Additional test and material parameters were needed such as frequency with life, strain rate with life and stress-strain relationships to apply methods of life prediction on the data. A complete detail of life prediction methods, equations and the types of tests needed to apply them is discussed in Chapter 6.

2.3. TRENDS IN THE LIFE PREDICTION METHODS

The trends in the life prediction methods (5-13) were identified in this section. To identify the trends, analysis was confined to specific life prediction methods that were assessed with the data presented in terms of batches in Chapter 4. Only Priest and Ellison (15) and Inoue et al, (16) conducted elaborate testing to assess their data with the methods of life prediction listed in section 2.2. Priest and Ellison (15) modified several methods (5, 9, 10) such that with those modifications (15) prediction capability of modified versions improved for their data and no other worker used those modified versions in life prediction for other data

batches. These details were aggregated batch by batch and tabulated in Chapter 6 to identify trends in the life prediction. In general, the capability of life prediction methods were dictated by test parameters such as temperature, hold times, strain rate and strain range. These features were identified for all the batches of data, where those details were available. From such an analysis trends in the life prediction of various methods were identified as set out in Chapter 6.

2.4. INVESTIGATION OF DAMAGE FEATURES FOR A IMI 829 AND A MAR M 002

Samples of previously tested specimens, under creep-fatigue conditions, were available for a titanium alloy IMI 829 (17) and a superalloy MAR M 002 (18). The chemical composition of the two alloys are tabulated in Tables 2.1 and 2.2.

Table 2.1. Composition of titanium alloy IMI 829 (in weight %).

Al	Mo	Zr	Si	Nb	Sn	Ti
5.5	0.25	3.0	0.3	0.25	3.5	balance

The microstructure of IMI 829 was in the form of Widmanstätten packets, produced by heat treatment cycle of 1.5 hours at 1050°C, oil quenched followed by 2 hours at 625°C. The composition of MAR M 002 is tabulated in Table 2.2.

Table 2.2. Composition of MAR M 002 (in weight %).

C	Si	Fe	Mn	Cr	Ti	Al	Co
0.15	0.2	0.5	0.2	9	1.5	5.5	10
W	Mo	B	Zr	Ta	Cu	Hf	Ni
10	0.5	0.02	0.05	2.5	0.1	2.5	Balance

The MAR M 002 superalloy was supplied by Rolls Royce Plc. in the form of hollow specimens ready for creep-fatigue testing. The MAR M 002 specimens received a five stage heat treatment which was:

1   4h/1190°C in vacuum, furnace cool (FC) to 1000°C at 5°C/min,

2   1h/1150°C in vacuum, FC to 1000°C at 5°/min,

3   aluminise at 906°C for 7.5 hours,

4   diffuse 1h at 1100°C in argon, and

5   age 16h at 870°C in argon.

Metallographic samples were prepared for both the materials IMI 829 and MAR M 002 from previously tested specimens under creep-fatigue (17-18). Samples of IMI 829 and MAR M 002 were polished and etched following these procedures:

IMI 829:   Final polishing to a 1 micron diamond finish. Swab etching was

                        performed in a solution of 2% hydrofluoric and 10% nitric acid in

                        water.

MAR M 002   10% phosphoric acid, electrolytic at 3V was used to reveal gamma

                        prime phase.

Samples were examined using optical and scanning electron microscope. Damage features were documented under different creep-fatigue test conditions for IMI 829 and MAR M 002 materials.

A five stage damage model was developed from the damage features documented from metallographic examinations. Oxidation was observed to occur in all test conditions for IMI 829 but only at 850°C and 1000°C for MAR M 002. Interpretation of the oxides and depletion of gamma prime phase which is an intermetallic compound of Ti and Al that imparts high temperature strength in the superalloys, was made from the published claims by Coffin (19, 20). However, such sources (19-20) also documented qualitative evidence and no quantitative analysis of the oxides was made in the literature. Other details such as

mechanical properties, creep-fatigue data and metallography of the two materials are presented in Chapter 7.

2.5. DEVELOPMENT OF AN EMPIRICAL LIFE PREDICTION MODEL FOR MAR M 002

Oxidation damage was found to occur under creep-fatigue test conditions for the superalloy, MAR M 002. The life prediction methods (5-11) discussed in section 2.2, did not account for the contributions of oxidation in degrading the mechanical properties and required several material parameters determined from specialised tests. Since no method (5-11) had been applied to the data on MAR M 002, in which, oxidation damage was evident, a new empirical method was developed accounting for the oxidation in life prediction. Those material parameters for MAR M 002 were unknown were assumed from published sources.

The applicability of the new empirical oxidation method developed in this research was assessed with the available data on MAR M 002. Several tests were incomplete and only one test was conducted for a particular condition of tensile, compressive and balanced hold times. Hence, material parameters determined form such data are likely to contain errors and require more work to assess and validate applicability of the empirical model developed in this investigation with a wide range of creep-fatigue data.

2.6. MODIFICATION AND APPLICABILITY OF DIERCKS EQUATION

Diercks equation (12), was used to extrapolate the creep-fatigue life for a stainless steel of the type SS 304 that was modified in this investigation and its applicability was extended to the creep-fatigue life prediction for low alloy steels. Diercks equation (12) required several test parameters to perform life prediction analysis. Data under numerous test types such as strain rates, temperatures, hold times and total strain ranges for SS 304 were used to derive a multivariate best fit equation. Hence, there were strain range, strain rate, temperature and

hold time parameters in Diercks equation. Modification and applicability of Diercks equation on the compiled creep-fatigue data for low alloy steels is discussed in Chapter 8.

2.7. RELIABILITY ANALYSIS

Reliability assessment for creep-fatigue life predicted by Diercks equation was carried out and compared with the reliability of other methods where those details were available. The ability of a method to predict the lives in a range from one half to two times the observed life , i.e., $\pm$ x2 , was considered to be a reliable life prediction. More data predicted by a method in $\pm$ x2 band enhanced the reliability of that particular method. Statistical standard error (SE) and equivalent factor on life (EF) values, determined the band in which the lives were predicted for the compiled data, were determined in Chapter 9.

Statistical analysis for every data point was performed for standard error (SE) and equivalent factor on life (EF) determinations. The SE and EF were determined to demonstrate the reliability of various life prediction methods.

2.8. SUMMARY

Methodologies adapted in various stages of this investigation to compile the creep-fatigue data bank for low alloy steels were discussed. The trends in the creep-fatigue behaviour and life prediction for low alloy steels were identified. Several unspecified test and material features were identified from the analyses of the compiled data. Life prediction is conducted by using an existing method or either developing a new method or modifying an available method to asses its applicability for a data bank. No attempts have been made in the past to compile a data bank and identify trends in the creep-fatigue behaviour and life prediction for low alloy steels. Hence, the methodology adapted in this investigation comprised compilation of data bank, determination of trends in the creep-fatigue behaviour, review and examination of trends in the life prediction methods, development of alternate approaches to the life prediction for MAR M 002 and metallographic investigations.

3. REVIEW OF CREEP-FATIGUE INTERACTIONS

3.1. INTRODUCTION

Components of power generating equipment and gas turbines operate in a hostile environment where they experience very high mechanical loading at high temperatures. High temperature low cycle fatigue (HTLCF) is a failure mechanism where more than one damage mechanisms such as creep or fatigue interact. The failure of these components occurs in the low cycle regime where lives are below 10,000 cycles. Therefore, the study of creep-fatigue interactions is very important to understand the failure mechanisms of components operating at high temperatures.

Engineering materials are not defect free and contain inherent discontinuities as well as stress concentration sites arising from complex geometry and fabrication processes. These are potential sites where fatigue damage develops. Fatigue is a progressive damage accumulation mechanism within the localised regions of discontinuities. The damage results from the cyclic action of load at high temperature and causes dislocations to generate, multiply and saturate to form a crack. Thus, the damage produced under HTLCF is irreversible and permanent. Therefore, fatigue is defined as a progressive, localised, irreversible, permanent deformation process (21).

High temperature may be defined in terms of a fraction 0.4 to 0.5 of the homologous temperature (T_h) which is the ratio of operating temperature to melting temperature of the material on the absolute scale. Such a temperature range is important because it establishes a boundary where creep becomes operative and allows interactions between creep and fatigue. A range of operating temperatures for various engineering applications is identified below and above $0.5 \, T_h$ in Table 3.1.

Table 3.1. Summary of high temperature applications.

High Temperature Applications	
High temperature	
Below 0.5Th	**Above 0.5Th**
Power Plant Components	Gas turbine components (turbine
Oil and Petroleum	discs and blades)
Nuclear Reactor	Space Shuttle (SS) main engine
Automotive IC Engines	components
Chemical Reactors	SS Structure
Accessaries and	Rockets and Missiles
Mountings	Solder joints
Pipe lines	
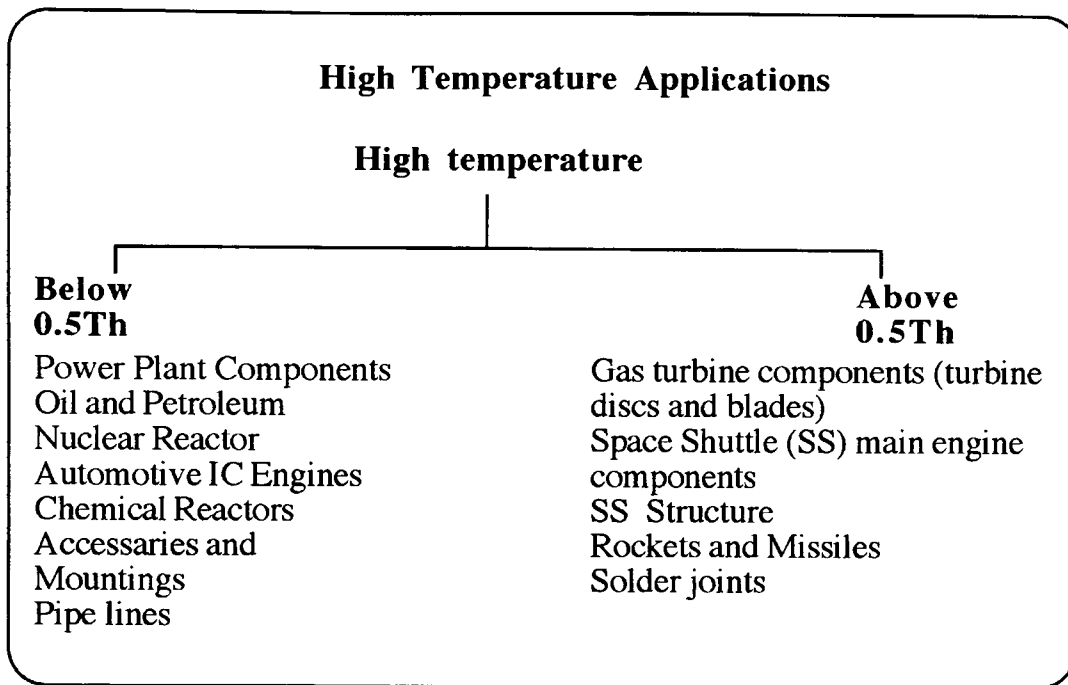
A conventional operating cycle of power generating equipment and gas turbines resembles a trapezoid, which has in addition to loading and unloading, a period of steady state loading condition. Growth of damage increases under trapezoidal loading conditions, because, in addition to time independent fatigue damage there, a time dependent creep damage occurs during the steady state period. This time dependent mechanical damage fraction is known as creep. Interaction of damage under creep and fatigue conditions is not yet fully understood and is the subject of the present research.

Conventionally, S-N type of fatigue data represented by cyclic stress amplitude range ($\Delta\sigma$) with cycles to failure (N_f) on a log-log scale are used in the design. A knee point in an S-N diagram appears in certain materials, at high stress lower life ($N_f < 10^4$), and also at low stress -longer life ($N_f > 10^7$) regimes. Since a small variation in the stress amplitude causes a large change in the cyclic life, material behaviour in the lower life region ($<10^4$) cannot be represented in terms of stress range versus life. Therefore, strain control testing is performed in the low cycle fatigue (LCF) regime where cycles to failure ($N_f = 2x$ reversals) is less than

10,000 cycles. Since HTLCF generally has a life range of less than 10^4 cycles, only strain control tests and methods of data correlation that will be used in this research are discussed below.

3.2. EXPERIMENTAL VARIABLES

3.2.1. Stress Based Approach

Wöhler (22) pointed out that the number of cycles to failure depends on the stress range (S_r) and value of S_r, $\{(S_{max} - S_{min})/2\}$ at any given number of cycles to failure (Nf), decreased as the mean stress (S_m) increased. Based on the Wöhler data, Goodman (23) proposed a straight line relationship, and equation of the form:

$$S_a = S_e [1 - \{ S_m / S_u \}] \tag{3.1}$$

where S_a = stress amplitude ($S_m + S_r$), S_e is the endurance limit and S_u is the ultimate tensile strength. Basquin (24), related semi -stress range (S) with cycles to failure (Nf) under predominantly elastic conditions in the following form:

$$N_f^{\beta'} S = \text{constant} \tag{3.2}$$

where β', is a material constant.

3.2.2. Strain Control Testing

When the total strain range is more than the elastic strain range $\Delta \varepsilon_t > \Delta \varepsilon_e$, a hysteretic phenomenon between stress and strain is usually observed. A hysteresis loop can be produced when ranges of stresses and strains are plotted in a X-Y recorder. However, when the total strain range is less than the elastic strain range, the loading and unloading traverse the same path within the linear elastic regime. A difference in loading and unloading paths forms a hysteresis loop that develops permanent damage in the material. Hence, life is shorter in the low cycle fatigue regime where plastic strain dominates than the high cycle fatigue regime where elastic strains dominate. The size and shape of a hysteresis loop

depends on test conditions, such as strain rate, total strain range and position of hold time at the peak tensile or compressive strain levels.

During strain control testing, every cycle is described by a hysteresis loop. If hysteresis loop tips are connected for different strain levels, the curve so obtained represents a cyclic stress-strain curve. Before the stress range saturates a small fraction of the life is lost after which the stress-strain behaviour stabilises. The total strain range and its elastic and plastic components can be correlated with cyclic life only after the saturation point, as shown in Fig. 3.1. Stress range variation with respect to fatigue cycles at a particular strain range shows the material behaviour to be either strain softening or hardening, depending upon the slope of the curve. Usually a material in a hard form (cold worked) softens and a softened material under annealed condition hardens, for example, 1Cr-Mo-V and 9Cr-1Mo softens, however, 2.25Cr-Mo hardens in the normalized and tempered condition. Such hardening and softening behaviour was observed up to approximately 30% of life in the case of the 2.25Cr-Mo (25). Strain range - cyclic life relationship for a titanium alloy IMI 829 is shown in Fig. 3.2 for different hold times (17). A stress range with percentage of cyclic life relationship is shown in Fig. 3.3 for a superalloy MAR M 002 tested at 1000°C by Plumbridge et al (18, 26).

In a creep-fatigue test under total strain control, extensometers are used to control either axial or diametral strain. Axial extensometers are used for cylindrical specimens whereas diametral extensometers are used for hourglass specimens. Diametral strain is converted to longitudinal strain which, in turn is controlled by a computer and very few direct diametral strain control tests were conducted (27-28). When a hold time was applied the stresses relax very rapidly with respect to time, which involves elastic strain conversion into plastic strain. Diametral extensometers overestimated the strain ranges (25) and were insensitive to measure the relaxed stresses. Over-estimation of longitudinal strains of up to 16% was reported (29) by diametral extensometers during testing of 2.25Cr-Mo at 427°C and 482°C and 5% for 1Cr-Mo-V and stainless steel of type SS 316 (30). However, no
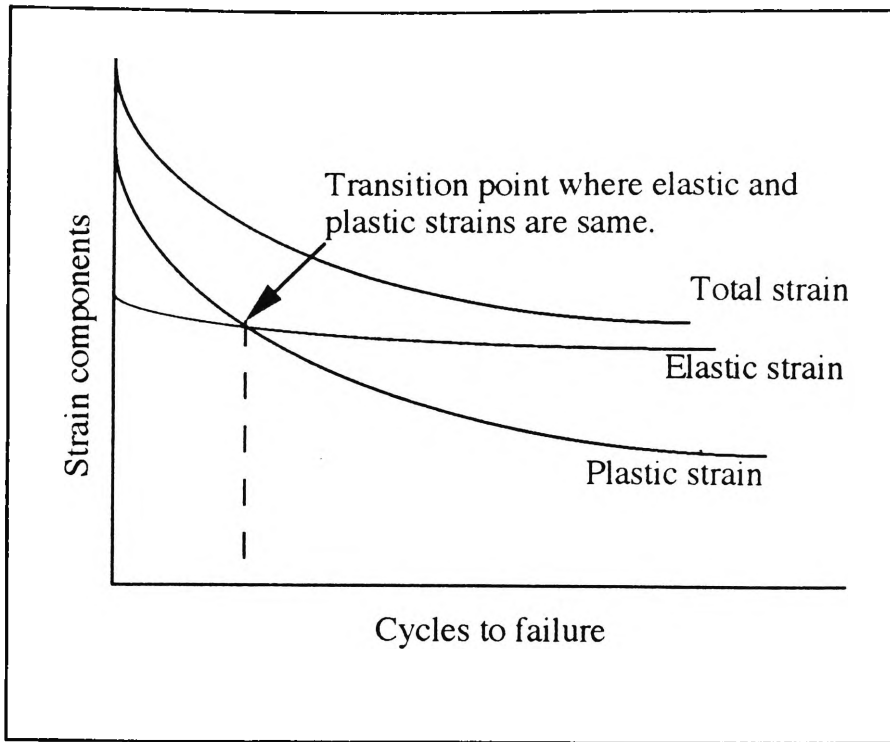
Fig. 3.1. Schematic representation of strain components with life.
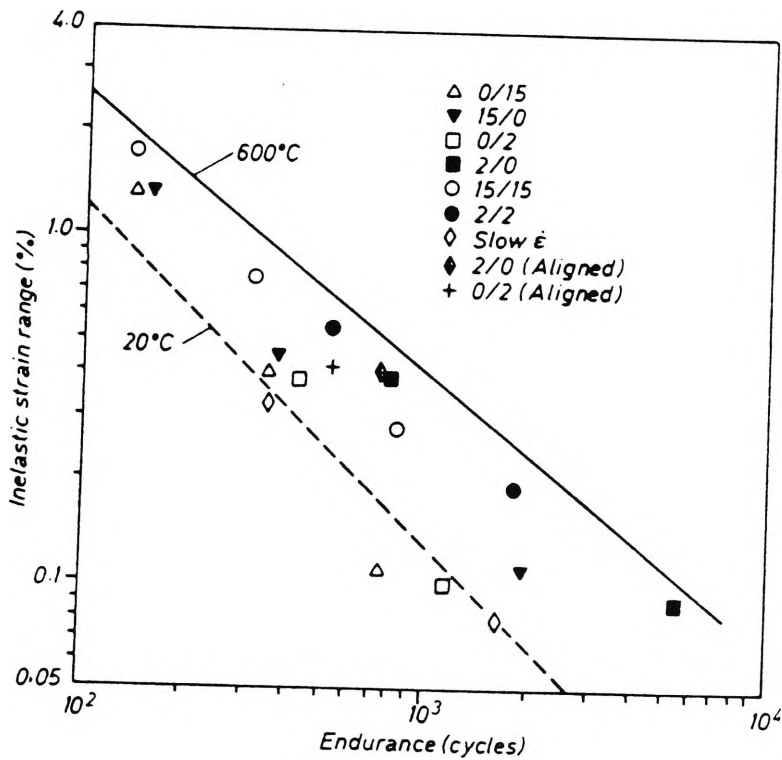
Fig. 3.2. Inelastic strain range with life relation for IMI 829 (17).
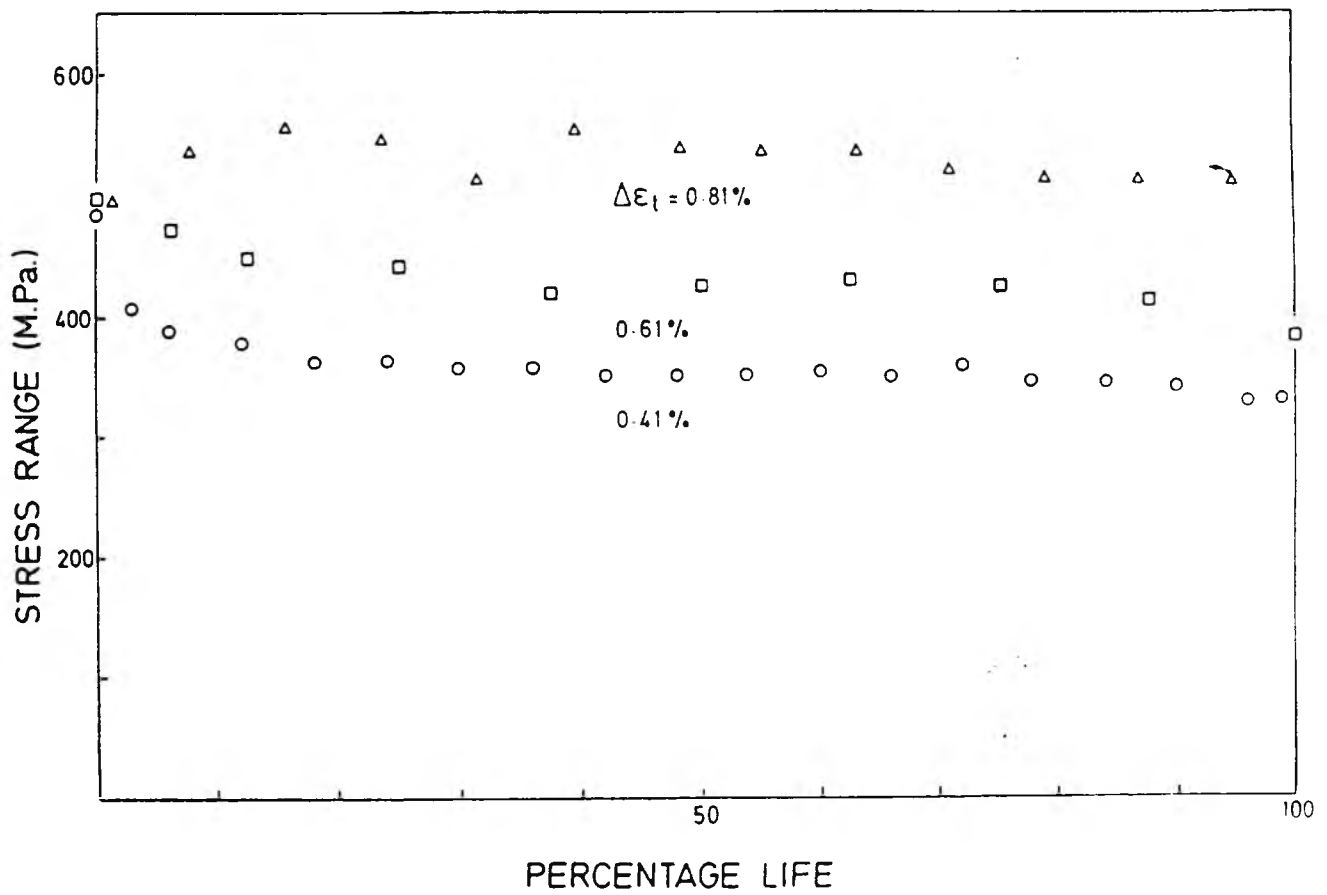
Fig. 3.3. Stress range change with life for MAR M 002 (18).

difference in the testing with hourglass and cylindrical specimens during the hardening of stainless steel of type SS 304 was reported in (31).

3.2.3. Waveforms in Creep-Fatigue Testing

Several types of waveforms that provide components of creep and fatigue damages are possible. A few common examples are shown in Fig. 3.4. To simulate service loading conditions hold time tests are conducted in the laboratory located in either peak tensile or compressive strain direction. When an equal hold time is applied at both peak tensile and peak compressive strain direction, the resulting cycle is known as a balanced cycle and when the duration of hold time is unequal in both the directions, the resulting cycle is known as unbalanced cycle. A hold cycle in either tension or compression direction results in the generation of a complex hysteresis loop. Partitioning strains in plastic fatigue and inelastic creep components of a complex hysteresis loop is very difficult. These loops have the components of total, plastic and transformed strains as shown in Fig. 3.4.

Some materials are sensitive to tensile hold times applied at the peak loading conditions whereas, other materials are sensitive to hold times in peak compression direction where a life debit results. Dwell sensitivity refers to a situation in which the interaction effect between creep and fatigue is more active in one loading direction than in the other, for example, 1Cr-Mo-V is found to be a tensile dwell sensitive (32), whereas, 2.25Cr-Mo is compressive dwell sensitive (33). Several nickel based superalloys are found to be compressive dwell sensitive (34). For 1Cr-Mo-V, a tensile hold results in cavitation (32), whereas for 2.25Cr-Mo, oxidation attack is observed under compressive hold cycles (35). In nickel based superalloys and titanium alloys, in general, a compressive dwell develops tensile mean stresses, which lowers the creep-fatigue life (36).

CONTINUOUS STRAIN CYCLING
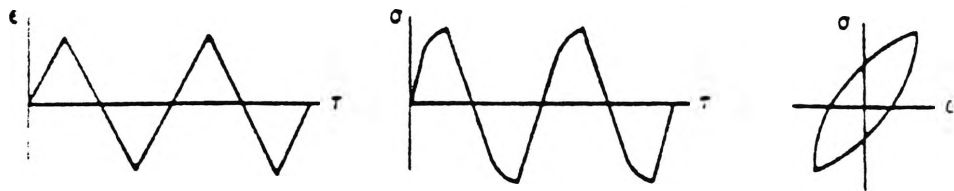
TENSION STRAIN HOLD
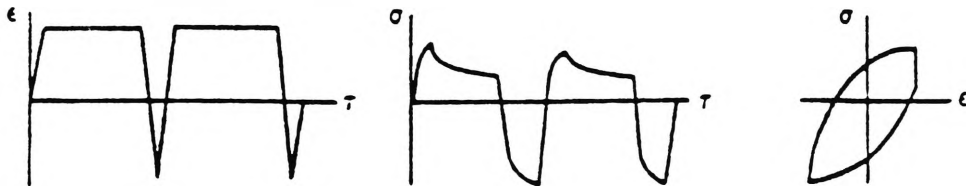
COMPRESSION STRAIN HOLD
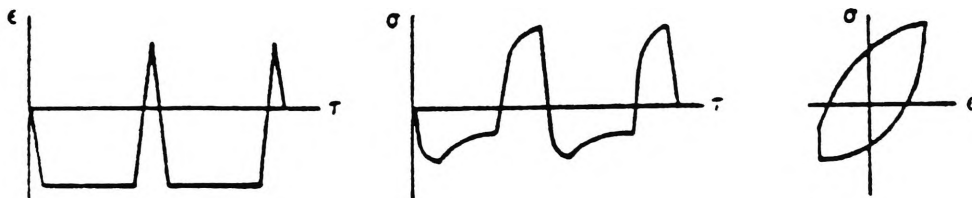
TENSION AND COMPRESSION STRAIN HOLD
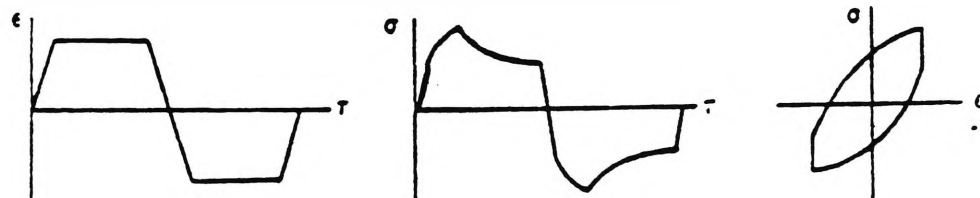
Fig. 3.4. Waveforms in high temperature low cycle fatigue testing.

3.2.4. Effect of Strain Rate on Creep-Fatigue Performance

The strain rate ($\dot{\varepsilon}$) is also represented in terms of frequency (v) only under continuous triangular waveforms (25). A relationship between strain rate, frequency and strain range, is described in equation 3.3.

$$\dot{\varepsilon}_t = 2v \, \Delta\varepsilon_t \qquad\qquad (3.3)$$

where $\Delta\varepsilon_t$, total strain range, $\dot{\varepsilon}_t$, total strain rate and v is frequency.

The strain rate, which is the rate of change of strain with time ($d\varepsilon / dt$), also implies that, with decreasing strain rate, life debits usually result. Strain rate has not yet been standardised for different test conditions, it varies from 10^{-3} to 10^{-5} /sec for an uniaxial tension test. During strain control fatigue tests, strain rate ranges from as high as 10^{-2} to a lower value of 10^{-6}/sec. Thus, during a constant strain hold, this rate of change is a zero term. Strain rate for a cycle which contains a hold period is expressed by the strain change per sec of the cycle (i.e., $\Delta\varepsilon$ / cycle time, where cycle time = [$1/v$ +hold time]. In the published data, strain rate is often omitted and data are presented either in terms of total strain range or plastic strain range with cycles to failure.

Wareing et al, (37) showed that as the plastic strain rate was reduced from 5×10^{-3} to 2×10^{-6}/sec. for a 20Cr-25Ni-Nb alloy at 750°C, the value of Cp (intercept) and the exponent β (slope of plastic strain versus cyclic life) in a Coffin-Manson equation (discussed in section 3.3.1 and equation 3.4), decreased from 1008 to 293 and 0.17 to 0.03 respectively. Negative strain rate effects, i.e., increases of cyclic strength with decreases in strain rate were observed for low alloy steels (38), and serrations appeared in the hysteresis loop during dynamic strain ageing.

3.3. DATA CORRELATION METHODS

Low cycle fatigue tests that are conducted under total strain control can either be represented in terms of total strain with life or plastic strain with life. These are discussed below.

3.3.1. Total Strain Based Approach

The loading of components is expressed in terms of percentage total strain. Total strain range may be partitioned into elastic and plastic strain components as follows.

$$\Delta\varepsilon_t = \Delta\varepsilon_e + \Delta\varepsilon_p$$

$$\Delta\varepsilon_e = \Delta\sigma / E, \text{ and also } =C_e (Nf)^{\alpha}$$

$$\Delta\varepsilon_p = C_p (N_f)^{\beta}$$

$$\Delta\varepsilon_t = \Delta\sigma / E + \Delta\varepsilon_p$$

$$\Delta\varepsilon_t = C_e (Nf)^{\alpha} + C_p (N_f)^{\beta} \tag{3.4}$$

where $\Delta\sigma$ is stress range, E is modulus, C_p, C_e, α and β are material constants.

Partitioned strain components are related with cyclic lives. A best fit equation determined to fit the data in terms of plastic strains with cycles to failure is known as the Coffin-Manson equation. Elastic (ε_e), plastic (ε_p) and total strain (ε_t) components are represented in an universal slope method (39), shown in Fig. 3.1, was derived by Manson by curve fitting HTLCF data for several materials. Equation 3.5 separates the total strain into elastic and plastic components below.

$$\Delta\varepsilon_t = 3.5 (\sigma_u / E) (N_f)^{-0.12} + \varepsilon_f^{0.6} (N_f)^{-0.6} \tag{3.5}$$

where σ_u is the tensile strength and ε_f fracture ductility.

Recently Muralidharan and Manson (40) modified the universal slope method in the following form.

$$\Delta\varepsilon_t = 0.0266 \varepsilon_f^{0.155} (\sigma_u / E)^{-0.53} N_f^{-0.56} + 1.17 (\sigma_u/E)^{0.832} N_f^{-0.09} \tag{3.6}$$

This equation was derived from the HTLCF data for 57 materials including steels, aluminium and titanium alloys. Equation 3.6 was claimed in (40) to be better approach than equation 3.5 since it was applicable for longer life regimes.

3.3.2. Plastic Strain Approach

The Coffin-Manson equation correlates plastic strain range with cyclic life as shown in equation 3.7

$$C_p \, (\Delta \varepsilon_p)^{\,\beta} = N_f \qquad\qquad (3.7)$$

where, C_p and β are material constants.

Cyclic stress range may be correlated with plastic strain range in the following stress-strain equation form:

$$\Delta \sigma = K \, \Delta \varepsilon_p^{\,n} \qquad\qquad (3.8)$$

where K is the intercept of cyclic stress range at unit plastic strain range and the exponent n is the slope of the curve. This is known as the cyclic stress-strain curve.

3.4. DAMAGE MECHANISMS UNDER CREEP-FATIGUE

A schematic representation of damage mechanisms under creep, fatigue and creep-fatigue interactions was reported by Hales (41). He (41) showed schematically that fatigue, creep-fatigue interactions and creep damage mechanisms occur under different waveforms which contain components of creep and fatigue. At high temperature, under axial loading, fatigue damage occurs by transgranular crack growth, whereas creep occurs by grain boundary sliding. Cavitation, as a result of creep, is a feature observed at grain boundary triple points. Creep cavitation together with a major crack, occurs under creep-fatigue interactions and is shown schematically in Fig. 3.5.

Damage under creep-fatigue interactions depends upon strain rate of the cycle. In creep-fatigue, cavitation results only at strain rates below some critical value, above which there is no creep damage. The critical strain rate in compression is much lower than that for tension and hence reversal of damage caused in tension occurs in compression half cycle (42). At low strain rates and stresses failure occurs by intergranular cavitation. However, at higher strain rates and stresses constrained intergranular cavitations occur. A strain rate dependent damage map for 1Cr-Mo-V was proposed by Priest and Ellison (43) and for SS 304 by Majumdar (42). The contribution of oxide scale formation along specimen surface with respect to exposure time under HTLCF has not been investigated. No standard tool is
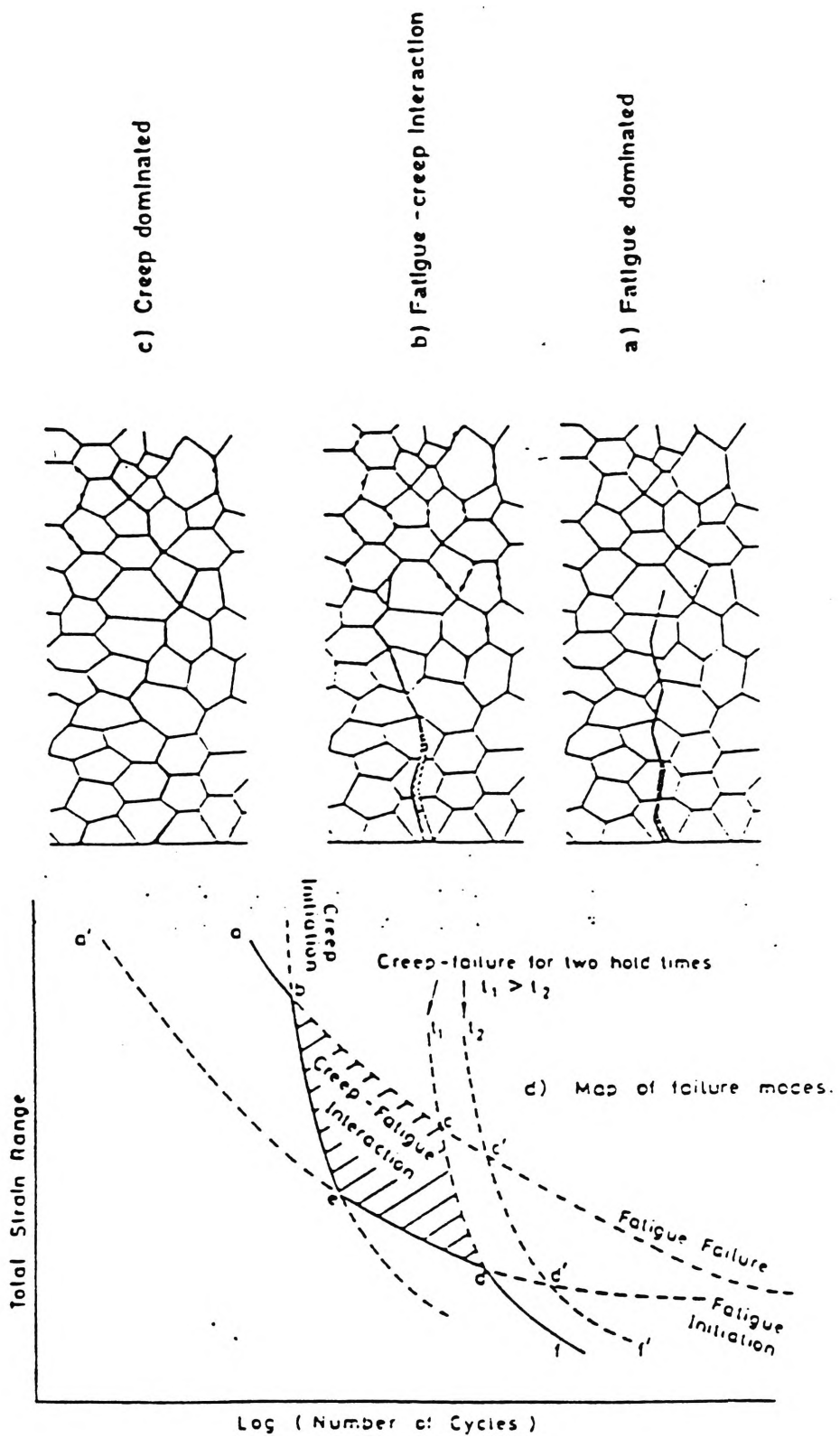
Fig. 3.5. Schematic damage map under creep-fatigue (41).

available to account for creep-fatigue and oxidation and their interactions (44-45) and modelling in terms of mechanistic methods.

3.5. SUMMARY

A brief review of creep-fatigue interaction is provided in this Chapter. The high temperature low cycle fatigue is a failure mechanism under creep-fatigue which results below 10^4 cycles. Experimental variables such as stress, strain ranges, strain rates together with conventional waveforms with different possibilities of hold times in testing were explored. The limiting value of strain rate below and above which damage by intergranular cavitation and constrained intergranular cavitation result was discussed. Data correlation methods in terms of stress-strain and strain range with cyclic life, expressed by Basquin and Coffin-Manson equations respectively, were reviewed.

4. COMPILATION OF CREEP-FATIGUE DATA FOR
LOW ALLOY STEELS

A creep-fatigue data bank for low alloy steels has been compiled in this Chapter for six steels of the type 0.5Cr-Mo-V, 1Cr-Mo-V, 1.25Cr-Mo, 2.25Cr-Mo, 2.25Cr-Mo-V and 9Cr-1Mo respectively. Published and unpublished creep-fatigue data were compiled for the six steels where data for a particular alloy was recorded in terms of a "batch", therefore, there were several batches of data for the same low alloy steel. Data "batches" in the same steel category were compared against each other to identify the creep-fatigue behaviour for the same material under different test conditions. In the open literature, numerous details related to material conditions, heat treatment parameters, microstructures and test parameters such as total strain rates and failure criteria were not revealed. As a result, there is a need to develop a consensus on standardization of laboratory test procedure in the creep-fatigue. One of the primary objectives of undertaking this research was to compile a creep-fatigue data bank for low alloy steels. The compiled data were used to identify trends in the creep-fatigue behaviour and life prediction for low alloy steels and to assess the applicability of a life prediction method modified in this investigation.

4.1. INTRODUCTION

Creep-fatigue data are of considerable importance since such data are used in the design of power plant components and in component life prediction. A volume of creep-fatigue data is not available in the public domain. In other cases, where data were published, the details related to microstructure, heat treatment conditions, failure criteria and material production histories were not reported. Research workers around the world were requested for the creep-fatigue data, additionally, a data bank was constructed from the published sources, therefore, this Chapter contains both the published and unpublished data.

Creep-fatigue data for the 0.5Cr-Mo-V, 1Cr-Mo-V, 1.25Cr-Mo, 2.25Cr-Mo, 2.25Cr-Mo-V and 9Cr-1Mo steels were collected. Each low alloy steel had been creep-fatigue tested in several laboratories in several countries. Creep-fatigue data for a particular low alloy steel, tested in one laboratory was denoted by a "batch". Hence, a large number of "batches" were formed from the data for the same and other low alloy steels. Thus, the terminology "batch" is used to identify a low alloy steel and its other particulars such as product form, test temperature and the source.

In fatigue, no two test conditions are the same since numerous parameters related to material surface finish, axiality, orientation, specimen dimensions, extensometry, load levels, difficulty in duplicating test parameters that a machine control system faces and material microstructures vary with specimens. As a result, each test varies with respect to the other test due mainly to associated test and material variability in creep-fatigue data. The "variability" that exists among batches of a particular low alloy steel are due to:

1   differences in the specimen geometry and orientation,

2   differences in extensometry employed in testing (longitudinal or diametral),

3   differences in composition of material,

4   differences in a particular heat treatment condition;

     (a) heating and cooling rates,

     (b) cooling media,

     (c) higher and lower tempering temperature ranges, and

     (d) time of hold at a specified temperature.

5   differences in microstructure of the same low alloy steel under N&T condition,

6   differences in material production routes,

7   differences in creep-fatigue test parameters;

     (a) test temperature,

     (b) strain rate,

     (c) type of heating e.g., induction and resistance, and

(d) test interruptions,

8 differences in the material product form e.g., casting and forging, and

9 differences in failure criteria employed in creep-fatigue testing.

In addition to the above items 1 through 9, there is also associated variability due to data generated in different countries. Since a code of practise does not exist or is in the developmental stage, standardisation of laboratory procedure is required to conduct creep-fatigue tests.

4.2. DATA COLLECTION

Creep-fatigue data from various international societies, laboratories, universities and private research institutions were collected and represented in "batches" for six low alloy steels. Table 4.1 describes the creep-fatigue data compiled on low alloy steel types, data representation in different batches and other details related to source, heat treatment or material conditions, test temperature and each data batch is duly referenced.

Table 4.1. Summary of the creep-fatigue data compiled.

Alloy Type	"Batch"	Source	Heat Treatment	Test Temperature	Reference
0.5Cr-Mo-V	1	CEGB	N&T	550°C	46
1Cr-Mo-V	1	NASA	N&T	540°C	47
	1	NASA	-do-	485°C	47
	2	G.E. Company	-do-	538°C	48
	2	-do-	-do-	483°C	48
	3	B.B. Company	Hot rolled	550°C	49
	4	Univ.of Bristol	Forged form N&T	565°C	50

	5	CEGB	Forged N&T	550°C	46
1.25Cr-Mo	1	Elcom, Victoria	As received	550°C	51
	2	N.I.of Metals Japan	N&T	600°C	52
2.25Cr-Mo	1	NASA	Annealed	540°C	47
	1	-do-	N&T	-do-	47
	1	-do-	Q&T	485°C	47
	2	G.E. Company	Annealed	538°C	48
	2	-do-	N&T	538°C	48
	2	-do-	Q&T	483°C	49
	3	J.S.M.S.	N&T	600°C	53
	4	O.R.N.L.	N&T	502°C	54
	5	M.H.Eng.	N&T	600°C	55
	6	European Communities	N&T	550°C	56
	7	University of Connecticut	N&T	593°C	57
	8	-do-	N&T	593°C	57
9Cr-1Mo	1	University of Bristol	N&T	550°C	58
	2	O.R.N.L.	N&T	538°C	59, 60

For a series of data batches, details of test and material parameters, for example, normalizing and tempering temperatures were unspecified for most N&T conditions that varied with batch to batch and steel to steel. These features were identified in this investigation and tabulated in Table 4.2.

Table 4.2. Summary of salient features of the compiled data.

1/2Cr-Mo-V Steel					
Batch	Source	Creep-fatigue Data Type	Heat Treatment	Salient Feature	Temp. °C
1	CEGB	0.5, 2 and 16 hrs tensile dwells	N&T	Unknown composition and stress ranges	550
1Cr-Mo-V Steel					
1	NASA	23 and 47 hrs. hold, Combined cycles (n).	N&T	Unknown composition and stress ranges	540 and 485
2	G.E.Co.	0/0, 23 and 47 hrs., combined cycles (n).	N&T	Unknown composition and stress ranges	538 and 483
3	B.B.& Co.	max. of 1/2 hr. unknown details	N&T	Unknown total strain range	550
4	Bristol University	0,1/2hr. t/0, t/t, 0/t & 18 hrs..	N&T	unknown test details.	565
5	CEGB	0.5, 2 and 16 hrs. tensile dwell	N&T	unknown heat treatment details	550
1.25Cr-Mo Steel					
1	Electricity com. (V)	up to 10 min.	as received condition	Not heat treated as N&T.	550
2	NIM	up to 1 hr.	N&T	known details	600

2.25Cr-Mo Steel

1	NASA	23 & 47 hrs.(n)	Annealed	unknown comp.	540
	NASA	23 & 47 hrs.(n)	N&T	-do-	540
	NASA	23 & 47 hrs.(n)	Q&T	-do-	485
2	G. E.Co.	0, 23 & 47hrs.n	Annealed	-do-	538
	G.E.Co.	0, 23 &47 hrs.n	N&T	-do-	538
	G.E.Co.	0. 23 &47 hrs.n	Q&T	-do-	483
3	J.S.M.	5 min. t/0, 0/t	N&T	only two tests	600
4	ORNL	6min. t/0, 0/t, t/t	N&T	one test each	502
5	MHE Co.	up to 0.54 hr.	N&T	unknown comp.	600
6	European commis.	up to 10 min.	N&T	N&T conditions unknown	550
7	Connecti- cut, Univ.	0/0 data	N&T	no hold time tests	593
8 2.25Cr- Mo-V	-do-	0/0 data, 2 frequencies	N&T	no hold time tests	593

9Cr-1Mo Steel

1	Bristol Univ.	0/0 data	N&T	Unknown comp. and N&T cycle.	550
2	ORNL	0.25, 0.5 and 1 hr. tensile holds	N & T	Unknown comp. N&T details	538 & 593

The salient features of the creep-fatigue data for all the batches are identified in Table 4.2. The detail of N&T heat treatment cycle was not known for most materials. Such details were published for a few cases in American Society of Testing Materials (ASTM) data series publication DS 58 (61), however, (61) also lacked those details. The heat

treatment details available in ASTM DS 58 and references (46-60) for different low alloy steels were compiled in Table 4.3.

Table 4.3. Summary of heat treatment parameters.

Material	Batch	Heat Treatment Parameters
1Cr-Mo-V	1	Normalized from 855°C, tempered at 676°C, slowly furnace cooled (FC).
	4	Soaked at 1000°C, furnace cooled to 690°C at 50°C, held for 70 hrs. Air cooled (AC).
		Re-heated to 975°C and soaked in salt bath. Quenched into another salt bath at 450°C, AC.
		After rough machining, re-heated to 700°C for 20hrs. Prior to finish, machining acts as tempering heat treatment and stresses relieved.
1.25Cr-Mo	2	930°C/1.5 hrs. AC, 710°C/1.5 hrs. AC, 680°C / 1 hr. FC.
2.25Cr-Mo	1 &2	Annealed: 927°C/2hrs, 593°C AC to RT, rate unknown.
	1&2	N&T: 955°C/6hrs.AC, Tempering 705°C/6hrs. AC
	1&2	Q&T: 955°C/6hrs.WQ, Tempered 621°C/6hrs, AC
	3	N&T: 930°C/0.5 hr, AC, 690°C/1.5hrs, FC.
	4	N&T: 930°C/1hr. FC, 705°C/2hrs. slow cooling.
	5	N&T: 927°C/1hr.704 @0.33°Ch^{-1}, hold at 704°C for 2 hrs.,cool to RT @ 1.31°C/hr..
	7 &8	N&T: 955°C/1hr,AC, tempered at 730°C/2hrs AC
9Cr-Mo	ASTM DS 58	N&T: 900°C, tempered 671°C. Unknown soaking.

There were considerable variations between the normalizing and tempering temperatures, periods of soaking and cooling rates within the same N&T condition where cooling types varied from furnace, air and water for the same heat treatment of the same low alloy steel. Thus, contributions of such variations on the creep-fatigue behaviour and life are unknown and their influence were isolated and ignored to identify trends in the creep-fatigue behaviour of low alloy steels.

4.3. SUMMARY OF MECHANICAL PROPERTIES

Mechanical properties of various low alloy steels for which the creep-fatigue data are compiled in this Chapter are summarized in Table 4.4. Ductility was calculated from equation 4.1, the percentage reduction in area of a tensile test, published in research literature and ASTM data series publications (61) as follows:

$$\text{Ductility} = \ln \{(100\text{-}\%\text{reduction in area})/100\}. \tag{4.1}$$

Table 4.4. Summary of mechanical properties of the compiled data.

Material details (batch)	Yield strength MPa	Tensile strength MPa	% elongation	Ductility %
1Cr-Mo-V (1-2)	614.5[a], 454.75[b]	771.6[a], 502.28[b]	22.6[a], 25.5[b]	0.87[a], 1.77[b]
1Cr-Mo-V (3)	698[a]	797[a]	24[a]	1.17[a]
1Cr-Mo-V (4)	635[a], 400[b],300[c]	805[a], 500[c],420[b]	36[a], 40[b]	1.02[a], 1.6[b]
1.25Cr-Mo (1)	330[a],191[b]	534[a], 285[b]	29[a], 48[b]	1.3[a], 2.3[b]
2.25Cr-Mo(1-2)	261.82[a], 174.4[b]	516.8[a], 336.3[b]	32.7[a], 37[b]	1.11[a], 1.70[b]
N&T (1-2)	520.2[a], 400[b]	658[a], 461.7[b]	25[a], 21[b]	1.32[a], 1.51[b]
Q&T (1-2)	799.3[a], 620.1[b]	892.3[a], 689[b]	21.5[a], 19[b]	1.28[a], 1.30[b]
N&T (3)	369[a], 240[b]	549[a], 262[b]	34[a], 36[b]	1.51[a], 2.40[b]
N&T (6)	301[a], 500[b]	218[a], 336[b]	28.8[a], 33[b]	1.46[a], 1.68[b]
N&T (7)	470[a], 597[b]	305[a], 354[b]	20[a], 34.5[b]	1.5[a], 2.04[b]
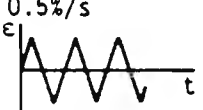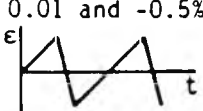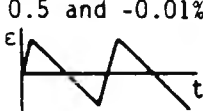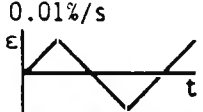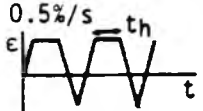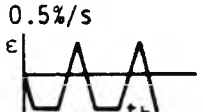
N&T (8)	620^a, 443^b	720^a, 456^b	18^a, 26.5^b	1.37^a, 1.73^b

4.4. CREEP-FATIGUE DATA

A large number of waveforms were utilized to generate the creep-fatigue data world-wide, where some workers used the ramp rates in which strain rate was different in tension and compression directions, others used the hold times (t) at the peak tension followed by no compression hold denoted by (t/0), or compression holds with no tension hold denoted by (0/t) cycles. When hold time was the same in both the directions, it was known as the balanced dwell cycle (t/t), however, when hold time was different in tension and compression, the cycle was known as an unbalanced dwell cycle (t_1/t_2). In most cases, the hold time was applied only in the tension direction (t/0) and very few compressive dwell tests (0/t) were conducted. Conventional types of waveforms popularly used in high temperature low cycle fatigue testing are shown in Figure 4.1. Complex combined cycles were used in the generation of creep-fatigue data under the Metals Properties Council Inc. (47-48) efforts. Combined cycles were used to investigate creep-fatigue interspersion effects, in that, a number (n) of pure fatigue cycles were applied at the end of a creep-fatigue hold time. A combined cycle employed by NASA (47) and General Electric Laboratories (48) is shown in Fig. 4.2. Creep-fatigue data for low alloy steels under different test combinations of hold times are tabulated in Tables 4.5-4.21.

---

[a] and [b] represent properties at room and creep-fatigue test temperatures (see Table 4.1).

No.	Strain wave pattern	Strain vs. time diagram	Δε (%)	th (min)
B-1	Faşt-fast	$\dot{\varepsilon} = 0.5\%/s$	2.0,1.2,0.8 0.6,0.4	—
B-2	Slow-fast	$\dot{\varepsilon} = 0.01$ and $-0.5\%/s$	2.0,1.2,0.8 0.6,0.4	—
B-3	Fast-slow	$\dot{\varepsilon} = 0.5$ and $-0.01\%/s$	2.0,1.2,0.8 0.6,0.4	—
B-4	Slow-slow	$\dot{\varepsilon} = 0.01\%/s$	2.0,1.2,0.8 0.6,0.4	—
B-5	Fast-fast with hold time in tension	$\dot{\varepsilon} = 0.5\%/s$	2.0	5
			1.0	5
			1.0	30
B-6	Fast-fast with hold time in compression	$\dot{\varepsilon} = 0.5\%/s$	2.0	5

Fig. 4.1. Illustration of waveforms used in the creep-fatigue characterization of 2.25Cr-Mo steel under benchmark project (53).
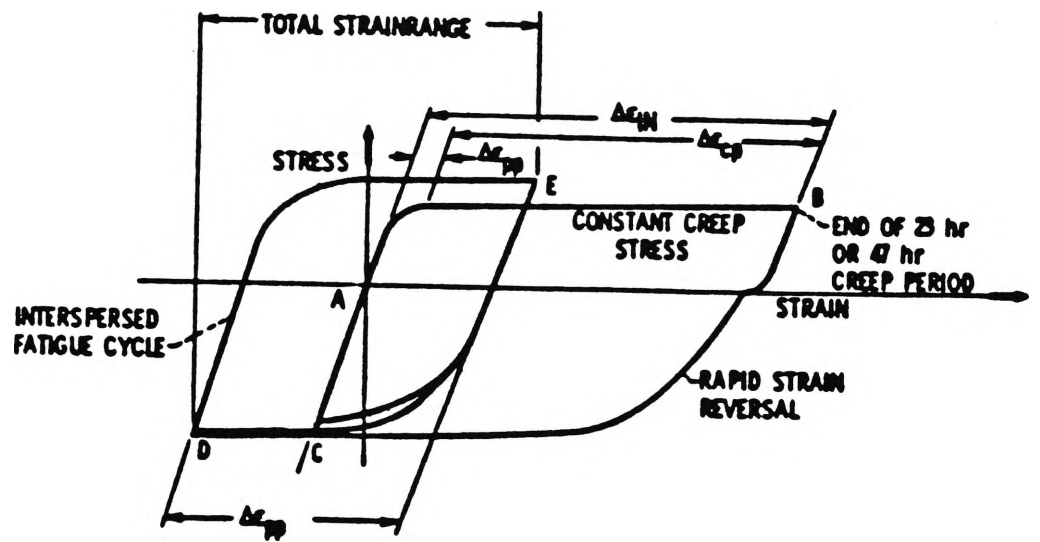
Fig. 4.2. Schematic hysteresis loops associated with MPC Creep-fatigue interspersion tests (47).

Table 4.5. Creep-fatigue data for 0.5Cr-Mo-V Batch 1 (46).

Total strain range (%)	Hold time (hours)	Test-temperature (°C)	Observed-cycles (Nf)	Remarks
1.51	0.5	550	375	
1	0.5	"	537	
0.70	0.5	"	998	
1.02	2	"	519	
1	16	"	340	
0.4	16	"	1590	
2.39	16	"	124	
1.25	16	"	314	
0.61	16	"	604	
0.43	16	"	675	
0.34	16	"	1249	
2.3	16	"	209	
0.92	16	"	611	
0.62	16	"	647	
0.4	16	"	1126	
0.3	16	"	1700	

Table 4.6. Creep-fatigue data for 1Cr-Mo-V Batch 1 (47).

Total strain range (%)	Hold time (hours)	Test-temperature (°C)	Observed-cycles (Nf)	Remarks
0.55	23	540	29	n=1

1.50	23	"	22	"
1.10	47	"	24	"
1.50	47	"	29	"
1.50	23	"	42	n=2
0.55	47	"	84	n=1
1.50	47	"	87	"
1.50	23	"	209	"
1.50	47	"	150	"
0.55	47	485	27	n=22
0.55	47	485	48	"
1.50	47	"	30	n=1
1.50	23	"	42	n=2
1.50	23	"	145	"
0.55	23	"	149	"
0.55	23	"	25	n=22
1.50	47	"	87	n=1
0.55	47	"	96	"

Table 4.7. Creep-Fatigue data for 1Cr-Mo-V Batch 2 (48).

Total strain range (%)	Hold time (hours)	Test-temperature (°C)	Observed-cycles (Nf)	Remarks
0.55	0	538	5105	
1.5	0	"	520	
0.55	23	538	130	n=22.5
1.5	23	"	68	n=5.5

0.55	0	483	8400	
1.5	0	"	500	
1.5	23	483	49	n=5.5
0.55	47	"	96	n=1.5
0.55	47	"	149	n=2.5
0.55	23	"	161	n=5.5

Table 4.8. Creep-fatigue data for 1Cr-Mo-V Batch 3 (49).

Inelastic strain (%)	Total Strain (%)	Test-temperature (°C)	Observed-cycles (Nf)	Remarks
1.27	1.95	550 (CC)	208	Hold times were
0.84	1.5	CC types	283	unspecified and
0.57	1.2		400	total strain range
1.6			165	was calculated
2.57			165	approximately.
2.29			90	
0.946	1.6	t/0 or CP types	340	
1.004	1.67		240	
1.038	1.72		180	
2.257			52	
0.95	1.62		171	
0.708	1.35		340	
1.554			113	
2.33		0/t or PC types	92	
1.297	1.98		285	

1.14	1.81		250	
2.18			95	
0.24	0.83		1460	
0.24	0.83		1230	
0.76	1.41		380	
1.32	2		185	
1.11	1.78		255	
0.5	1.13		590	
0.3	0.9	t/t or CC types	625	
0.57	1.2		350	
1.167	1.84		180	
1.923			108	
0.892	1.55		260	
0.369	0.98		600	
0.093	0.6		950	

Table 4.9. Creep-fatigue data for 1Cr-Mo-V Batch 4 (50).

Total strain range (%)	Hold time (hours)	Test-temperature (°C)	Observed-cycles (Nf)	Remarks
1.5	0	565	327	Stress range was
1.0	0	"	490	unknown,
0.7	0	"	960	inelastic strain
1.96	3		97	range unknown
1.08	3	"	150	
1.96	0.5	"	135	

1.08	0.5	"	220	
0.53	0.5	"	435	
0.86	1	"	1275	
1.06	0.5/0.5	"	385	
1.46	0.5/0.5	"	220	
2.0	0.5/0.5	"	215	
1.4	0.5/0.5	"	390	
1.3	16	"	73	
1.3	16/0.003	"	208	
2.0	0.5	"	180	
1.5	0.5	"	215	
1.0	0.5	"	300	
2.0	0/0.5	"	300	
1.5	0/0.5	"	374	
1.1	0/0.5	"	560	
2.04	0/0.5	"	320	
1.24	0/0.5	"	562	
1.53	0/0.5	"	362	
0.85	0/0.5	"	500	

Table 4.10. Creep-fatigue data for 1Cr-Mo-V Batch 5 (46).

Total strain range (%)	Hold time (hours)	Test-temperature (°C)	Observed-cycles (Nf)	Remarks
3.2	0.5	550	80	
2	0.5	"	176	

1	0.5	"	382	min. value
0.9	0.5	"	500	
0.6	0.5	"	1456	
0.5	0.5	"	2300	
1	2	"	448	
3.19	16	"	86	
1.23	16	"	244	
0.84	16	"	454	
0.63	16	"	1033	
0.5	16	"	3557	
3.74	16	"	122	
1.16	16	"	645	
0.61	16	"	2347	
0.48	16	"	4084	

Table 4.11. Creep-fatigue data for 1.25Cr-Mo Batch 1 (51).

Total strain range (%)	Hold time (hours)	Test-temperature (°C)	Observed-cycles (Nf)	Test end criterion
0.5	0	550	5284	20% load drop
0.7	0		1667	"
1.0	0		945	"
0.5	0.0166		3919	"
0.7	0.0166		1475	"
1.0	0.0166		769	"
0.5	0.166		3896	40%

0.7	0.166		1311	33%
1.0	0.166		820	20%
1.0	0.5		601	20%

Table 4. 12. Creep-fatigue data for 1.25Cr-Mo Batch 2 (52).

Total strain range (%)	Hold time (hours)	Test-temperature (°C)	Observed-cycles (Nf)	Saturated stress range(Nf/2) MPa.
2.01	0	600	560	575
1.52	0	"	760	527
0.98	0	"	1500	505
0.62	0	"	6100	460
0.59	0	"	5800	459
0.48	0	"	5000	438
2.04	0.03	"	418	599
1.04	"	"	871	526
2.05	0.08	"	327	583
0.95	"	"	772	533
2.04	0.16	"	292	583
1.04	"	"	605	522
2.03	0.5	"	230	551
1.04	"	"	455	488
2.03	1	"	195	528
0.99	"	"	418	481

Table 4.13. Creep-fatigue data for 2.25Cr-Mo Batch 1 (47).

Total strain range (%)	Hold time (hours)	Test-temperature (°C)	Observed-cycles (Nf)	Remarks
0.55	47	540	67	n=1 (annealed)
1.50	23	"	141	"
2.30	47	"	59	"
2.30	23	"	73	"
1.50	23	"	202	"
1.50	23	"	50	n=1 N&T
0.55	47	"	13	"
2.3	47	"	24	"
2.3	23	"	43	"
0.55	47	"	60	"
1.5	23	"	110	"
0.55	47	485	23	n=1 Q&T
1.50	23	"	31	"
2.3	47	"	15	"
2.3	23	"	29	"
0.55	47	"	48	"
1.50	23	"	77	"

Table 4.14. Creep-fatigue data for 2.25Cr-Mo Batch 2 (48).

Total strain range (%)	Hold time (hours)	Test-temperature (°C)	Observed-cycles (Nf)	Remarks
0.55	0	538	3655	Annealed

1.5	0	"	930	"
2.3	0	"	348	"
0.55	47	"	67	n=1.5
0.55	23	"	103	n=5.5
1.50	23	"	13	n=5.5
0.55	0	538	2990	N&T
1.5	0	"	672	"
2.3	0	"	281	"
0.55	47	"	13	n=1.5
0.55	23	"	32	n=5.5
0.55	47	"	60	n=1.5
1.5	23	"	13	n=22.5
0.55	0	483	7440	Q&T
1.50	0	"	474	"
2.3	0	"	265	"
0.55	47	"	23	n=1.5
0.55	23	"	90	n=5.5
1.50	23	"	77	n=1.5

Table 4.15. Creep-fatigue data for 2.25Cr-Mo Batch 3 (53).

Total strain range (%)	Hold time (hours)	Test-temperature (°C)	Observed-cycles (Nf)	Remarks
2.0	-	600	257	Five strain rates
"	-	"	355	fast -fast (FF)
1.2	-	"	780	0.5%/s

"	-	"	668	slow-fast
0.8	-	"	2008	0.01 and-0.5%/s
"	-	"	1294	fast-slow
0.6	-	"	3865	0.5 & -0.01%/s
"	-	"	2100	slow-slow
0.4	-	"	7786	0.01%/s
"	-	"	6742	FF with tensile
"	-	"	6075	hold=0.5%/s
2.1	-	"	112	FF with comp.
1.3	-	"	308	hold = 0.5%/s
1.2	-	"	350	
0.87	-	"	731	
0.8	-	"	1048	
0.68	-	"	1140	
0.6	-	"	2129	
0.4	-	"	7346	
2.0	-	"	305	
1.2	-	"	540	
"	-	"	678	
0.8	-	"	1049	
"	-	"	1138	
0.62	-	"	2095	
0.6	-	"	2560	
0.4	-	"	5630	
2.0	-	"	224	
"	-	"	168	

1.2	-	"	325	
"	-	"	496	
0.86	-	"	915	
0.8	-	"	955	
0.6	-	"	1768	
"	-	"	1229	
0.4	-	"	9227	
2.0	0.083	"	312	
1.0	0.083	"	720	
2.0	0/0.083	"	325	
1.0	0/0.083	"	894	

Table 4.16. Creep-fatigue data for 2.25Cr-Mo Batch 4 (54).

Total strain range (%)	Hold time (hours)	Test-temperature (°C)	Observed-cycles (Nf)	Saturated stress range (Nf/2)MPa.
0.5	0/0.1	502	61111	216
0.5	0.1	"	20147	209
0.5	0.1/0.1	"	3420	209
1.0	-	"	3721	259
1.0	0/ 0.1	"	1924	264
1.0	0.1	"	2059	252

Table 4.17. Creep-fatigue data for 2.25Cr-Mo Batch 5 (55).

Total strain range (%)	Hold time (hours)	Test-temperature (°C)	Observed-cycles (Nf)	Inelastic strain range %
1.01	0.23	600	1360	0.79
1.99	0.22	"	472	1.75
1.00	0.01	"	1070	0.79
1.07	0.54	"	820	0.9
1.02	0.08	"	940	0.85
1.97	0.22	"	410	1.78

Table 4.18. Creep-fatigue data for 2.25Cr-Mo Batch 6 (56).

Total strain range (%)	Hold time (hours)	Test-temperature (°C)	Observed-cycles (Nf)	Saturated stress range(Nf/2) MPa.
3.20	0.016	550	234	697
2.15	"	"	410	647
0.54	"	"	5200	485
1.05	"	"	1520	549
4.30	"	"	200	722
3.20	"	"	208	687
2.20	"	"	380	630
1.20	"	"	150	736
0.52	"	"	6100	422
1.05	"	"	1450	510
4.25	0.034	"	165	657

3.00	"	"	280	608
2.10	"	"	440	574
1.15	"	"	1200	490
0.68	"	"	2200	432
4.1	0.166	"	180	549
3.0	"	"	265	520
2.2	"	"	345	515
1.2	"	"	1070	427
0.66	"	"	2300	353
4.0	"	"	220	530
3.1	"	"	255	535
2.1	"	"	410	471
1.1	"	"	1180	408
0.60	"	"	2750	334

Table 4.19. Creep-fatigue data for 2.25Cr-Mo Batch 7 &8 (57).

Total strain range (%)	Hold time (hours)	Test-temperature (°C)	Observed-cycles (Nf)	Saturated stress range (Nf/2)MPa.
0.523	-	593	7179	478
0.544	-	"	5100	436
0.773	-	"	2980	478
0.84	-	"	799	492
0.86	-	"	1065	402
0.92	-	"	2647	498
0.927	-	"	2699	520

0.973	-	"	1623	450
0.993	-	"	2443	450
1.41	-	"	1109	492
1.84	-	"	777	510
2.33	-	"	555	582
0.557	**Batch 8**	"	5072	535
0.571	-	"	4645	591
0.813	-	"	2734	634
0.933	-	"	505	622
0.94	-	"	1201	536
0.984	-	"	301	680
1.024	-	"	1904	613
1.027	$v = 1.027\%/s$	"	2159	632
1.040	$=0.042\%/s$	"	1519	470
1.40		"	861	620
1.90		"	605	685

Table 4.20. Creep-fatigue data for 9Cr-1Mo Batch 1 (58).

Total strain range (%)	Hold time (hours)	Test-temperature (°C)	Observed-cycles (Nf)	Remarks
2.0	-	550	780	other details were
"	-	"	935	unknown
"	-	"	947	
1.2	-	"	1839	
"	-	"	1852	

"	-	" .	1740	
0.6	-	"	16960	
"	-	"	13000	
"	-	"	10300	

Table 4.21: Creep-fatigue data for 9Cr-1Mo Batch 2 (59).

Total strain range (%)	Hold time (hours)	Test-temperature (°C)	Observed-cycles (Nf)	Saturated stress range(Nf/2) MPa.
0.5	0/0	538	13786	535
0.5	0/0	"	15455	604
0.7	0/0	"	6844	556
0.7	0/0	"	9676	549
0.78	0.25	"	3537	482
0.5	0.25	"	8840	475
0.5	0.5	"	6975	508
0.51	0.5	"	7770	513
0.52	0/0	593	13125	505
0.49	0/0	"	7420	472
0.5	0.5	"	3360	426
0.5	0.5	"	4150	465
0.5	1	"	3207	370
0.5	1	"	2870	203
0.5	1	"	2882	363
0.5	1	"	2900	429

4.5. COMMENTS ON THE DATA COMPILED

In all the batches of creep-fatigue data tabulated in Tables 4.5- 4.21, several features were found to be unspecified in the open literature, for example, the effects of microstructure on the creep-fatigue life was evidently ignored by all workers. Strain rates during creep-fatigue tests were mostly unspecified in the open literature. Total strain range and hold times were unspecified (48) for 1Cr-Mo-V "batch" 3, in Table 4.8. For Table 4.8, total strain ranges ($\Delta\varepsilon_t$) were derived using the equations 4.2 for the approximate determination,

$$\Delta\varepsilon_t = \Delta\sigma / E + \Delta\varepsilon_p$$

$$\text{where } \Delta\sigma = K (\Delta\varepsilon_p)^n \tag{4.2}$$

where $\Delta\varepsilon_t$ is total strain range, $\Delta\sigma$ is stress range, E is modulus of elasticity, $\Delta\varepsilon_p$ is plastic strain range, K, and n are the material parameters.

Value of K and n were assumed for "batch" 8 from Jaske and Mindlin (62), who found them 1008 MPa and 0.09 respectively for 1Cr-Mo-V tested at 538°C. Such conversion from inelastic strain to total strain was made below inelastic strain range of 1.4% (25, 62). Beyond this limit, the two values assumed, changed (62). The approximate analysis performed in this section randomises the data which will be useful in assessing the applicability of a method of life prediction and must not be used in design analyses.

Another aspect of the data relates to the saturated stress range which was sparingly available in the literature. Hence, saturated stress range appear in the data tables where details were available. In most cases, longitudinal extensometers were used with cylindrical specimens. However, complete details of the specimens, extensometry and how the temperature and strain rates were controlled were not generally specified in the open literature. The failure criteria also varied from laboratory to laboratory and in one particular case for 1.25Cr-Mo "batch" 1 from tests to tests. Why different failure criteria were used for different tests was not specified in the open literature.

A code of practice (63) is in the developmental stage in the United Kingdom, however, several test parameters such as strain rates in tension and compression and hold

times and their directions as well as other parameters are not standardised in this code. An elaborate standard of practice in laboratory generation of creep-fatigue tests is highly desired.

5. CREEP-FATIGUE BEHAVIOR OF LOW ALLOY STEELS - TRENDS

A creep-fatigue data bank has been compiled for low alloy steels in Chapter 4 which was used in this Chapter to identify trends in the creep-fatigue behaviour of low alloy steels. Several material and test parameters were identified in Chapter 4 that enhanced the variability in creep-fatigue testing. How numerous variables, identified in Chapter 4, affect the creep-fatigue life of materials are unknown, hence, effects of unknown variables in creep-fatigue response are isolated to identify the trends in the creep-fatigue behaviour of low alloy steels. Effects of composition on the creep-fatigue behaviour of low alloy steels were assessed in a range of chromium content from 0.5 to 9 weight percent, where the creep-fatigue behaviour in general improved with the increase in chromium content. When other elements (e.g., vanadium) were added to a 2.25Cr-Mo steel, the creep-fatigue performance deteriorated. Effects of hold times in tension and compression directions were assessed to investigate the dwell sensitive behaviour of the materials. A material was dwell sensitive if there was associated decrease in life when either a tension or a compression hold at peak strain range was applied. The 2.25Cr-Mo steel was observed to be compressive dwell sensitive, whereas, 1Cr-Mo-V steel was tensile dwell sensitive. When a number (n) of pure fatigue cycles were applied at the end of a creep-fatigue cycle, known as combined cycles, either improvement or deterioration of creep-fatigue resistance occurred and the response depended upon the number of combined cycles employed.

5.1. INTRODUCTION

Creep-fatigue tests are conducted to simulate the actual service conditions of engineering components operating in the creep range. The microscopic damage features are also investigated to document failure modes under creep-fatigue that aid in the development of life prediction or extension methods. These studies are conducted to gain more knowledge on the high temperature low cycle fatigue (HTLCF), which is a candidate failure mechanism of

components operating in the creep range. Effects of numerous material and test parameters on the creep-fatigue behaviour of low alloy steels are not understood, therefore, the influence of several variables are isolated to identify trends in the creep-fatigue behaviour of low alloy steels. The trends in the creep-fatigue behaviour of low alloy steels are discussed below.

5.2. ANALYSES OF CREEP-FATIGUE DATA

Creep-fatigue data, in which the plastic strain dominates, usually the life ranges from 10^3 to 10^4 cycles and elastic strain component is found smaller than plastic. The data compiled in Chapter 4 are represented by total strain range and cycles to failure, hence total strain range and life data were fitted with a least square best fit equation on a log-log scale. A least square best fit equation was determined for at least 50 combinations of continuous fatigue and hold time test sequences. The best fit equation so obtained had an intercept (A) and a slope (m), known as material parameters. Only two data points were used to determine the parameters of linear extrapolation when only two data points were available. Such equations are questionable and should not be used in the design by extrapolating total strain and life combinations. As intercept (A) and negative slope (m) increased creep-fatigue life decreased. The equation has the following form :

$$\Delta \varepsilon_t = A \, (Nf)^m \tag{5.1}$$

where A and m are material parameters.

Material parameters were determined for various combinations of tests tabulated in Table 5.1. Thus, Table 5.1 is a source table from which the information on creep-fatigue behaviour of low alloy steels can be gathered and a total strain- life relationship can be determined.

Table 5.1. Material parameters of total strain versus life equation of the compiled data.

Material / (Batch)	Temperature	Slope	Intercept	Remarks
0.5Cr-Mo-V (1)	550°C	-0.77	2.12	0.5 hour tensile hold.
	550°C	-0.84	2.18	16 hours tensile hold.

1Cr-Mo-V (1)	540°C	-3.63*	4.30	23 hour hold. (n=1)
	485°C	-0.80*	1.46	23 hour hold. (n=2)
	485°C	-10.2*	19.9	47 hour hold. (n-1)
Batch 2	538°C	-0.44*	1.36	0/0 continuous fatigue.
	483°C	-0.36*	1.36	0/0 continuous fatigue.
	483°C	-0.84*	1.6	23 hour hold. (n=5.5)
Batch 3	550°C	-1.03	2.47	CC type of SRP loop#.
	550°C	-0.54	1.27	CP type of SRP loop#.
	550°C	-0.17*	0.40	PC type of SRP loop#.
	550°C	-1.04	2.45	CC type of SRP loop#.
Batch 4	565°C	-1.36*	3.0	3 hours hold data.
	565°C	-1.22*	2.89	1/2 hour hold data.
	565°C	-0.85	2.22	Balanced dwell of 1/2 hr.
	565°C	-1.34	3.31	1/2 hr. hold.
	565°c	-1.04	2.87	0/0.5 hr.hold.
Batch 5	550°C	-0.56	1.52	0.5 hour tensile hold.
	550°C	-0.51	1.4304	16 hours tensile hold.
1.25Cr-Mo (1)	550°C	-0.39	.96	0/0 continuous fatigue.
	550°C	-0.42	1.19	0.016 hr. hold.
	550°C	-0.42	1.19	0.16 hr. hold
Batch 2	600°C	-0.52	1.67	0/0 continuous fatigue.
	600°C	-0.92*	2.71	0.03 hr. hold.
	600°C	-0.89*	2.5	0.08 hr. hold.
	600°C	-0.92*	2.58	0.16 hr. hold
	600°C	-0.98*	2.6	1/2 hr. hold.

	600°C	-0.94*	2.46	1 hr. hold.
2.25Cr-Mo (1)	540°C	-11.25*	20.3	47hr. hold, Annealed(A)
	540°C	-0.419*	1.14	23 hr. hold, A.
	540°C	-2.83*	4.99	23 hr. hold, N&T.
	540°C	-1.56*	2.5	47 hr. hold, N&T.
	485°C	-6.4*	9.73	23 hr. hold, Q&T.
	485°C	-3.34*	4.29	47 hr. hold, Q&T.
Batch 2	538°C	-0.61	1.94	0/0 continuous fatigue A.
	538°C	-0.61	1.87	0/0, N&T.
	483°V	-0.40	1.32	0/0, Q&T.
Batch 3	600°C	-0.44	1.25	0/0 N&T.
	600°C	-0.83*	2.3	0.08 hr.tensile hold N&T
	600°C	-0.68*	2.0	0.08 hr. compression.
Batch 4				Not enough data.
Batch 5				Not enough data.
Batch 6	550°C	-0.46	1.51	0.016 hr. hold.
	550°C	-0.69	2.17	0.034 hr. hold.
	550°C	-0.7	2.18	0.166 hr. hold.
Batch 7	593°C	-0.46	1.48	0/0 continuous fatigue.
Batch 8	593°C	-0.274	0.83	0/0 continuous fatigue.
9Cr-1Mo (1)	550°C	-0.42	1.5	0/0 continuous fatigue
Batch 2	538°C	-0.49	1.72	0/0 continuous fatigue
	538°C	-0.49*	1.62	1/4 hr. tensile hold.
	538°C	0.18*	-1.01	1/2 hr. tensile hold, within $\Delta\varepsilon_t$=0.5-0.51%

	593	0.11	-0.72	0/0 continuous fatigue within $\Delta\varepsilon_t$=0.52-0.49%

In situations, where material parameters are determined from two data points are denoted by (*). The symbol, (#) is used with inelastic strain range versus life relations.

5.3. CREEP-FATIGUE BEHAVIOR OF LOW ALLOY STEELS - TRENDS

In this section the data compiled and presented in Chapter 4 were used to identify the trends in the effects of waveform, product form and composition on the creep-fatigue behaviour for six low alloy steels having compositions as follows:

Steel No. 1: 0.5Cr-Mo-V

Steel No. 2: 1Cr-Mo-V

Steel No. 3: 1.25Cr-Mo

Steel No. 4: 2.25Cr-Mo

Steel No. 5: 2.25Cr-Mo-V

Steel No. 6: 9Cr-1Mo.

5.3.1. Effects of waveform

5.3.1.1. Steels No. 1: Creep-fatigue data for a 0.5Cr-Mo-V steel (46) are presented in Fig. 5.1. The hold times applied were one-half and sixteen hours only at peak tensile strain direction and no hold times in the compression were tested as a result comparison of the tensile and compressive properties for this steel can not be made. The material parameters of equation 5.1 exhibited similar values for 30 min. and sixteen hours tensile holds. The life debits associated with a hold, when compared with continuous fatigue, depended upon strain range where life debit was more at low strain ranges which, with the increase in total strain range saturated.
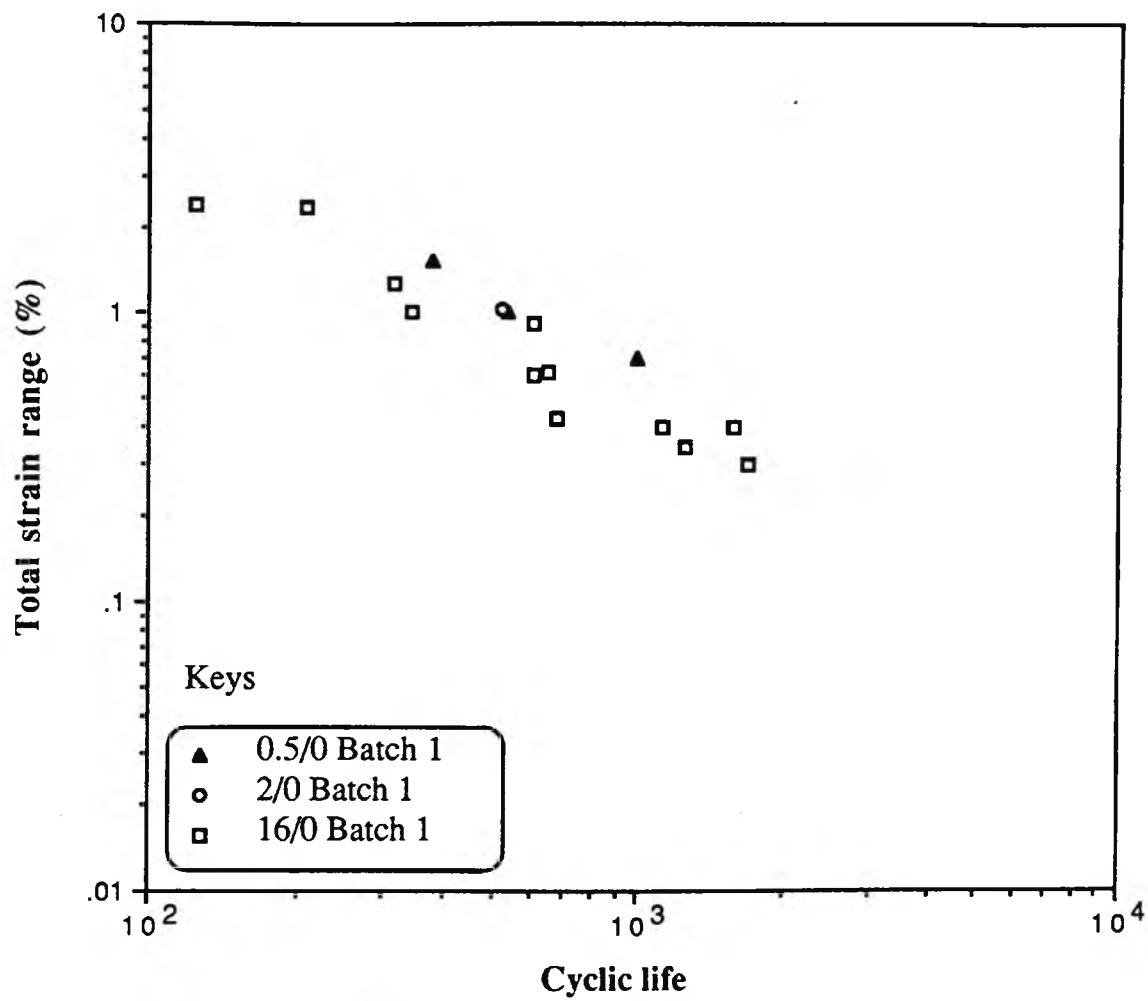
Fig. 5.1. Creep-fatigue behavior of 0.5Cr-Mo-V steel with different hold times.

5.3.1.2. Steel No.2: This steel has been extensively tested for creep-fatigue performance under different tension and compression holds, where a tensile hold caused more damage than hold in the compression, balanced hold and unbalanced holds for "batch 4" (36, 50). Although the same hold periods were applied in tension and compression at the same strain range, tensile holds were nearly two times more damaging. Material parameters, such as slope of 30 min. tensile dwell cycles were more negative than the same compressive dwell cycles shown in Table 5.1. The material parameter (m) of equation 5.1 for one-half hour tensile dwell cycles was -1.22, whereas for the same compressive hold cycles it was -1.04. For unbalanced cycles (t_1/t_2), with 16 hours tensile hold, followed by 10 seconds hold in compression, caused a healing effect. With the application of 16h/10 sec. cycle, life enhanced by a factor of 3 from only tensile hold of 16 hours shown in Fig. 5.2.

In creep-fatigue condition, where damage accrues by creep-fatigue interaction is interpreted in terms of relaxed strains when a hold time is applied at constant stress level and stress relax when a hold time is applied at constant strain. In both the cases, the plastic strain component is increased, such that, when the magnitude of relaxed strains exceed the creep ductility of the material, failure occurs. Creep ductility is a variable quantity which depends not only upon stress, temperature and time, but also, upon microstructure, grain size, heat treatment and material composition. For a typical estimate, for "batch 4" (32, 36, 50), it was found 5%, however, no consideration of factors that influence the creep ductility was made. The rates of stress relaxation were assumed (11) to be the same in both tension and compression directions, however, the mechanistic features of damage observed under tension and compression holds were different (32), that implies rates of stress relaxation in tension and compression directions to be different.

Data for various hold time cycles were normalized with continuous fatigue data, in terms of normalized cycle ratio (NCR), which was a ratio of number of cycles to failure under hold time cycle with continuous fatigue at the same strain ranges. The NCR was presented with total strain range for 1Cr-Mo-V steel in Fig. 5.3. When the NCR of various

Fig. 5.2. Creep-fatigue behavior of 1Cr-Mo-V steel with different hold times.
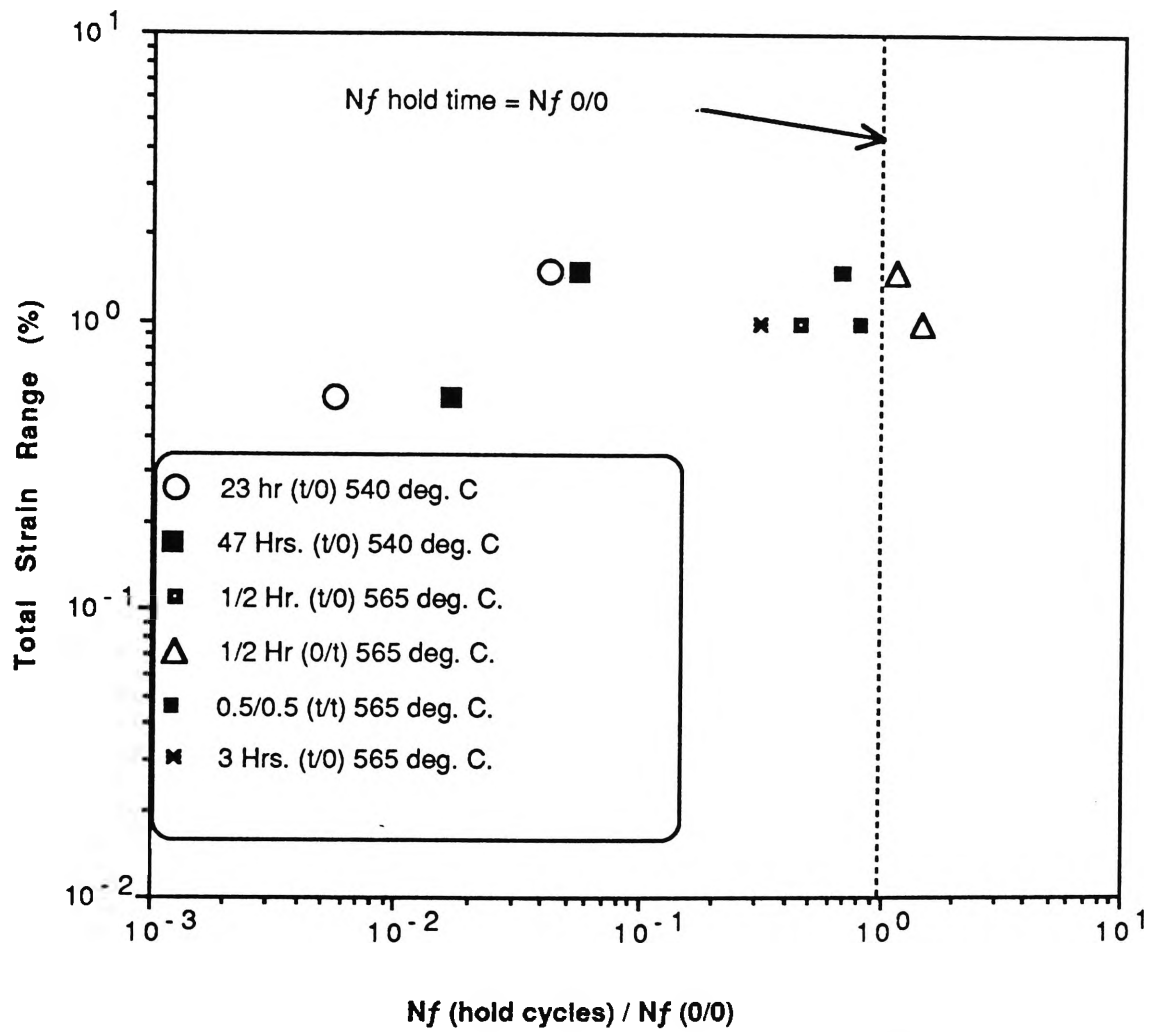
Fig. 5.3. Normalized life ratio of various dwell cycles of 1Cr-Mo-V steel.

tensile dwell containing cycles were less than unity, the material was tensile dwell sensitive. However, when the normalized cycle ratios of the compressive dwell containing cycles were more than unity, those cycles were beneficial than continuous fatigue (0/0).

5.3.1.3. Steel No. 3: For this steel the material conditions and heat treatment details were not specified in the literature (51) for "batch" 1. The data compiled for two batches of 1.25Cr-Mo steels were compared against each other by isolating the effects of material conditions. A difference of 50°C existed in the test temperatures for two batches which contributed to lower the tensile properties of the material. When compared at the same total strain ranges, both materials performed identically when no hold time was applied. With 10 and 30 minutes tensile holds creep-fatigue response for "batch 1" was slightly better than "batch 2" as shown in Fig. 5.4 at the same strain range. It may not be possible to conclude from the available data whether a decrease in temperature from 600 to 550°C, raised the life by 1.25 times or, ignoring the effects of temperature, material in as-received condition was superior.

Various hold time data were normalized by continuous fatigue data in terms of NCR and presented with total strain range in Fig. 5.5. As the NCR of various tensile dwell cycles was much less than one, the material was tensile dwell sensitive. Since no compressive hold time data was available, and the normalized cycle ratios of tensile hold data were less than one, it was considered to be a tensile dwell sensitive material.

5.3.1.4. Steel No. 4: This is a compressive dwell sensitive material, where compressive dwell at a strain range and temperature causes more damage than the dwell in the tension direction (33). Challenger et al (54), explained that a possible reason for such behaviour was mainly oxidation of the material. The oxide cracking that occurs in the case of 2.25Cr-1Mo steels was a function of strain range, temperature and time of hold in peak compressive loading direction. Later evidence for oxidation at 593°C of this alloy was reported by
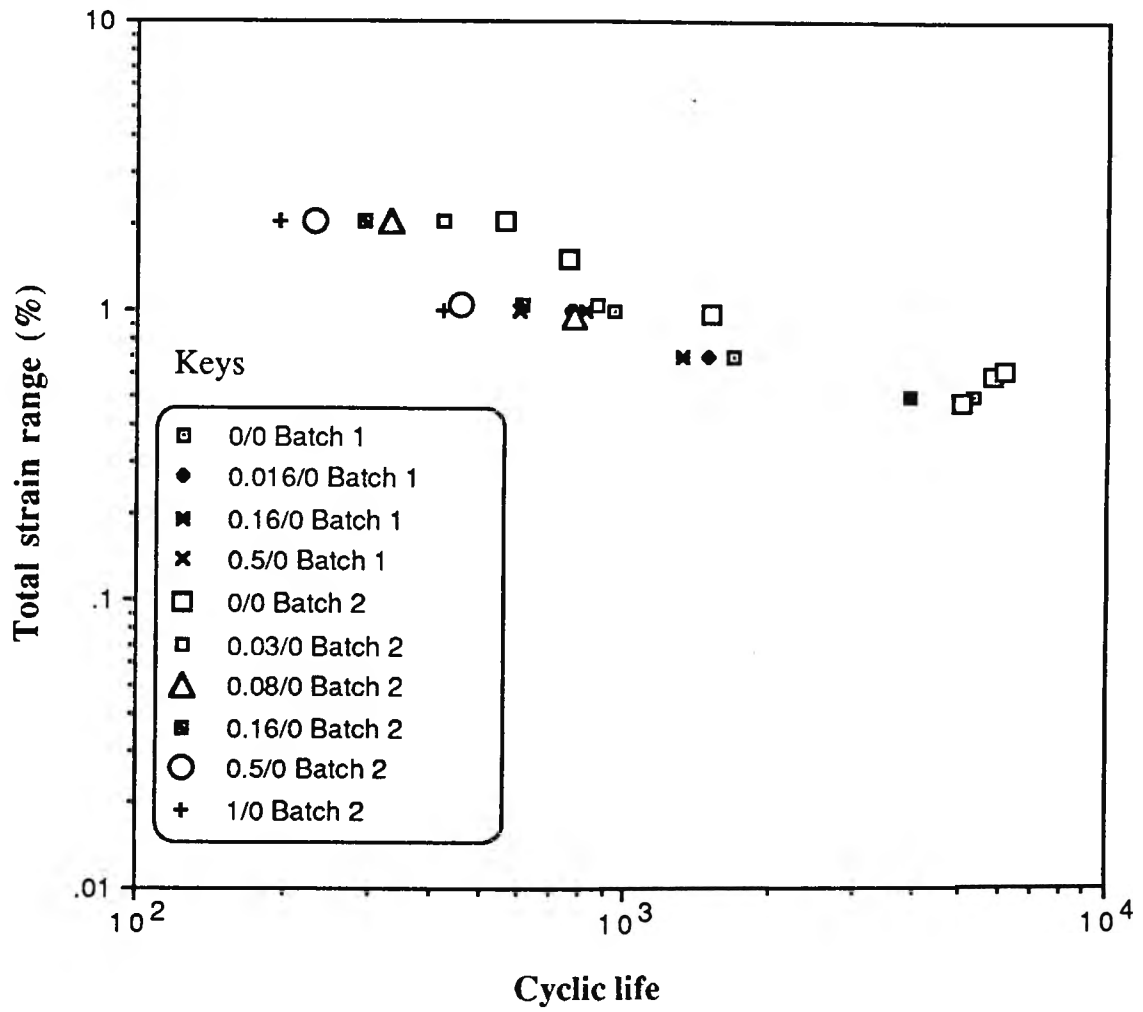
Fig. 5.4. Creep-fatigue behavior of 1.25Cr-Mo steel with different hold times.

Fig. 5.5. Normalized life ratio of various dwell cycles of 1.25Cr-Mo steel.

Teranishi and McEvily (57) and Narumuto (64). A threshold in the temperature range was observed (33, 64), above which the oxidation damage occurred. This temperature was found to be 450°C in (33) and was lower (250 - 350°C) for 2.25Cr-Mo steel (64).

Apart from a threshold in temperature there also was a hold time criterion, below which life debit did not occur. Five minutes tensile and compressive holds were compared with continuous fatigue data in Fig. 5.6 tested at 600°C for 2.25Cr-Mo steel (53) "batch" 3. Creep-fatigue lives under such hold periods were between the maximum and mean response of continuous fatigue behaviour.

Creep-fatigue life for various dwell data were normalized by continuous fatigue data and NCR with total strain range was presented in Fig. 5.7. As the normalized cycle ratio for various tensile dwell containing cycles was more than compression dwells, the material was compressive dwell sensitive.

5.3.1.5. Steel No. 5:   Only two batches of creep fatigue data were available with several hold times and continuous fatigue combinations with only two tests conducted for every condition. The best fit equations determined from two data points are questionable and should not be extrapolated for other total strain range and life combinations. Creep-fatigue data for 9Cr-1Mo steel are shown in Fig. 5.8.

Creep-fatigue life under various dwell cycles were normalized by continuous fatigue life and presented with total strain range in Fig. 5.9. Since there were no compressive hold time data and the normalized cycle ratio of various tensile dwell containing cycles were much less than one, the material was assumed tensile dwell sensitive.

5.3.1.6. Effects of combined cycles on Steel No. 2: A combined cycle comprised in addition to a tensile dwell, a specified number of pure fatigue cycles represented by n, as shown in Fig. 4.2, in Chapter 4. Combined cycles were applied after a tensile hold of 23 and 47 hours in (47-48). The effects of combined cycles on creep-fatigue performance of "batch
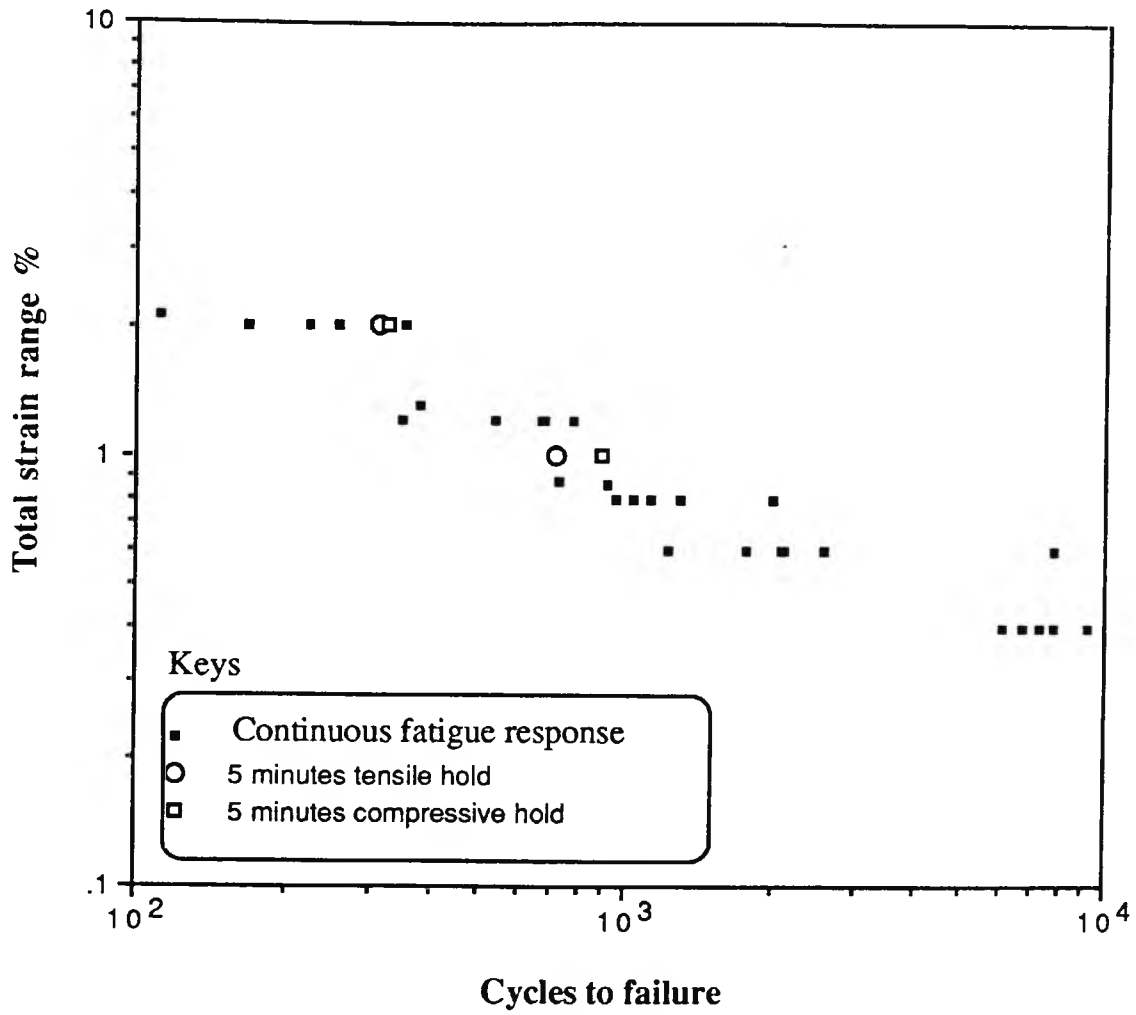
Fig. 5.6. Scatter plot with 5 minutes and with out hold of 2.25Cr-Mo steel (Batch 3).
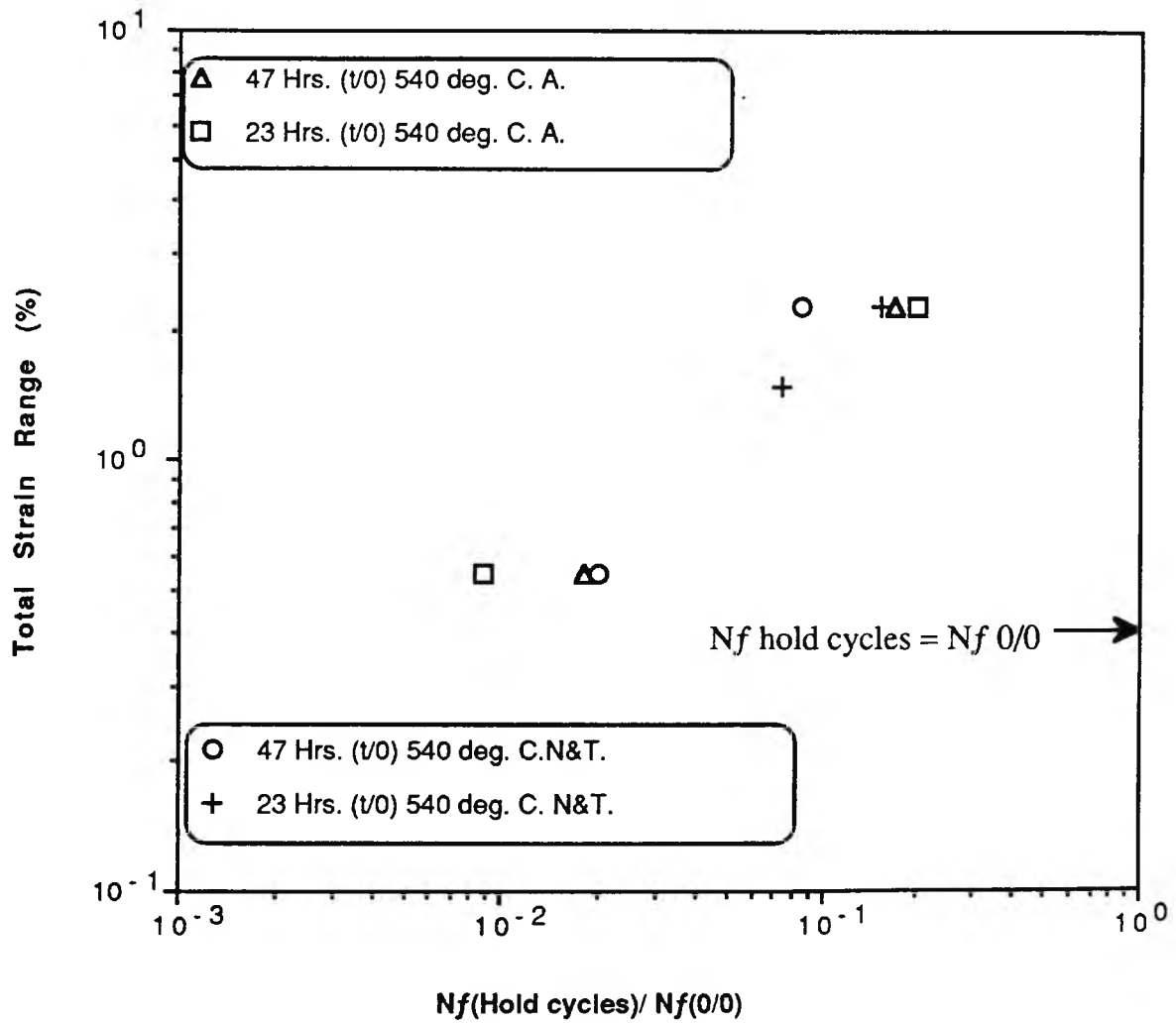
Fig. 5.7. Normalized life ratio of various dwell cycles of 2.25Cr-Mo steel.
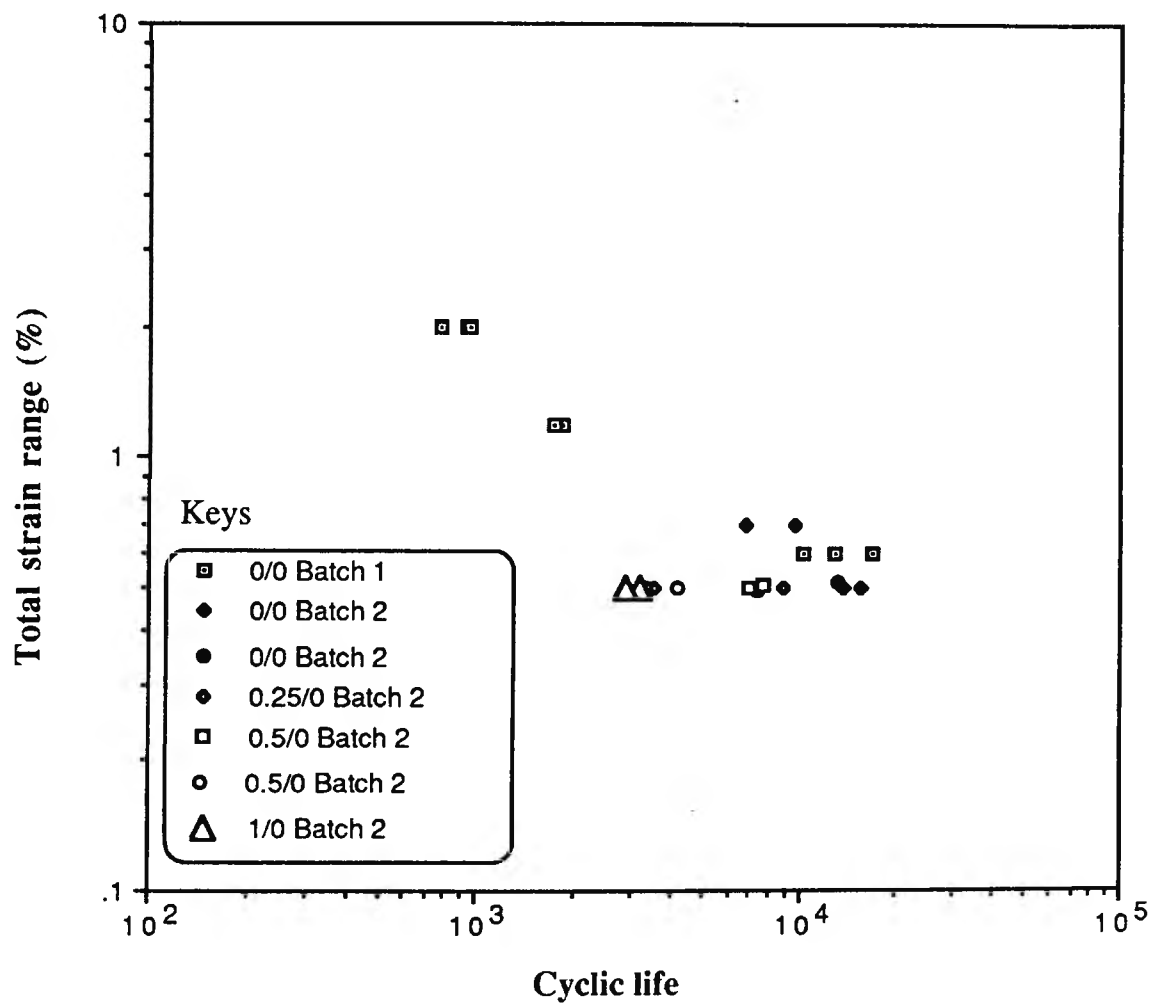
Fig. 5.8. Creep-fatigue behavior of 9Cr-Mo steel with different hold times.
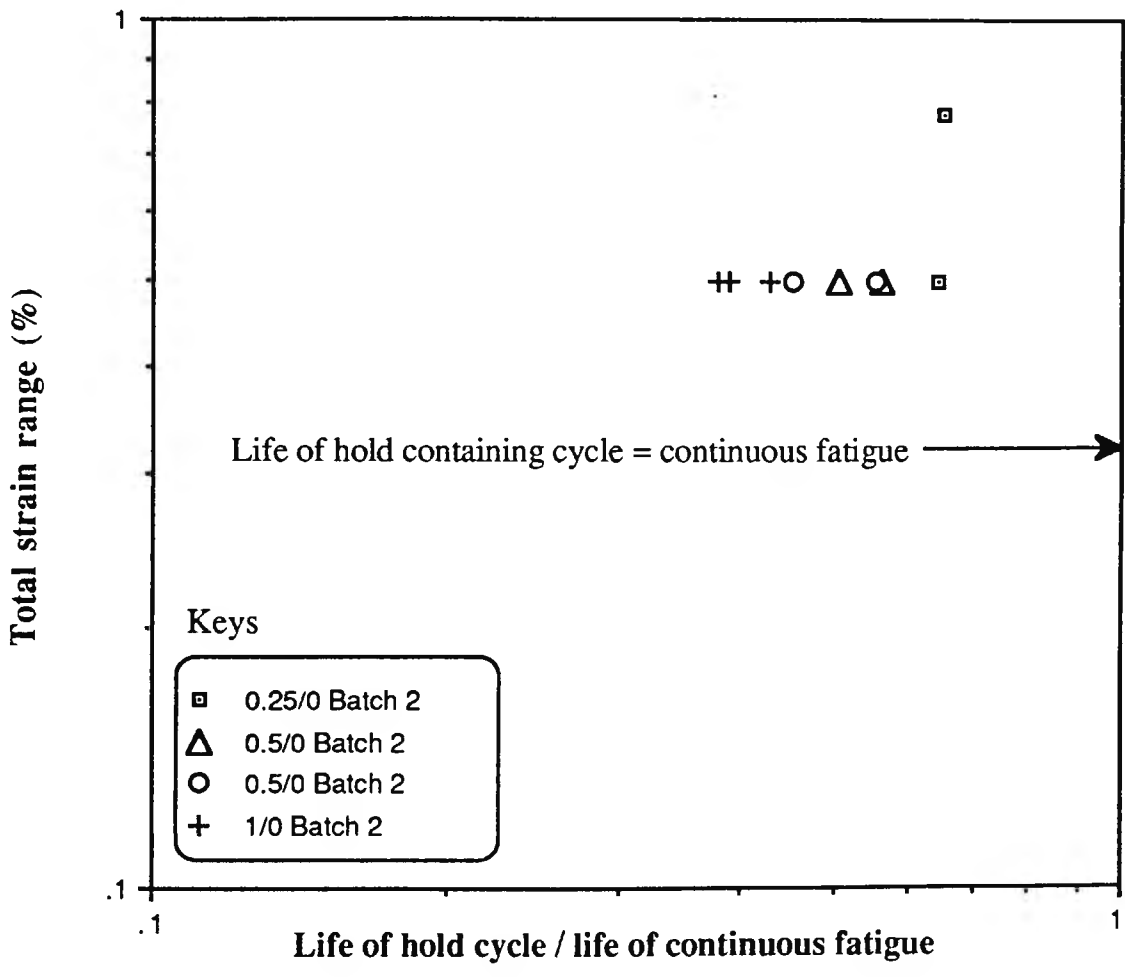
Fig. 5.9. Normalized cycle ratio of various dwell cycles of 9Cr-1Mo steel.

1 and 2" are tabulated in Table 5.2. Continuous fatigue behaviour were compared with tensile hold data for 23 and 47 hours where number of pure fatigue cycles ranging from n=1 to 22.5 were applied. Life lowered 311 times from continuous fatigue data for test combinations of a 47 hours hold at 485°C with (n=1) when the total strain range was 0.55%. At the same strain range and 540°C the life reduced by 170 times from continuous fatigue behaviour shown in Table 5.3. However, with 1.5% strain range at 540°C with 23 hour hold time and n=1, the life was 24 times lower than continuous fatigue performance shown in Table 5.4. When the number of fatigue cycles was increased from 1 to 22, the creep-fatigue life decreased with respect to n=1 data. A maximum beneficial effect was observed when number of pure fatigue cycles was from 1 to 5.5. In the case of n=22, a decreasing trend in life compared with n=1 was observed. The effect of combined cycles for Steel no. 2 are tabulated in Tables 5.2-5.4.

Table. 5.2. Effect of combined cycles on the performance of 1Cr-Mo-V steel.

Strain range %	Hold time hrs.	Temp. °C	N_f	no. of fatigue cycles (n)	Life Increase from 47 hr. and n=1	Life Debit from 0/0 data
0.55	0	483	8400	0	-	-
0.55	47	485	27	1		311
0.55	47	483	96	1.5	3.55	87.5
0.55	47	485	149	2	5.51	56.4
0.55	47	483	149	2.5	5.37	58
0.55	47	485	48	22	1.7	175

Table. 5.3. Effect of combined cycles on the performance of 1Cr-Mo-V steel.

Strain range %	Hold time hrs.	Temp. °C	N_f	no. of fatigue cycles (n)	Life Increase from 47 hr. and n=1	Life Debit from 0/0 data
0.55	0	538	5105	0	-	-
0.55	23	540	29	1		170
0.55	23	538	157	5	5.4	32.5
0.55	23	540	130	22	4.48	39.3

Table 5.4. Effect of combined cycles on the performance of 1Cr-Mo-V steel.

Strain range %	Hold time hrs.	Temp. °C	N_f	no. of fatigue cycles (n)	Life Increase from 47 hr. and n=1	Life Debit from 0/0 data
1.5	0	538	520	0	-	-
1.5	23	540	22	1		23.63
1.5	23	538	68	5.5	3.09	7.64
1.5	23	540	11	22	0.5	47.27

5.3.1.7.: Effect of Combined Cycle on Steel No. 4: The effects of combined cycles in the case of a 2.25Cr-Mo steel were quite similar to those observed for a 1Cr-Mo-V steel. Very limited data for the 2.25Cr-1Mo steel were available in the annealed condition that were analyzed collectively from "batch 1 & 2", and presented in Table 5.5.

Table 5.5. Effect of combined cycles on the performance of 2.25Cr-Mo steel.

Strain range %	Hold time hrs.	Temp. °C	N_f	no. of fatigue cycles (n)	Life Increase from 47 hr. and n=1	Life Debit from 0/0 data
1.5	0	538	930	0	-	-
1.5	23	540	141	1		6.5
1.5	23	540	75	5	-	12.4
1.5	23	538	92	5.5	1.2	10.1
1.5	23	540	29	22		31.8

5.3.2. Effect of Product Form

5.3.2.1.: Effect of Product Form on the Performance of Steel No. 2: The details of heat treatment, microstructure, grain size composition and product form were not investigated in the creep-fatigue behaviour of low alloy steels. Creep- fatigue performance of "batches 2, 3 and 4" (47-49) for the 1Cr-Mo-V steel were presented in Fig. 5.2. "Batch 3", was in hot rolled bar form, whereas the other batches were in normalized and tempered condition from a forging. "Batch 3" had a higher life compared to the forged conditions of other batches. The continuous fatigue behaviour at the same total strain range for "batch 2" was superior than "batch 4" when there was a temperature difference of 25°C. "Batch 4", at the same total strain range and tensile dwells, had inferior life than "batch 3". The test temperature for hot rolled bar, "batch 3", was 15°C lower than "batch 4". Test details such as strain range and hold times for "batch 3" were not published and several assumptions were made to determine them. Only few data points with CP sequence for "batch 3", involved tensile holds of 30 min. (65) were compared with "batch 4", where "batch 4", was found inferior to "batch 3". For a 30 minutes tensile dwell at 2% total strain range, life was at least 150% in the case of "batch 3" at 550°C, than "batch 4" at 565°C. It may not be possible to

address if a temperature increase of 15°C reduced creep-fatigue life for "batch 4", or material condition for "batch 3" enhanced creep-fatigue performance. A conclusion may be drawn from Fig. 5.2, that though there were differences in the testing parameters and material conditions, "batch 3" had higher lives in a ferritic form at the same strain range and tensile dwells, compared with the tempered bainitic form of "batch 4".

5.3.2.2.: Effect of Product form on the Performance of Steel No. 4: "Batches 1 and 2" (47-48) were characterized with identical material conditions, heat treatments, compositions and the test parameters. At same total strain range and temperature, material in the annealed condition had longer lives than the normalized and tempered (N&T) condition. At 0.55% total strain range for quenched and tempered (Q&T) tested at 485°C the creep-fatigue behaviour was found superior than N&T and annealed conditions tested at 55°C higher temperatures. A cross over in the behaviour was observed at a strain range of nearly 1% for both N&T and annealed conditions, below which Q&T was found superior as shown in Fig. 5.10. However, a temperature difference of 55°C was quite considerable and no conclusion should be drawn from such trends.

5.3.3. Effects of composition

5.3.3.1. Effects of composition on the performance of low alloy steels: Low alloy steels are investigated in the order of percentage chromium content from 0.5 to 9 they are 0.5Cr-Mo-V, 1Cr-Mo-V, 1.25Cr-Mo, 2.25Cr-Mo, 2.25Cr-Mo-V and 9Cr-1Mo steels. Creep-fatigue behaviour of these alloys with or without hold periods, are shown in Fig. 5.11. Limited data points are analyzed in Fig. 5.11 which show the scatter in the creep-fatigue data. In general, the creep-fatigue performance of materials improved with the increase in chromium content. Isolating several factors such as temperature differences, material conditions, strain rates and microstructures, properties of 1Cr-Mo-V steel was at the lower extreme. Better properties were found with the increase in chromium to 9%.
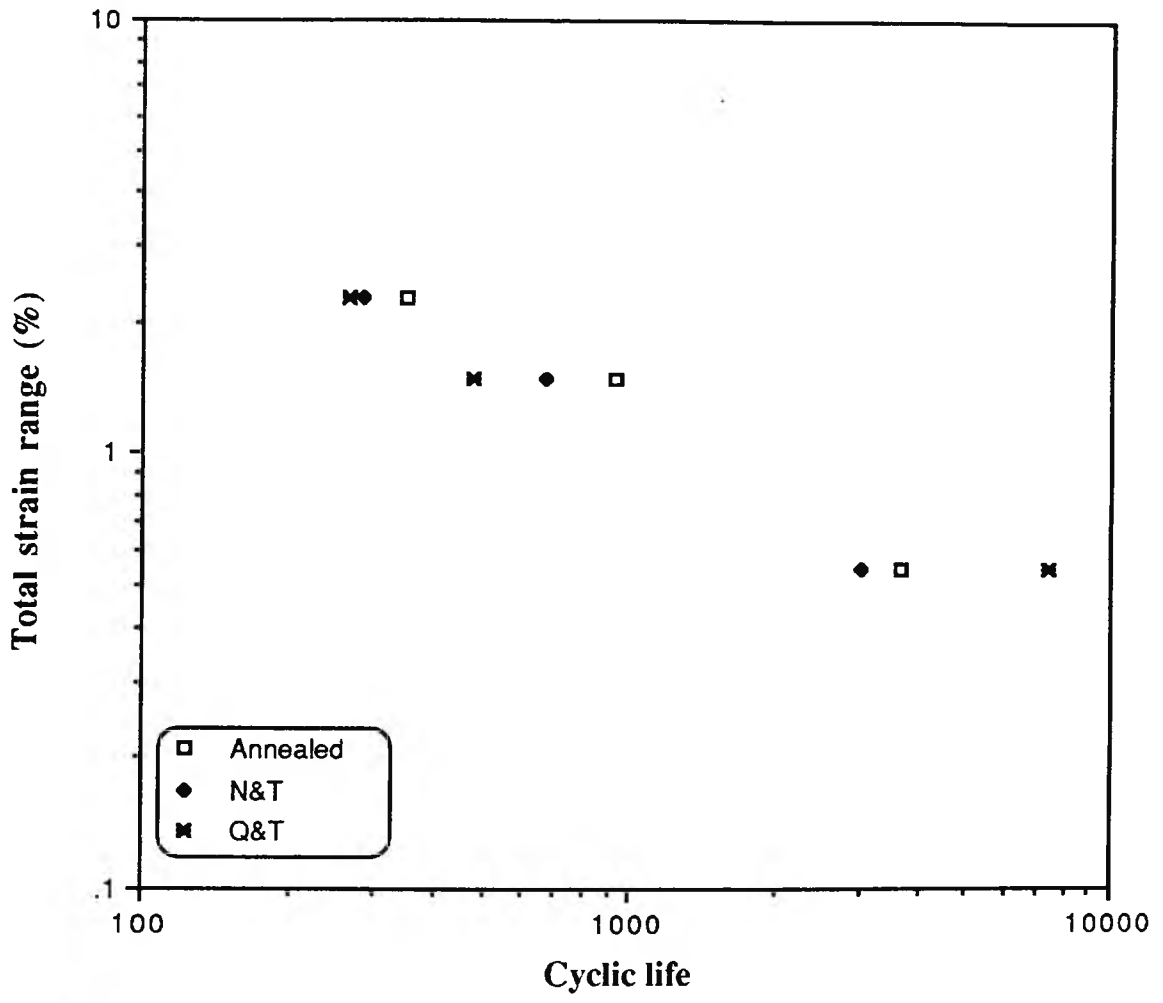
Fig. 5.10. Effect of heat treatment on the creep-fatigue performance of 2.25Cr-Mo steel.
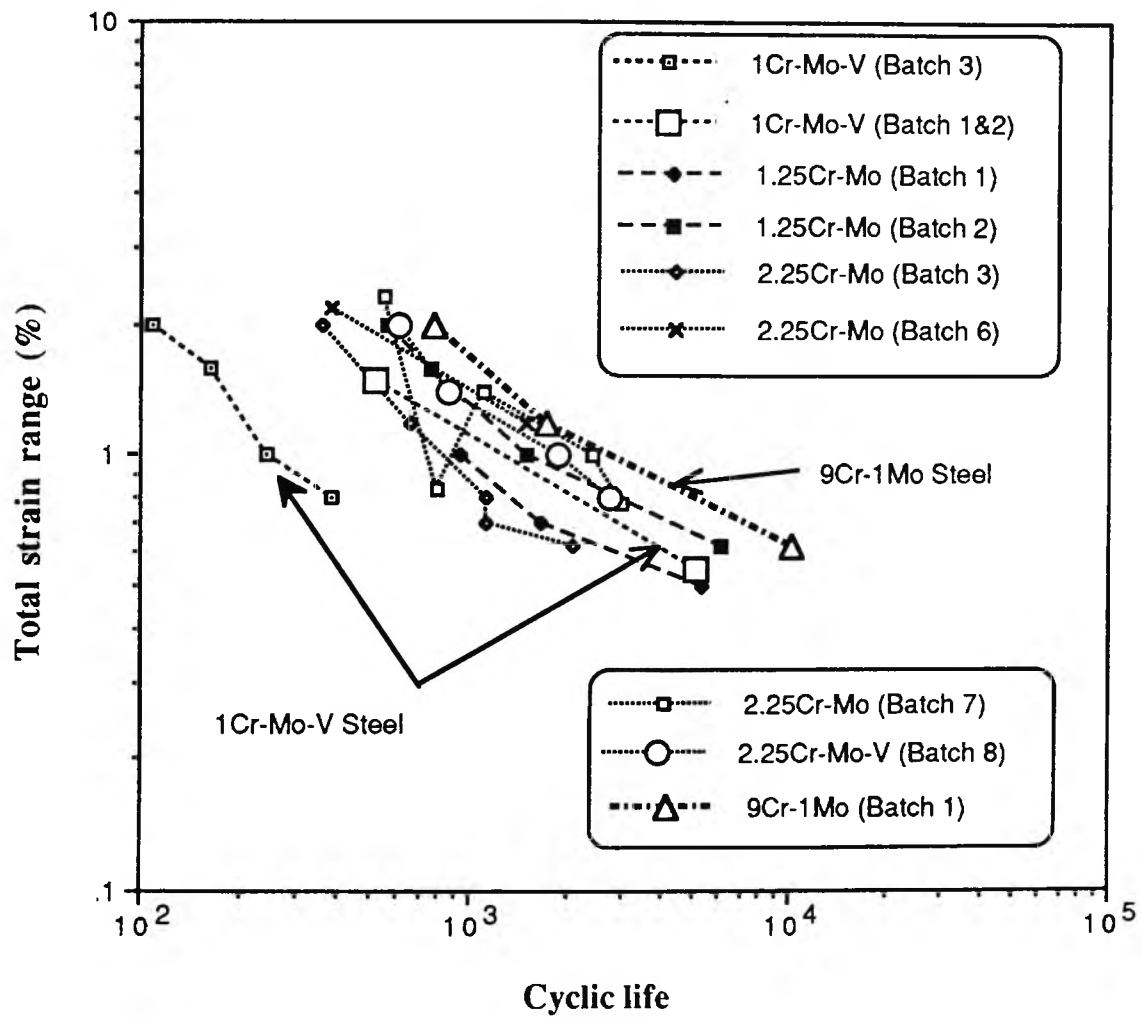
Fig. 5.11. Effect of composition on the creep-fatigue behavior of low alloy steels.

5.3.3.2.: Effect of vanadium on creep-fatigue behaviour of Steel No. 4:

"Batches 7 and 8" (57) were investigated to determine the effect of vanadium on the HTLCF properties of 2.25Cr-Mo steel as shown in Fig. 5.12. With the inclusion of vanadium in 2.25Cr-Mo steel, the HTLCF life deteriorated. This observation was on the basis of only two data sets, (Batch no. 7 and 8) with limited creep-fatigue tests. Therefore, additional data (several batches) will be needed to validate such a hypothesis.

Nevertheless, the inferior life with vanadium addition was hypothesized from monotonic properties of both the materials. The yield and the tensile strength of the alloy improved with the increase in the total element addition in 2.25Cr-Mo-V steel. With the increase in element addition, modulus (E) and proof strength increased. As strength increased the ductility and % elongation decreased as shown in Table 5.6. Under total strain control testing, plastic strain reduces with the increase in strength achieved by element additions. The saturated stresses at half-life in the case of 2.25Cr-Mo-V steel were 50 to 75 MPa higher than at the similar strain ranges for 2.25Cr-Mo steel. As a result, mean stresses in the 2.25Cr-Mo-V steel were higher than the 2.25Cr-Mo steel. Such behaviour was also observed for a titanium alloy IMI 829 and a superalloy MAR M 002 under HTLCF, where the plastic strain per cycle reduced and enhanced retained mean stresses (26, 66). The same was observed also in 2.25Cr-Mo-V steel, when increased strength resulted in lower plasticity. Retained mean stresses caused life shortening effects, however, compared with the 2.25Cr-Mo steel, which has more plastic strains and less mean stresses in Table 6, 2.25Cr-Mo-V steel performed inferior under HTLCF.

Table. 5.6. Monotonic properties of the 2.25Cr-Mo steel (57).

Alloy	Temperature	YS MPA	UTS MPa	% Elongation
2.25Cr-Mo	RT	470	597	20
-do-	593	305	334	34.5
2.25Cr-Mo-V	RT	620	720	18
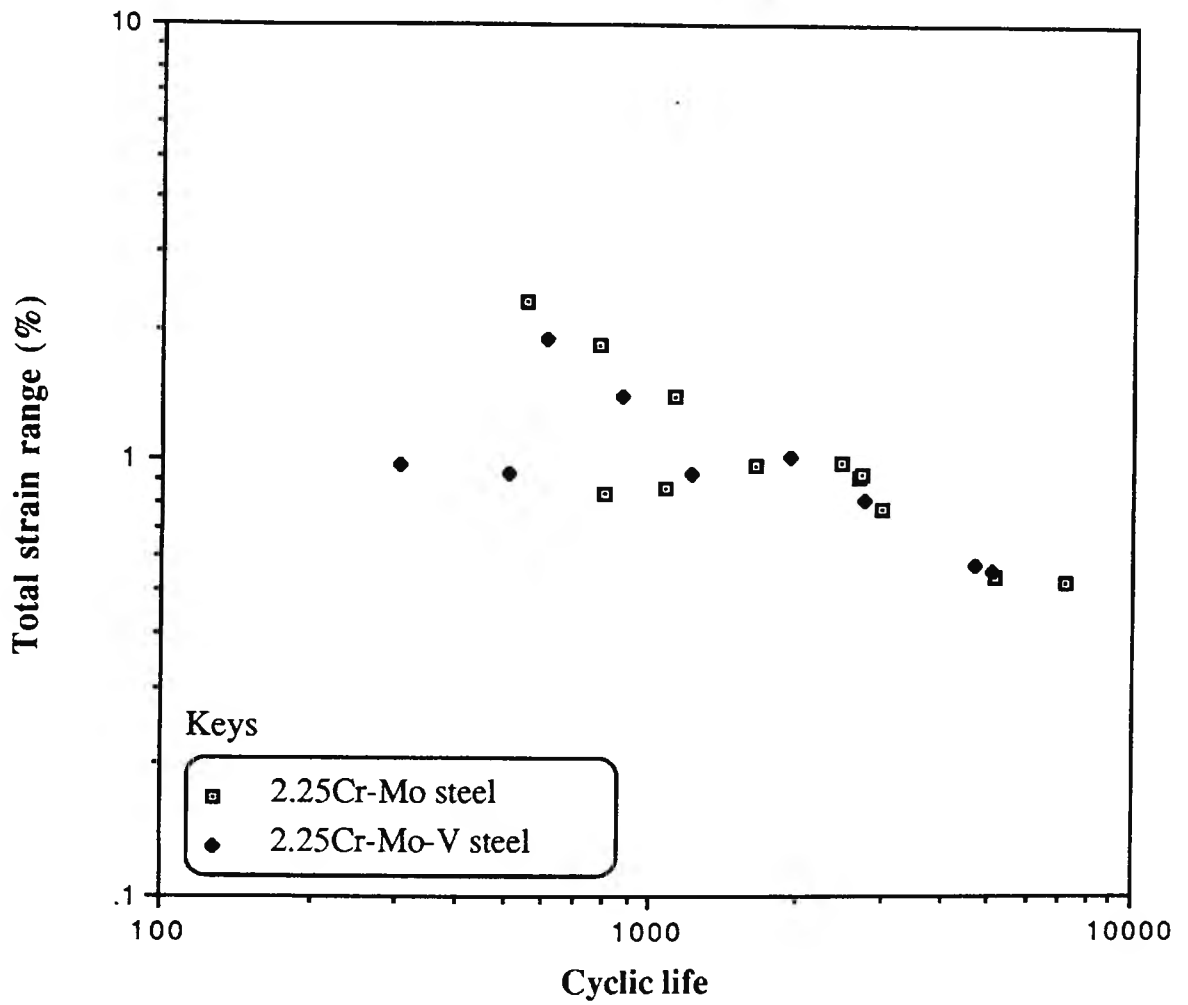
Fig. 5.12. Effect of vanadium on the creep-fatigue behavior of 2.25Cr-Mo steel.

-do	593	443	456	26.5

5.4. SUMMARY

The following trends were observed:

(1)   isolating variations in the materials arising from microstructures, N&T heat treatments and test parameters such as temperature and strain rate, the creep-fatigue response of low alloy steels improved with the increase in chromium content,

(2)   dwell sensitivity of low alloy steels with hold times in either tension or compression and associated life debits were different for different low alloy steels,

(3)   vanadium additions to a standard 2.25Cr-Mo alloy, caused deterioration to the high temperature creep-fatigue response, and

(4)   there was a limiting value in the test temperature, direction of hold time and the strain rate above which only the life debit occurred for 2.25Cr-Mo steel.

6. CREEP - FATIGUE LIFE PREDICTION : METHODS AND TRENDS

Creep-fatigue data for low alloy steels were compiled and presented in Chapter 4. Using these data, trends in the creep-fatigue behaviour of low alloy steels were identified in Chapter 5. The information presented in Chapters 4 and 5 are used, in general, to develop "phenomenological" life prediction methods. A review of existing life prediction methods within the phenomenological framework is provided in Chapter 6. As every life prediction method requires different types of creep-fatigue data and material parameters, knowledge of creep-fatigue test requirements for different methods is very important to the design of experimental programs. Details of test requirements and material parameters are not critically examined for different life prediction methods in the open literature. Capability of life prediction methods assessed by various workers for different batches of six low alloy steels were aggregated to identify trends in the life prediction of various methods in this Chapter.

6.1. INTRODUCTION

Development of a reliable life prediction method for creep-fatigue interactions is very important to the conduct of structural analyses and the prediction of lifetimes of engineering components operating at high temperature. Development of life prediction approach requires creep-fatigue data bank. Much of creep-fatigue data is classified and not available in open literature. There also is a lack of publications describing the analysis of a life prediction method with creep-fatigue data. Presently, there are only two publications (15-16) that describe the analysis of life prediction for low alloy steels. Two low alloy steels of the type 1Cr-Mo-V and 2.25Cr-Mo were assessed in those publications to compare the prediction capability of methods with each other. Hence publications (15-16) play a key role in discussion of the applicability of life prediction methods.

Two reviews (67, 68) were published on the methods of life prediction and analysis conducted for low alloy and stainless steels, however, neither examined the capabilities of

methods for life prediction with an international data bank. Hence, to overcome this deficiency, prediction capabilities of various methods (5-14, 69-91) for different "batches" of the same and six low alloy steels are examined in this Chapter. Comparison of prediction capability for different methods under a range of conditions such as test temperature, hold time and material conditions will be useful in applying methods of life prediction or identifying where a method will be more suitable.

6.2. REVIEW OF LIFE PREDICTION METHODS

6.2.1. Linear Damage Summation

Conceptually this method was similar to the linear damage summation technique proposed by Miner (69) for fatigue analysis. Life prediction under creep-fatigue was proposed by Robinson (70) and modified by Taira (71). Damage under creep-fatigue utilizes linear summation of time dependent creep fraction and time independent fatigue fraction separately. Damage culminates to final failure when the linear summation of fraction creep and fraction fatigue becomes unity. The fatigue or cycle fraction, is a ratio of number of cycles (n) at a stress or strain level with cycles to failure (Nf) at the same loading conditions, whereas, the creep or time fraction is a ratio of time of hold (t) with time to rupture (t$_f$), at same loading conditions. Equation 6.1 shows the linear damage summation:

$$\Sigma\, n\,/\,N_f + \Sigma\, t\,/t_f = D = 1 \text{ at failure} \qquad (6.1)$$

where, n / N$_f$ and t / t$_f$ are cycle and time fractions respectively. Linear damage summation method was accepted by the American Society of Mechanical Engineers as a code in the design of pressure vessel and piping under Code Case N 47 1597 (5). Deficiencies were observed in the life prediction of balanced dwell cycles since this method assumed same the time fractions for tension and compression dwells. Hold times at very low strain ranges in peak tensile direction produced a damage parameter (D) much less than unity. Interaction effects among creep and fatigue and others were unaccounted, which, in the case of 2.25Cr-1Mo, reduced the creep-fatigue life (35) when hold was applied in compression direction.

6.2.2. Frequency Modified and Frequency Separation Approach

To account for the environmental and other time dependent effects, Coffin (72-74) introduced time effects in the Coffin-Manson relationship by a frequency term . Thus the Coffin-Manson equation $\{\Delta\varepsilon_p = C_i(N_f)^{-\alpha}\}$ becomes

$$\Delta\varepsilon_p = C_i \, (N_f \cdot \nu^{k-1})^{-\alpha} \tag{6.2}$$

where $\Delta\varepsilon_p$ is plastic strain range, N_f is cyclic life, ν is frequency, and C_i, k and α are material parameters. Life for complex creep-fatigue cycles were predicted using material parameters determined from continuous fatigue data and other test types. Thus, with the frequency term in equation 6.2, and transferring strains in terms of stress by the Basquin relation, several expressions for life prediction could be obtained.

for hold time cycles:

For test types the required Basquin stress-strain equation was:

$$A' \, (N_f)^{-\beta'} \nu^{K'} = \Delta\sigma \tag{6.3}$$

where, K', β' and A' are material parameters that can be obtained by conducting regression analysis of the stress range and cyclic life data on log-log scale. The number of cycles to failure (N_f) is given by:

$$N_f = (A' / \Delta\sigma_{sf})^{1/\beta'} \, [\nu_{t/2}]^{K'/\beta'} \tag{6.4}$$

where $\Delta\sigma_{sf}$ is stress range with unequal ramp rates and ν_t is the tensile frequency. The frequency is separated in tension and compression in equation 6.4 and the predicted life was good for simplified cycles. Further modifications were made to enable the applicability of this method for unequal ramp rates and for hold time cycles.

Life prediction for unequal ramp rate cycles:

The frequency modified approach was found to be not effective for prediction of creep-fatigue life when there were unequal ramp rates in which strain rates in tension and compression (9) were different. It was assumed that the damage occurred only during the tensile part of the cycle in a hysteresis loop. However, such an assumption is inappropriate

for dwell sensitive materials in which damage caused by a hold cycle was more in one direction compared to the same hold applied in other. The equation for stress range ($\Delta\sigma_f$) for unequal ramp rate cycles was partitioned in terms of frequency in tension or compression directions in frequency separation approach, as follows:

$$\Delta\sigma_f = 0.5 \ A'' \ \Delta\varepsilon_p^{\ n'} \ [(v_t \ /2)^{K_1} + (v_c/2)^{K_1} \ ] \tag{6.5}$$

where, A'', n' and K_1 were coefficients of the Basquin relation obtained from unequal ramp rates data:

$$\Delta\sigma = A'' \Delta\varepsilon_p^{\ n'} v^{K_1} \tag{6.6}$$

The use of unequal ramp rates as equivalent to hold times is quite questionable. Therefore, a further modification was made by Coffin in terms of frequency separation approach.

Frequency separation approach:

Frequency separation approach requires coefficients from balanced loops with equal tension and compression holds are accounted for by separating the tensile and compressive strain rates. The material parameters in the above model were determined from continuously cycled tests and also from some hold time tests that may be applied to any complex creep-fatigue cycle for life prediction in equation 6.7.

$$N_f = [\ F/\Delta\varepsilon_p]^{\ 1/\beta'} \ [v_t \ / \ 2]^{\ 1-K} \ [v_c/v_t]^d \tag{6.7}$$

In the equation 6.7 v, β' and K are material parameters obtained from balanced loop data and d was obtained from unbalanced hold data to predict life for hold time cycles.

Frequency modified and separation models were criticized for under-predicting the life. The damage produced by a tensile hold was considered to be the same irrespective of the location in a cycle where a hold was applied. Tensile mean stresses were not accounted that a compressive hold cycle produced. With increasing peak tensile hold this method predicted shorter life, that may not be the case as the opposite was found in the case of SS 304 (9), 2.25Cr-Mo (35) and superalloys (34), where a tensile hold was less damaging compared to compressive holds.

6.2.3. Strain Range Partitioning Technique

Manson, Halford and Hirschberg (7) developed a technique known as strain range partitioning (SRP) in which plastic fatigue (P) and inelastic creep (C) strains were separated in a hysteresis loop. Representation of strain components in two directions resulted in combined PP, PC, CP or CC loops so that four base-line relationships were involved in describing combinations of plastic and inelastic strains with respect to cyclic life. Strain components $\Delta\varepsilon_{pp}$, $\Delta\varepsilon_{pc}$, $\Delta\varepsilon_{cc}$ and $\Delta\varepsilon_{cp}$ represented the combination of strains where the subscripts denoted p for plasticity and c for creep and the first subscript refers to be in tension direction and the second refers to the compression direction.

Representation of life was made in terms of the Coffin-Manson equation

$$N_{ij}=A_{ij}\Delta\varepsilon_{ij}^{\theta jk} \tag{6.8}$$

where N_{ij}, A_{ij} and $\Delta\varepsilon_{ij}$ is cyclic life, a material constant and the strain range respectively, θ is slope and ij refers to plasticity (p) or creep (c) combinations.

Damage fractions, F_{ij} were added by an interacting damage rule.

$$F_{ij} = F_{pp} / N_{pp} + F_{pc}/N_{pc} + F_{cc}/N_{cc} + F_{cp}/N_{cp}$$

i.e., $F_{ij}=\Delta\varepsilon_{jk}/\Delta\varepsilon_{in}$ \hfill (6.9)

where $\Delta\varepsilon_{in;}$ was the inelastic strain range

$$\Delta\varepsilon_{in} = \Delta\varepsilon_{pp}+\Delta\varepsilon_{pc}+\Delta\varepsilon_{cc}+\Delta\varepsilon_{cp} \tag{6.10}$$

The technique, SRP was criticized for the difficulty in partitioning the loop and the omission of environmental terms in the damage criterion. Bounds on life relationships generated with four baseline strain combinations such as PP, PC, CP and CC, where PP, PC, CP and CC response determined a particular combination was the the most damaging. Behaviour of four baseline strain-life relations when observed as parallel lines one of them was considered representing service condition in the design. For gas turbine blade materials such as IN 100 and MAR M 200, these combinations coincided (76) and helped as a design criterion. However, for other materials such as stainless steels and some low alloy steel, for example, 2.25Cr-Mo and 9Cr-1Mo steels, these lines intersected (33) and posed difficulties in selecting

a particular line appropriate to the service condition. This model was further modified as a total strain version of SRP (77) to account for mean stresses, low strain range and long hold time situations.

6.2.4. Damage Rate Approach

Majumdar and Maiya (9, 78-79) developed damage rate approach in which it was assumed that, under high temperature fatigue, the rate of fatigue or creep damage accumulation depended upon plastic strain rate. Damage was thought to be micro crack growth, which occurred differently under tension and compression from an initial length (a_0) to a final length (a_f). Scaling factors in tension (T) and compression (C) were introduced, as follows:

$$da/dN = a [T] [\varepsilon_p]^m [\dot{\varepsilon}_p]^k \quad \text{(in the presence of tensile stress)}$$

$$da/dN = a[C] [\varepsilon_p]^m [\dot{\varepsilon}_p]^k \quad \text{(in the presence of compressive stress)} \qquad (6.11)$$

where m and k are material parameters which remain constant over a range of plastic strain rate $\dot{\varepsilon}_p$ and plastic strain range $\Delta\varepsilon_p$. Scaling factors T and C were introduced to account for the differences in crack growth rate (da/dN) that occurred under tension or compression holds. Crack growth by fatigue and cavity growth by creep were dealt with independently. The cavity growth equation was expressed as follows:

$$1/c \, da/dt = G [\varepsilon_p]^m [\dot{\varepsilon}_p]^{k'} \qquad (6.12)$$

where c is the cavity size, t the test duration and G is a material constant.

Material parameters of the equations 6.11-6.12 are determined from completely reversed cycle data at different strain rates. However, prediction of longer hold time data required hold time tests to determine the material parameters of the equation 6.11-6.12.

6.2.5. Damage Function Method

The change in internal energy per unit volume of material in a time interval from 0 to a particular time t or (0, t) was assumed to be a measure of damage, as follows:

$$U = \int \alpha_{ij} \, \sigma_{ij} \, \varepsilon_{ij} \, dt - \int h \, dt \qquad (6.13)$$

where α_{ij} and h_{ij} are shape factors where the former corrects a distorted hysteresis loop, whereas latter term accounts for the heat generated in plastic deformation respectively. Morrow (80) proposed that hysteretic energy per cycle be considered as a measure of fatigue damage in equation 6.14.

$$C = \Delta W \, N_f \, \nu \qquad (6.14)$$

where, ΔW is an energy term, C is a material constant and ν the frequency.

Damage function model was developed within the premise that the energy of a hysteresis loop contributes to damage. Only tensile part of a hysteresis loop was assumed to contribute to damage (10) since the crack tip remained open during tensile half loading. There was also a limiting value of tensile energy above which damage accumulated and below that limiting value closure occurred. For a strain controlled, low cycle fatigue test, since identification of closure limit line was difficult, it was proposed (10) to consider the total tensile energy as damaging.

Ostergren (10) introduced a damage function, $\alpha \, \sigma_T \, \Delta \, \varepsilon_p$ where the product of stress and strain or the energy was used in frequency modified equations as follows:

$$C = \alpha \, \sigma_T \, \Delta \varepsilon_p \, N_f^{\beta} \, \nu^{\beta(K-1)} \qquad (6.15)$$

where C, β, and k are material parameters, σ_T the maximum tensile stress and α is a shape factor. Since equation 6.15 considered the energy term which was difficult to define, life predicted by this method was also depended upon type of creep-fatigue cycle.

6.2.6. Damage Parameter Approach

Historically, Kachanov (81) described creep rupture behaviour in terms of a damage parameter (ω), which was related to the cavitated area fraction of grain boundaries. The damage parameter was unity at failure and zero for the virgin or undamaged condition. To describe the damage parameter, the concept of material continuity (ψ) was introduced which was unity when there was no damage for the virgin condition and zero at failure. The change of continuity was expressed by Kachanov as:

$$d\psi/dt = -A \, (\sigma/\omega)^n \qquad (6.16)$$

where (σ/ω) is an effective stress term and σ is the nominal stress. Equation 6.16 can be integrated between extremes of the virgin and failure conditions. The damage under creep-fatigue interactions was described by the rate of damage accumulation, a function of effective stress:

$$d\omega/dt = f[\, \sigma / (1-\omega)] \qquad (6.17)$$

This concept has been explored further in the literature (82-83). Chrzanowski (8) proposed damage parameter approach based upon the above damage concepts of equation 6.17 assuming that:

(1)   damage comprised time dependent and time independent parts,

(2)   damage by fatigue increased as stress increased, whereas in creep damage increased by both positive and negative stress rates, and

(3)   rates of fatigue and creep damage were zero under negative stresses in compression directions.

Damage was considered to occur only under positive stress increments and the damage law was expressed by a non linear equation which describes the rate of damage accumulation, as a function of effective stress:

$$d\omega/dt = [\, Co \; \{\sigma/(1-\omega)\}^{Vo} \, d\sigma/dt \; H \, (d\sigma) + C\{\sigma/ (1-\omega)^{\,v}\}] \, H \, (\sigma) \qquad (6.18)$$

The first and second terms represent fatigue and creep damage respectively, and Co, C, v_0 and v are material parameters and H is the heaviside function of tensile stress. Life prediction under creep-fatigue interactions by equation 6.18 can be performed by integrating a known stress-time history to predict life.

6.2.7. Assessment Procedure R 5

Code R 5 was developed by the Nuclear Electric Inc., as "An assessment procedure for the high temperature response of structures" (11). The cyclic endurance of a component subjected to an arbitrary cycle in which a dwell of any length may be present, can be

described by "assessment procedure R 5". It was assumed that the endurance can be expressed in terms of fatigue and creep components of damage which can be linearly summed to produce a damage term representative of the service cycle. Fatigue damage was assumed to be proportional to the inverse of the continuous fatigue endurance (N_o) corresponding to the initiation of a crack of depth (a_o). The fatigue damage was determined for a total strain range calculated as the difference between the extreme strain values in the hysteresis loops. If N_l is the number of cycles to failure in a continuously cycled laboratory specimen, and, at the time of failure the corresponding crack depth is a_l, then the required number of cycles (N_o), to initiate and grow a crack to depth a_o, can be expressed in terms of the following:

$$N_o = MN_l + (1-M)N_i \qquad (6.19)$$

where N_i, is the number of cycles undergone in initiating a defect of depth $a_i = 20 \ \mu m$, irrespective of the section thickness, and given by:

$$N_i = \exp(1.306 \ln N_l - 3.308) \qquad (6.20)$$

This expression is valid for $50,000 > N_l < 15$ cycles. The creep damage per cycle, D_c, was evaluated using the ductility exhaustion method by performing an integral over the dwell time t_h.

$$D_c = \int_0^{t_h} \dot{\varepsilon} / \varepsilon_f(\dot{\varepsilon}) \ dt \qquad (6.21)$$

where $\dot{\varepsilon}$ is the instantaneous strain rate during the dwell and $\varepsilon_f(\dot{\varepsilon})$ is corresponding creep ductility. The total damage per cycle was simply expressed as:

$$D_t = 1/N_o + D_c \qquad (6.22)$$

The creep-fatigue endurance N_o* was given by:

$$N_o* = 1/D_t \qquad (6.23)$$

Equation 6.20 becomes simplified if the ductility ε_f was pessimistically assumed to be independent of $\dot{\varepsilon}$ and equal to the lower shelf ductility ε_l. The equation then became:

$$D_c = Z\Delta\sigma' / E \varepsilon_l \qquad (6.24)$$

where $\Delta\sigma'$ was the stress relaxation in time t_h and E was young's modulus.

Similarly if the dwell occurred in the compressive part of the cycle then equation 6.24 simplifies to:

$$D_c = Z\Delta\sigma' / E\varepsilon_u \tag{6.25}$$

The arbitrary value of Z was estimated by:

calculating the 0/0 endurance (N_o) from N_l (equation 6.19), and the

endurance N_o^*, including the effects of hold times, using

$$N_o^* = (1/N_o + Z D_c)^{-1} \tag{6.26}$$

where D_c calculated from $Z = 1$ in equation 6. 25 and with higher values of Z, the life prediction was found to be too pessimistic.

"Assessment procedure R-5" was assessed with very limited creep-fatigue data in (11), using tensile hold times from 3 min. to 16 hours, and, sparingly with compressive holds.

6.3. EMPIRICAL METHODS

Empirical methods were pursued as an alternate to the phenomenological life prediction models due mainly to the limitations in the use of phenomenological methods. One of these models is the Diercks equation which has been successfully applied in the creep-fatigue life prediction for low alloy steels.

6.3.1. Diercks Equation

Diercks and Raskey (12) compiled a bank of creep-fatigue data for stainless steel of type SS 304 and obtained a multivariate best fit equation for creep-fatigue life extrapolation in regression functions of various test parameters as follows:

$$(\log N_f)^{-1/2} = 1.20551064 + 0.66002143*S + 0.18040042\ S*S - 0.00814329*S^4 +$$

$$0.00025308\ R*S^4 + 0.00021832TS^4 - 0.00054660\ RT^2 - 0.005567RH^2 -$$

$$0.00293919HR^2 + 0.0119714H*T - 0.00051639H^2T^2 \tag{6.27}$$

with strain range parameter $S = (\Delta\varepsilon_t / 100)$,

strain rate parameter $R = (\log \dot\varepsilon)$,

temperature parameter $T = (T_c / 100)$, and,

hold time parameter $H = \log(1 + t_h)$, in a multivariate form,

where T_c, was the test temperature and t_h the time of hold. Equation 6.27 was used to extrapolate the creep-fatigue life for SS 304 and was recommended by ASME Code 1749 (5) to design fatigue diagrams (13, 85) in terms of strain and life.

Kitagawa et al (13) extended equation 6.27 for creep-fatigue life prediction for the 2.25Cr-1Mo and the 9Cr-1Mo low alloy steels and assessed with creep-fatigue data. However, their proposed modification required:

1) a cycle ratio (α), which was a ratio of fatigue life for SS 304 to that for a low alloy steel, shown schematically in Fig. 6.1 under same strain range, temperature (°C) and strain rate,

2) a temperature parameter (T) that compares iso-stress creep rupture life of a low alloy steel with the life for SS 304 in Fig. 6.2, where iso-stress creep rupture life was defined as the temperature at which both SS 304 and the low alloy steel had the same creep rupture life under the same stress, and

3) a temperature correction $(T_t + T_a)/100$, where T_t was the test temperature for the low alloy steel and T_a was the temperature difference in iso-stress creep rupture lives in °C.

Kitagawa et al (13), successfully extended Diercks equation with the above modifications for creep-fatigue life prediction of the 2.25Cr -1Mo and the 9Cr-1Mo steels where the range of Diercks equation was from pure fatigue to creep.

6.4. REQUIREMENTS OF PREDICTION METHODS

Requirement of various life prediction methods related to number of tests, type of tests, material and test parameters is not published which is very important to know how each method is determined. Since the description of test variables, tension/compression stresses, hysteretic behaviour in X-Y plots (σ – ε and with time) and loop stabilization histories were not quantitatively known, application of methods of life prediction to the compiled data was not possible. On the other hand, application of the phenomenological methods of life

Cycle ratio = N*f* (SS 304) / N*f* (low alloy steel) at the same conditions (strain range)

Strain Range %

SS 304

Low alloy
steel

Cyclic life
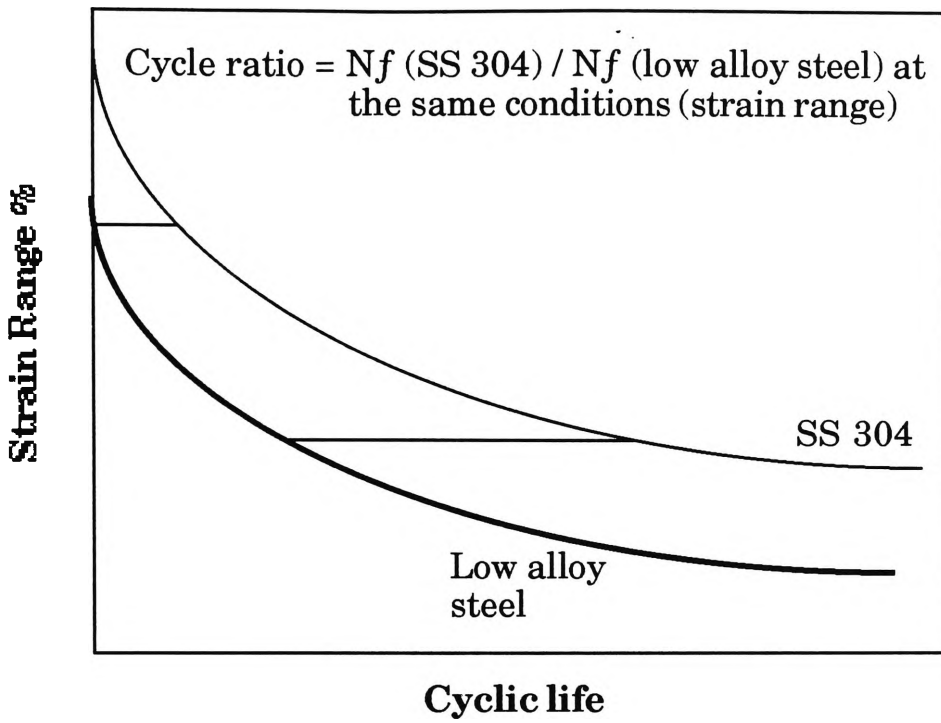
Fig. 6.1. Shematic determination of cycle ratio.

Rupture time

100,000
hours

SS 304

low alloy steel

100 hours

iso-stress lines

Inverse temperature (absolute scale)
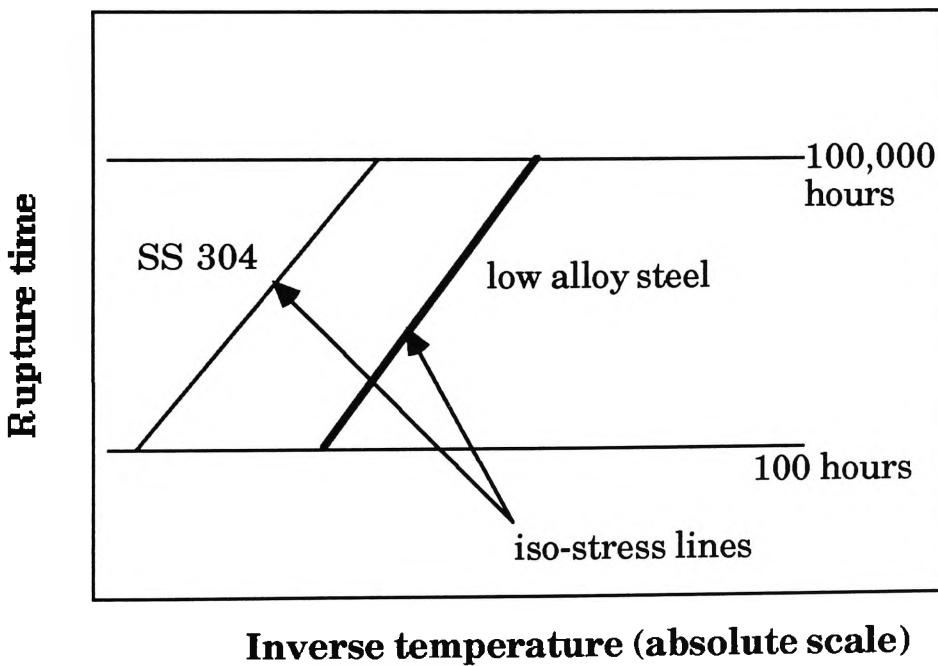
Fig. 6.2. Schematic determination of temperature correction factor.

prediction to creep-fatigue data requires a large number of test information, and material parameters such as:

(a)   creep rupture properties at the same test temperature employed in creep-fatigue, the stress and time to rupture data provided two material parameters in each linear behaviour as the trends were bilinear above or below a stress,

(b)   stress relaxation with respect to hold time,

(c)   total strain and life relationships provided four parameters representing elastic and plastic behaviours,

(d)   stress - strain relationships that provided two parameters,

(e)   tests with balanced and unbalanced hold times and unequal ramp rates,

(f)   apart from these, several parameters that may be needed to apply a method e.g., SRP needs 8 such parameters, inelastic strain with life components, and

(g)   frequency - life data.

In the laboratory, creep-fatigue tests are conducted by controlling the total strain. Under hold time waveform, when a hold is applied at constant strain, stress changes with respect to time, where the stress is much higher at the begin of a cycle than at the end due to stress relaxation. The log-log relationship between creep rupture time and applied stress is often found to be a bilinear. Ellison and Walton (86), compiled such data for 1Cr-Mo-V tested at 565°C. They observed a bilinear trend below or above 280 MPa. The ratio of two slopes and intercepts (stress value at unit rupture time) was 2.15 and 2×10^{20} respectively, between stresses above and below 280 MPa.. A slight difference in stress resulted in a large variation in the extrapolated rupture life. Also, creep rupture properties changed considerably with slight increase in temperature. The iso-stress (15 Kgf/mm^2) creep rupture properties in the case of low alloy steels, varied from 50 to 10^5 hours in a temperature range of 485 to 590°C. Hence applicability of life prediction methods cannot be assessed with the material parameters determined from one set of data.

Table 6.1 summarizes requirements of individual life prediction methods. Methods of life prediction, conditions under which they apply.

Table 6.1. Constants of the phenomenological approaches.

Method of life prediction	Life prediction equation	No. of constants (n)	Details of the tests
Linear life fraction	$1 = \sum n / Nf + \sum t / T_r$	- strain -life data (4) - creep-rupture (2 to 4)	0/0 tests (ε_t-Nf) creep rupture°C. stress relaxation
Frequency modified Approach	$N_f = [F/\Delta \varepsilon_p]^{1/\beta'}$ $[v_t / 2]^{1-k}[v_c / v_t]^d$	-strain-life data (4) - frequency vs. life (2) - stress-strain (2)	0/0 tests. some hold times frequency -life
Strain range partitioning	$N_{ij}=A_{ij}\Delta \varepsilon_{ij}^{\theta jk}$ ij represent PP, PC, CP and CC loops.	four inelastic strain vs. life relations. (2x4)	Tests producing complex loops PP, PC, CP and CC.
Damage Rate Approach. (n o creep damage)	$da/dN = a [T] [\varepsilon_p]^m [\dot{\varepsilon}_p]^k$ $da/dN = a[C] [\varepsilon_p]^m [\dot{\varepsilon}_p]^k$	scaling factors (2) strain -life (4) strain rate -life (2) assuming a crack size	0/0 tests. metallographic evidence. hold time tests.
with creep	$1/c \, da/dt = G [\varepsilon_p]^m [\dot{\varepsilon}_p]^{k'}$	scaling factor in creep cavity size (1) strain-life and rate (6)	metallographic evidence. creep data. test duration

Damage function method	$C = \sigma_T \Delta\varepsilon_p N_f^{\beta} v^{\beta(K-1)}$	strain-life (4)	0/0 data.
		frequency-life (2)	frequency data
		stress-strain (2)	stress-life data
		shape correction factor	hold time data.
Damage parameter approach	$d\omega/dt = [\text{ Co } \{\sigma/(1-\omega)\}^{v0}$ $d\sigma/dt\ H\ (d\sigma) + C\{\sigma/\ (1-\omega)$ $^v]\ H\ (\sigma)$	material constants (3)	stress versus
		fatigue -damage (2)	damage in creep
		creep-damage (2)	and fatigue.

6.5. DISCUSSION ON THE APPLICABILITY OF METHODS

Applicability of life prediction methods for low alloy steels under different test combinations such as hold times waveforms and temperatures had been examined by various workers with the data compiled in Chapter 4 are aggregated to identify trends in the prediction capability of methods discussed below.

6.5.1. Linear Damage Summation

Under constant tensile strain hold, steady state creep strain rate was computed and integrated for duration of test. During a dwell, stress relaxation was modelled by Σ t / t_f, where t was hold time and t $_f$, rupture time at the same load levels. It was pointed out (50) for 1Cr-Mo-V, "batch 4", at 565°C, that the magnitude of relaxed stresses was considerable even at the end of first cycle. Relaxed stresses accounted for 43% of the peak tensile stress after a 0.5 hour hold. However, peak tensile stresses were rising with the increase in number of cycles. At 50% life, the relaxed stresses were 33% of the peak stresses, hence, exact knowledge of creep rupture behaviour was extremely important which was not discussed in the literature.

Applicability of damage summation method was assessed for 1Cr-Mo-V, 1.25Cr-Mo and 2.25Cr-Mo steels in Table 6.2 where percentage of test data points predicted in a factor of $\pm$ x 2 of observed life for different batches of low alloy steels was tabulated. It can be

seen that applicability of this method depends upon material conditions and test temperatures in Table 6.2. With the decrease in temperature from 600 to 485°C, the prediction capability improved for both 1Cr-Mo-V and 2.25Cr-Mo steels. At 485°C damage summation approach predicted 100% of test data points in a factor of $\pm$ x2, for both N&T and Q&T conditions. For annealed condition, prediction capability was very poor, and this method was not applicable. With increase in temperature to 600°C, 2.25Cr-Mo, "batch 3 and 7" in N&T condition the prediction was quite poor. Hence, the life predicted by damage summation approach was influenced by test parameters such as temperature and material conditions as identified in Table 6.2.

Table 6.2. Prediction Capability of Damage Summation Approach.

Material	Batch no.	Heat Treatment	% Data in $\pm$ x 2	Temp °C
1Cr-Mo-V	1	N&T	69	540
	1	N&T	100	485
	4	N&T	57	565
	4	N&T	43	565
2.25Cr-Mo	1	Annealed	29	540
	1	N&T	82	540
	1	Q&T	100	485
	3	N&T	70	600
	5	N&T	0	600

6.5.2. Frequency Modified Approach

Frequency modified approach (FMA) underestimated life for constant tensile load cycles and longer tensile hold cycles for 1Cr-Mo-V in (15). Effects of unbalanced cycles, 16 hours/16 sec. were beneficial to creep-fatigue response that were unaccounted by this model (6).

Melton (65), observed excellent agreement between experimental and predicted results for 1Cr-Mo-V, "batch 3", within $\pm$ x 1.5 for a hot rolled bar material. The parameter of equations 6.2 - 6.7, $\beta'(K-1)$ was = -0.076 for "batch 3", which in the case of "batch 4" was -0.46. The FMA method was not well explored for other low alloy steels since it required the material parameters determined from tests with unequal ramp rates and balanced and unbalanced dwells. Table 6.3 describes the prediction capability for FMA method.

Table 6.3. Prediction capability of Frequency Modified Approach.

Material	Batch	Heat Treatment	% tests in $\pm$ 2	Temperature °C
1Cr-Mo-V	3	N&T	100	550
	4	-do-	66	565

6.5.3. Strain Range Partitioning Technique

A base line relationship involved four PP, PC, CP and CC combinations in strain and life in the following form (6)

$$N_{CP \text{ or } PC} = F_{CP \text{ or } PC}/ (\ 1/N_{obsrv}. - F_{pp}/ N_{pp}) \qquad (6.28)$$

Two steel grades of the 1Cr-Mo-V and the 2.25Cr-Mo types have been assessed in the literature. Trends in the prediction capability for longer tensile dwell data were reasonable, which was not good for too short or long dwell cycles for 1Cr-Mo-V and 2.25Cr-Mo "batch 3" (65) and "batch 4". However, there were conflicting opinions about SRP prediction capability for 1Cr-Mo-V alloy (15), type 304 SS (87), IN-738 LC (88) whereas, it was shown as a reliable technique for, type SS 304, SS 316, 2.25Cr-Mo (89), IN 100 (90), 1Cr-Mo-V rotor steel (91) and many others (92). Bicego et al (84, 91) examined predicted and experimental data for forged 1Cr-Mo-V steel at various strain rates and temperatures, where specimens were machined from different positions of a rotor forging. In some cases, life

shortening effects were observed with strain rates of 3×10^{-6} /sec, which was over-predicted by SRP, resulting in conservative predictions. Life reductions were moderate with the increase in temperature beyond total strain ranges 0.8% or above observed in (91).

Life prediction by SRP is tabulated in Table 6.4, where it is quite evident that SRP is better than other methods under annealed and normalized and tempered (N&T) conditions for 2.25Cr-Mo steel e.g., "batches 1, 3 and 4" for 1Cr-Mo-V in N&T and "batch 1" in annealed and "batch 3 and 5" in N&T condition for 2.25Cr-Mo steels. Trends in the prediction capability improved with increase in test temperature for several batches of 2.25Cr-Mo steel. However, Lloyd and Wareing (68) concluded from the data (87, 89) on SS 316, that with increase in temperature from 600-700°C or 650 to 750°C, trends in the predicted life were outside the factor of 2 band. Prediction capability of SRP was found questionable only for quenched and tempered condition for 2.25Cr-Mo steel shown in Table 6.4, that needs to be established with additional data.

Table 6.4. Prediction capability of Strain Range Partitioning Technique (SRP).

Material	"Batch"	Heat Treatment	% tests in± 2	Temperature °C	Remarks
1Cr-Mo-V	1	N&T	75	540	
	1	N&T	100	485	
	3	N&T	100	550	
	4	N&T	85	565	SRP
	4	N&T	100	Modified eq.	(15)
2.25Cr-Mo	1	Annealed	100	540	
	1	N&T	96	540	
	1	Q&T	58	485	worse case
	3	N&T	100	600	2 points
	5	N&T	100	600	

6.5.4. Damage Rate Approach

Plumbridge et al (32), investigated the metallographic damage development for "batch 4" 1Cr-Mo-V steel where fatigue and creep damages were independent of each other. Since, damage rate approach accounted for growth of fatigue damage in terms of cracks and creep damage by cavities, a very good prediction for "batch 4" of the 1Cr-Mo-V steel and "batch 3" of the 2.25Cr-Mo steel (15-16) were observed, in Table 6.5.

Table 6.5. Prediction capability of Damage Rate Approach.

Material	"Batch"	Heat Treatment	% tests in $\pm$ x2	Remarks
1Cr-Mo-V	4	N&T	100	at 565°C
2.25Cr-Mo	3	N&T	100	at 600°C with two data points, 5 min. hold.

6.5.5. Hysteresis Energy Approach

The prediction capability of hysteresis energy approach for only tensile hold data for 16 hours duration was found non conservative for 1Cr-Mo-V steel, "batch 4"[1]. However, prediction for compressive and balanced data was within a factor of $\pm$ x2. A further modification made on the approach proposed by Ostergren (10) in (15) by using the hold time data to determine the material parameters. This improved the prediction capability for "batch 4" 1Cr-Mo-V steel, as set out in Table 6.6. The equation proposed in (15) had the following form:

$$[N_f v^{K-1} (v_t / v)^r] \alpha \Delta \varepsilon_p \sigma_t = C \tag{6.29}$$

With the modifications equation 6.29 was assessed with very limited creep-fatigue data. Only "batch 4" 1Cr-Mo-V steel was assessed and applicability of equation 6.29 needs to be established with additional data.

Table 6.6. Prediction capability of Hysteresis Energy Approach.

Material	"Batch"	Heat Treatment	% tests in± 2	Remarks
1Cr-Mo-V Original	4	N&T	61	565°C by Ostergren (10)
Modified method	4	N&T	78	565°C by Priest et al,(15)
2.25Cr-Mo	3	N&T	100	at 600°C for 0/0 and two tests with 5 min. hold.

6.5.6. Damage Parameter Approach

A non-conservative prediction was observed for tension only hold periods for the 1Cr-Mo-V steel batch 4 as shown in Table 6.7. Though better predictions were observed for compression only hold, further work and extension of this model to both dwell cases needs to be established.

Table 6.7. Prediction capability of damage Parameter Approach.

Material	"Batch"	Heat Treatment	% tests in± 2	Remarks
1Cr-Mo-V 4	4	N&T	50	at 565°C
2.25Cr-Mo 3	3	N&T	100	at 600°C with 0/0 and two tests of 5min. hold.

6.5.7. Assessment Procedure R 5

Two low alloy steels of the type the 0.5Cr-Mo-V and the 1Cr-Mo-V were reviewed. In the case of the 0.5Cr-Mo-V steel, 75% of the test data points were predicted in a factor of ± x2. It was observed in the analysis of the data as the life range reduced, the trend in the prediction capability was found to improve. In the case of the 1Cr-Mo-V steel, 56% of the test data

points were predicted in a factor of $\pm$ x2. The same trend follows also in the case of the 1Cr-Mo-V steel, that the prediction capability improved only at lower life ranges of few hundred cycles. As "Assessment procedure R-5" is new and not yet widely assessed with a range of creep-fatigue data, applicability of R-5 remains as a topic for future investigations.

6.5.8. Diercks Equation

Kitagawa et al (13), assessed Diercks equation (12) with the creep-fatigue data for the 2.25Cr-Mo and the 9Cr-1Mo steels. A maximum of 10 min. tensile hold times were assessed, where 100% test data points were predicted in a factor of $\pm$ x2. Prediction capability of this method was presented in the recent literature (13, 85) as better than other methods mainly because it is a simple statistical equation which predicts life and does not require any details of creep-fatigue tests as shown in Table 6.8. However, the applicability of Diercks method needs to be determined by assessing it with a large data bank.

Table 6.8. Prediction capability of Diercks Empirical Method.

Material	"Batch"	Heat Treatment	% tests in$\pm$ 2	Remarks
2.25Cr-Mo	Data unknown classified	N&T	100	at 470°C with 10 min. hold.
9Cr-1Mo	Data unknown classified	N&T	100	at 600°C. (unknown holds)

6.6. SUMMARY

The following trends were identified:

(1)   there is a lack of publications describing creep-fatigue data, assessing creep-fatigue data with methods of life prediction and requirements of various methods related to material and test parameters,

(2)   various material parameters determined from one type of tests for one low alloy steel type cannot be extended to other creep-fatigue data for other low alloy steels,

3)   the life prediction methods within the phenomenological approach require a large number of material parameters and laboratory tests where parametric relationships are evolved by fitting those data, which often lack generalization to global creep-fatigue data,

4)   trends in the methods of life prediction depend upon test and material parameters, such as strain rate, temperature, material condition and heat treatment where the prediction capability of most methods deteriorated with increase in temperature,

5)   the empirical methods of creep-fatigue life prediction were recommended in the literature as promising, and

6)   several modifications of the existing life prediction methods are possible, specific to a data type, hence, any modification made on an existing method should be examined with a data bank before proposing the applicability of the modified version.

7. CREEP-FATIGUE BEHAVIOUR AND LIFE PREDICTION
OF GAS TURBINE MATERIALS

In this Chapter creep-fatigue behaviour and life prediction of two gas turbine materials are examined. Low alloy steels are used for power equipment, whereas, titanium alloys and superalloys are used in gas turbines. Only limited studies were conducted to investigate either the deformation mechanisms under creep-fatigue or life prediction for gas turbine and power equipment materials. As a result there is a lack of interaction between the two groups of researchers in power generation and gas turbines, hence, to provide an unification, damage features under creep-fatigue for a titanium alloy (IMI 829) and a superalloy (MAR M 002) were investigated and compared with low alloy steels in this research. The combined study of low alloy steels the titanium alloy, and the superalloy, conducted in this research, will advance the knowledge of creep-fatigue behaviour and life prediction for high temperature materials.

7.1. INTRODUCTION

Previously tested specimens were available (17, 18) from which metallographic samples were prepared and examined for high temperature low cycle fatigue (HTLCF) damage mechanisms for a titanium alloy (IMI 829) and a superalloy (MAR M 002). Samples were machined, etched and polished to conduct metallographic and fractographic investigations to document the damage development under creep-fatigue. Since limited tests were conducted (17-18), assessment of any life prediction method with the data was not possible (18). Due to this limitation, research in the development of an empirical life prediction method, and its applicability to the available data on MAR M 002 was undertaken. However, more work needs to be done to propose the applicability of the method developed in this investigation in creep-fatigue life prediction for high temperature materials.

7.2. CREEP-FATIGUE DATA FOR IMI 829 AND MAR M 002

Metallographic samples for IMI 829 (17) and MAR M 002 (18) had been prepared and examined by optical and scanning electron microscope. Damage under creep and fatigue has been extensively examined in terms of transgranular and intergranular cracking in the literature. Also, tortuous crack paths and multiple cracking together with cavitations were observed for titanium alloy IMI 829 under HTLCF at 600°C (93). In the case of MAR M 002 (18) wedge cracking and multiple crack sites in the coating were observed, in addition, oxidation was found present for both the materials investigated in this research.

Two microstructural details were investigated (93) for titanium alloy IMI 829 which is a α-β alloy comprising α platlets either align in β grains known as "aligned" microstructure or in a Widmanstätten pattern. The IMI 829 was tested (17) at 600°C under total strain control whereas, MAR M 002 was tested (18) at three different temperatures 750°C, 850°C and 1000°C with different hold times applied in tension and compression directions. Microstructures for MAR M 002 were varied (18) through ageing heat treatment conducted by Rolls Royce Plc Inc. Derby, United Kingdom where the ageing cycle reduced the creep-fatigue life of MAR M 002 considerably. Data for IMI 829 and MAR M 002 are tabulated in Table 7.1-7.2 respectively.

Table 7.1. Summary of creep-fatigue data of IMI 829 (17, 66).

Material Type.	Total Strain range (%)	Hold time (hr)	Cycles to failure	Test Temp. (°C)
WP	1.0		3355	600
	1.0	0.0333	5500	Widmanstätten Packets
	1.0	0 / 0.0333	1182	
	1.0	0.033/0.033	1800	
	1.0	0.25 / 0	1963	
	1.0	0 / 0.033	755	

	1.0	0.25 / 0.25	819	
	1.5		1115	
	1.5	0.0333 / 0	781	
	1.5	0 / 0.0333	423	
	1.5	0.033/0.033	536	
	1.5	0.25	371	
	1.5	0 / 0.25	349	
	1.5	0.25 / 0.25	311	
	2.5		271	
	2.5	0.25 / 0	153	
	2.5	0 / 0.25	134	
	2.5	0.25 / 0.25	136	
Aligned	1.5		941	
	1.5	0.033 / 0	753	
	1.5	0 / 0.033	536	

Table 7.2. Creep-fatigue data on MAR M 002 (18).

NICKEL BASED SUPERALLOY MAR M 002				
Strain range % Inelastic	Total	Hold time (hr.)	Cycles to failure	Test Temp. (°C)
0.076	0.896	0/0	352	750
0.048	0.772		1099	
0.032	0.601		8490	
0.178	0.946		94	850

0.094	0.799		549	
0.055	0.587		2590	
0.411	0.808		127	1000
0.256	0.606		160	
0.117	0.408		835	

Summary of data in unaged condition

0.076	0.896		352	750
0.094	0.900	0 / 0.0833	133	
0.115	0.906	0.0833 / 0	330	
0.178	0.946		94	850
0.219	0.897	0 / 0.0833	28	
0.133	0.664	0 / 0.0833	356	
0.264	0.888	0.0833 / 0	290	
0.410	0.921	0.0833/0.083	49	
0.411	0.808		127	1000
0.541	0.816	0 / 0.0833	161	
0.465	0.819	0.0833 / 0	127	

Summary of data in aged condition

0.095	0.706		15*	850
0.029	0.506		417*	
0.331	0.922	0 / 0.0833	2	
0.111	0.514	0 / 0.0833	39*	
0.40	0.81		68	1000
0.18	0.52		952	

|				
0.059	0.26		>5420	
0.38	0.74	0 / 0.0833	38	
0.41	0.73	0.0833 / 0	65	

(* 10% load drop.)

7.3. METALLOGRAPHIC INVESTIGATIONS AND DEVELOPMENT OF A DAMAGE MODEL

Samples from the tabulated test conditions set out in Tables 7.1-7.2 were examined for metallographic features that occurred under HTLCF. For IMI 829, Widmanstätten packet (WP) morphology was mainly tested (93) except for few tests on α aligned structure. A "scale" interpreted in this study as oxides formed on the specimen surface due to high temperature exposure in all tests. The "scale" was seen under an optical microscope as "black irregular bands" on the specimen gauge surface which contained multiple crack sites. Since quantitative characterization and or, analysis of oxides required advanced capabilities, interpretation of oxidation was made from published sources. The publications describing the oxidation were also in terms of qualitative interpretations from the evidence of "black bands" for different materials. The crack paths were mainly of the tortuous type dominating in the case of the IMI 829 alloy. However, for superalloys, depletion of intermetallic phases (γ') were reported by Coffin (19-20) and other workers (94) from the metallographic observations. For MAR M 002, oxide banding was observed together with γ' depleted regions. At 850°C and 1000°C, grain boundary wedge cracking, oxidation and γ' depletion were more prevalent than at 750°C.

Metallographic observations made on the samples from the gauge section, revealed "oxide scales" on the external surfaces for both materials. Accumulation of this scale resulted in "oxide banding", the shape of which was found to depend upon the specimen surface finish. Since each specimen contained surface irregularities where the surface finish changed from point to point, these were reflected on the depth of "oxide band" when microscopic studies were conducted shown in photomicrographs Fig. 7.1 (a-d).

Bakelite Mounting

Oxide Band

Matrix

30 μm
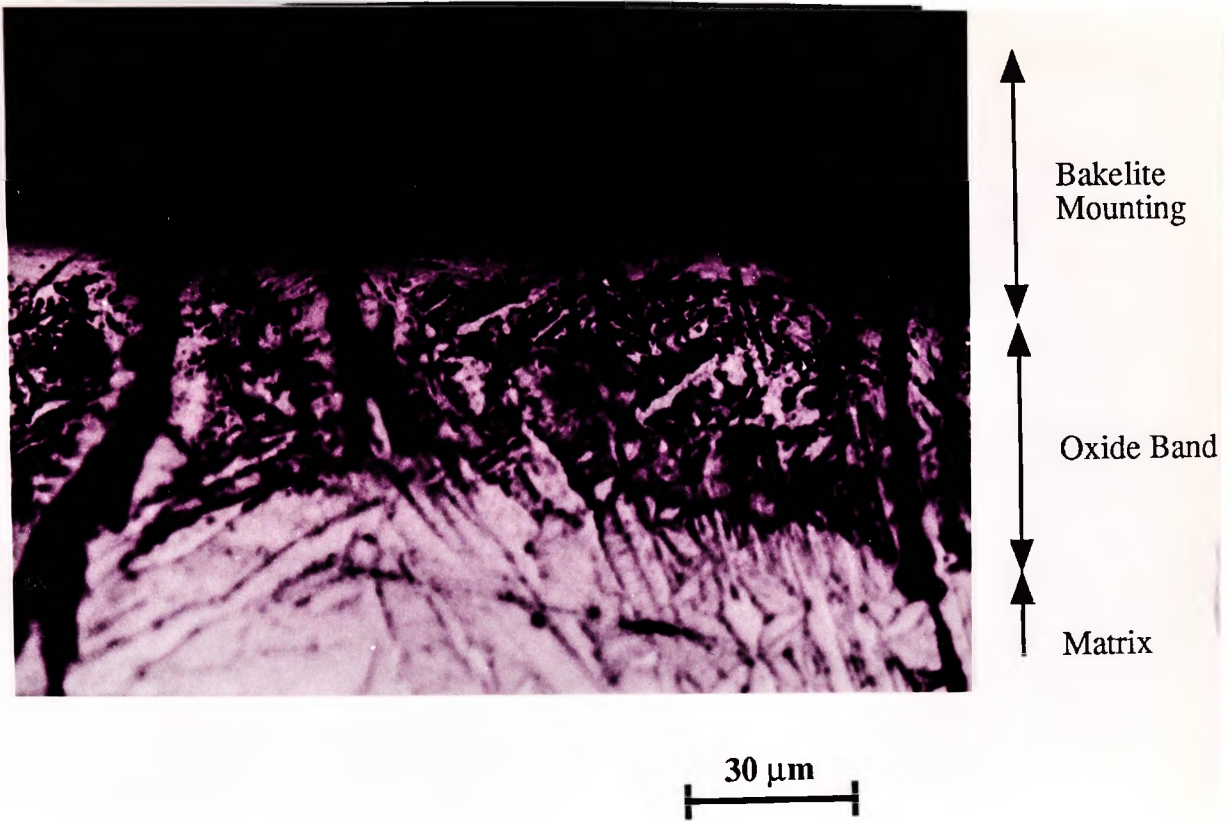
Fig. 7.1 (a). Oxide band formation and multiple intrusions in IMI 829 (at 600° C, a balanced cycle 15/15 min. and 1% total strain range).



Bakelite Mounting

Oxide Band

Matrix

60 μm
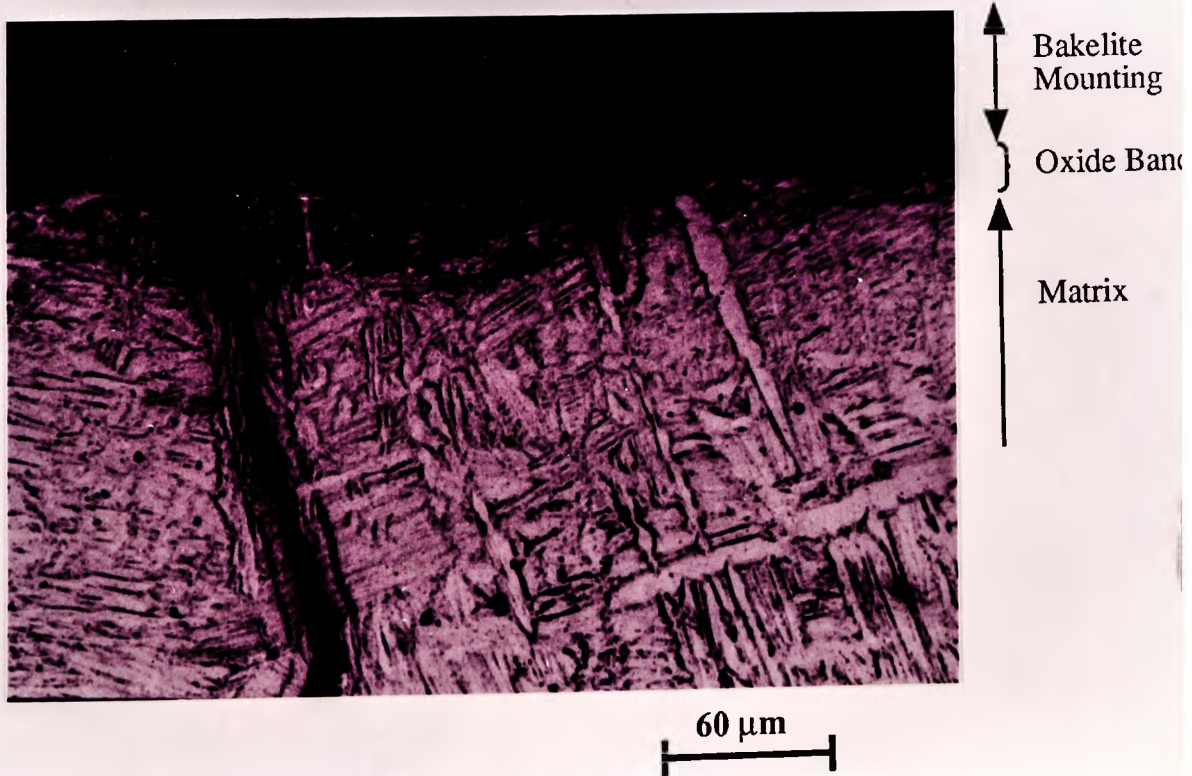
Fig. 7.1 (b). Oxide band formation and multiple intrusions in IMI 829 (at 600°C, a balanced cycle 15/15 min. at 1% total strain range).

Depending upon oxide band size, surface roughness and loading conditions, localised stress concentrations developed along surface irregularity valleys. From the regions of higher stresses, oxide scale penetrated further into the matrix by oxide spikes. For MAR M 002, which was strengthened by γ', which is an intermetallic compound of Al and Ti, depletion of the γ' occurred. The depletion of γ' was thermal activation dependent which at high temperatures enhanced the diffusion processes such that elements Al and Ti diffused in the matrix and along the main crack for MAR M 247 (45). Also, depletion of γ' occurred along the grain boundaries that resulted in intergranular wedge cracking. Wedge cracking, transgranular and intergranular cracking together with γ' depletion were observed for MAR M 002. Depleted γ' regions for MAR M 002 are shown in Fig. 7.2 (a-b) where interpretation of γ' depletion is made from such claims (19-20, 94) in the published literature.

A threshold temperature was identified (33, 64) in Chapter 5 for the 2.25Cr-Mo steel only above that temperature oxidation results. When oxidation occurs it accelerates the damage of fatigue, creep and their interactions. The interactions among creep-fatigue and other processes are in the research stage and not much is known about their mechanisms. The threshold temperature for a 2.25Cr-Mo steel was in a range of 250 - 450°C (33, 64) which was 0.3 times the homologus temperature (T_h). Oxidation was found to accelerate transgranular crack growth under fatigue (45), whereas, the same effect with creep cavitation and intergranular cracking occurred when oxidation interacted with creep (45). The contribution of oxidation in accelerating the fatigue and creep damage and in reducing life is not yet established because the complexities involved in three interacting mechanisms are difficult to model.

From the metallographic features documented under creep-fatigue for IMI 829 and MAR M 002, a model describing various stages in which damage under fatigue, creep and oxidation developed is proposed in this investigation. "Damage" is defined as a change in material state (microstructure) that occurs due to high temperature testing which can be observed under metallographic examination. A change in the microstructure was first
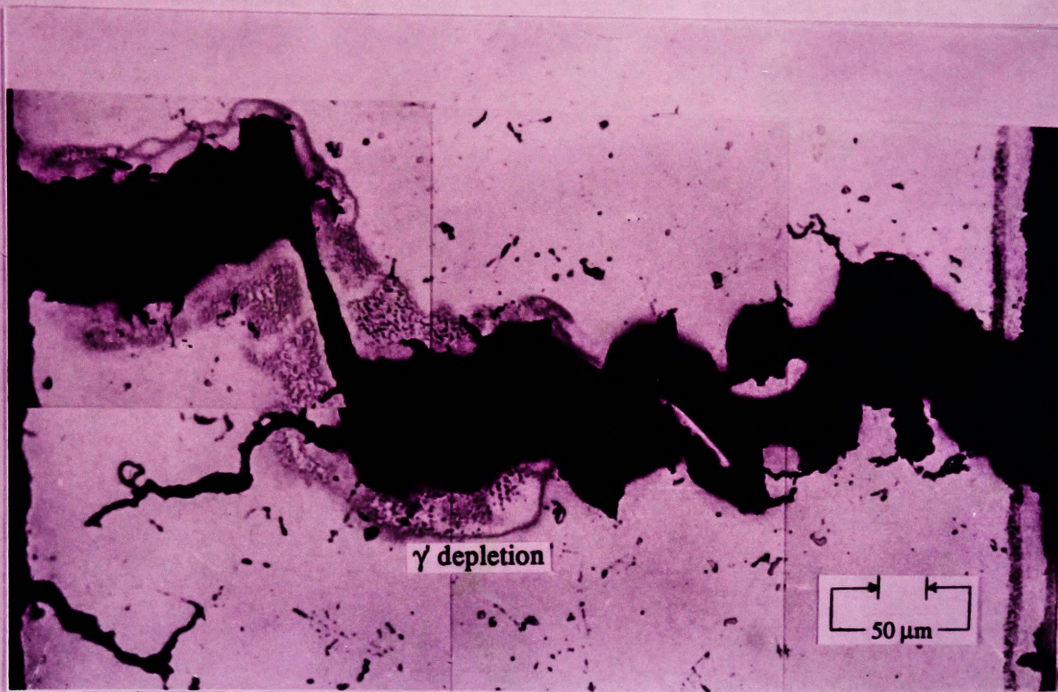
Fig. 7.2 (a). Multiple intrusions, main crack and γ' depletion in MAR M 002 (1000°C, a tensile dwell cycle 5/0 min. at 0.819% total strain range)
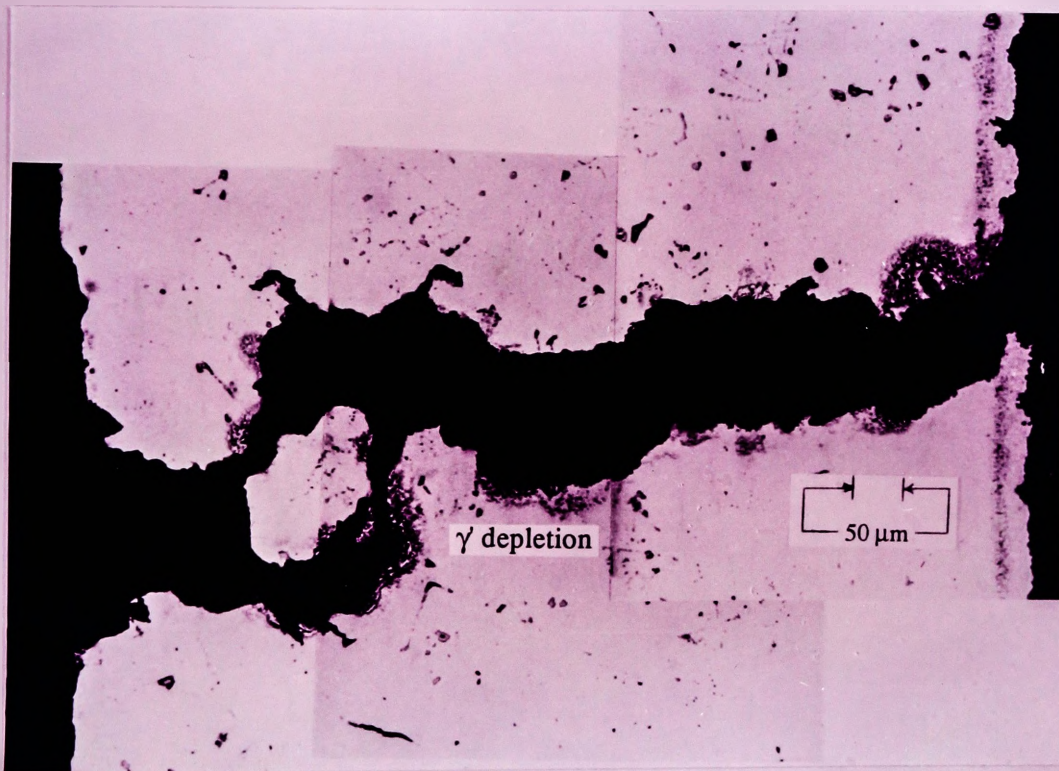
Fig. 7.2 (b) Multiple cracking, intrusions, and γ' depletion in MAR M 002 (1000°C, continuous fatigue cycle, at 0.808% total strain range)

observed on the specimen surface when oxide scales formed due to exposure at high temperature. Rate of oxide scale formation was enhanced with the increase in exposure time at high temperature and load for several superalloys (95). As a result, specimen circumference over the gauge length was covered with oxide scales and away from the specimen out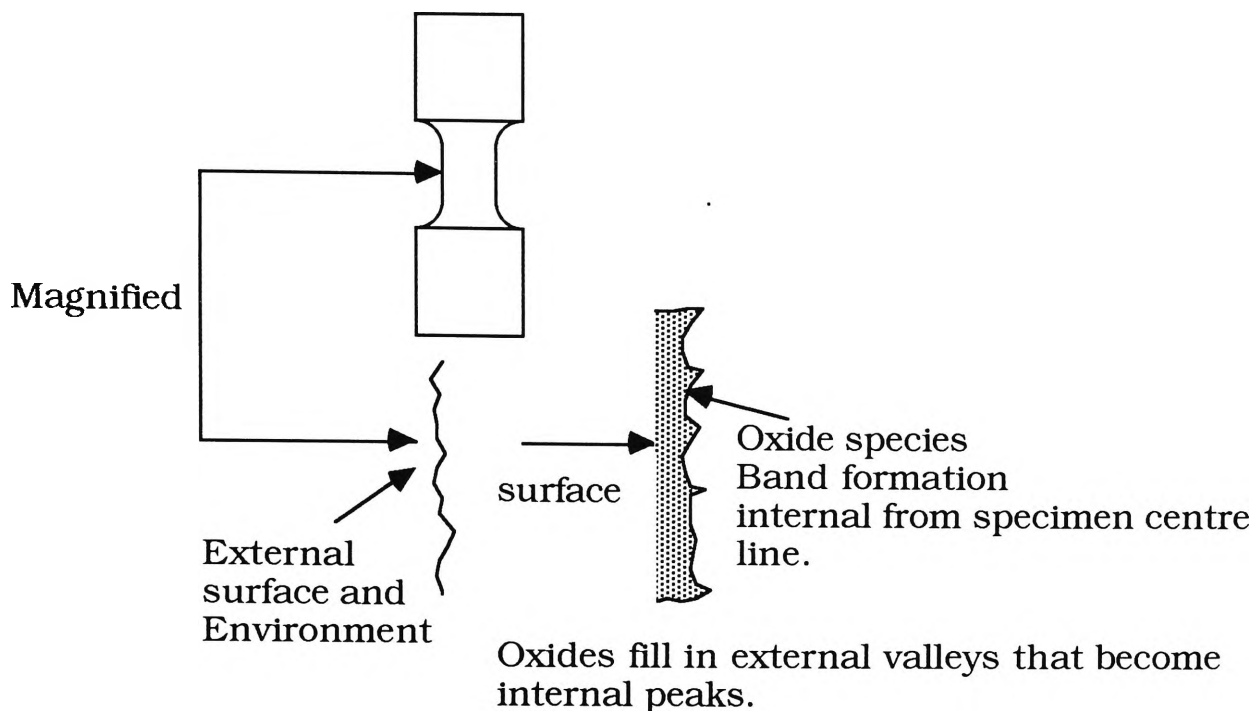er surface, changes in the matrix such as cracking and cavitation for IMI 829 were also observed. The five stages in which damage developed are shown in Fig.7.3 where individual steps are described below.

'Stage I': describes the formation of oxide scale on the specimen surface because of high temperature exposure. Stress concentration developed at the regions of surface irregularities due to fatigue cycling. Depending upon exposure time and loading, new layers of oxides developed and accumulated on the specimen surface, where thickness of "oxide layers" was different from point to point.

'Stage II': growth of the oxide bands took place externally as well as in the internal matrix depending upon the strain concentrations and the diffusion of alloying elements. Since diffusion of alloying elements such as aluminium and titanium in a superalloy resulted in the depletion of γ', oxidation damage was accelerated. Also the external surface irregularities in term of peaks and valleys with exposure time became filled with products of oxides. When observed internally from the matrix, external peaks transformed into internal valleys and external valleys into internal peaks respectively as shown in Fig. 7.3 (Stage I). When the thickness of the oxide scale reached a critical value a layer of material ruptured as shown in Fig. 7.3.

'Stage III': the rate of oxide scale formation and subsequent rupture of material layers increased with time and load cycling. Multiple oxide layers formed and ruptured with the increase in time and load cycling.

'Stage IV': the concentration of numerous ruptured material layers resulted in the formation of an oxide spike into the matrix. The process of generation of an oxide spike functioned as a micro-crack by intrusion. Intrusions so generated were of the order of a few

Magnified

surface

External
surface and
Environment

Oxide species
Band formation
internal from specimen centre
line.

Oxides fill in external valleys that become
internal peaks.

Stage I: Oxide formation due to high temperature exposures.

Oxide spikes

first layer

following layers.
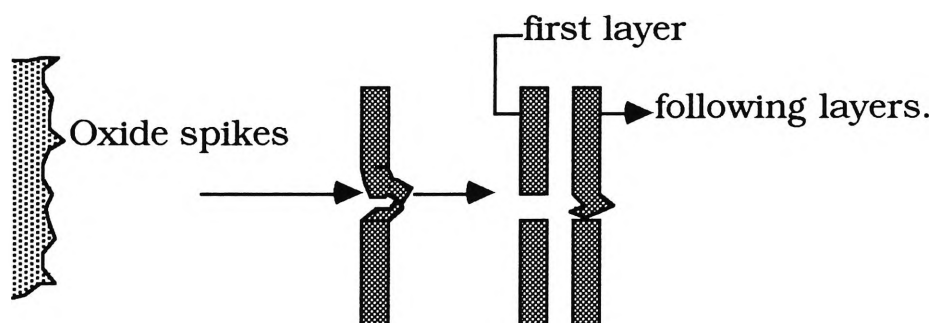
Stage II: Surface irregularities filled with oxides and penetration.

Oxide growth and
penetration in
the matrix.

Multiple layers oxidation
and rupture.
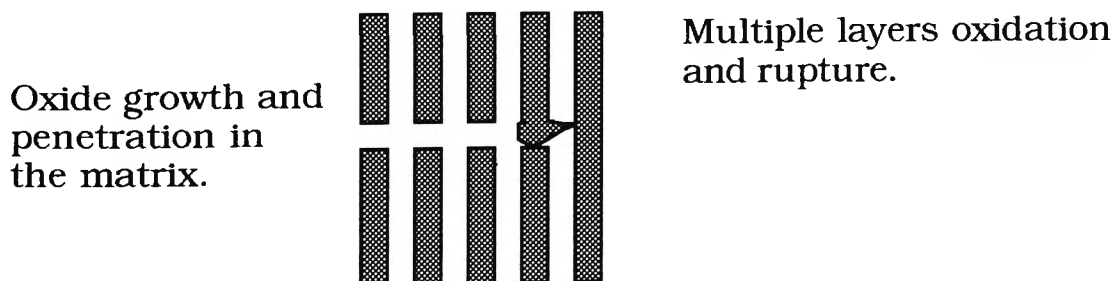
Stage III. Multiple layers of material are being ruptured.
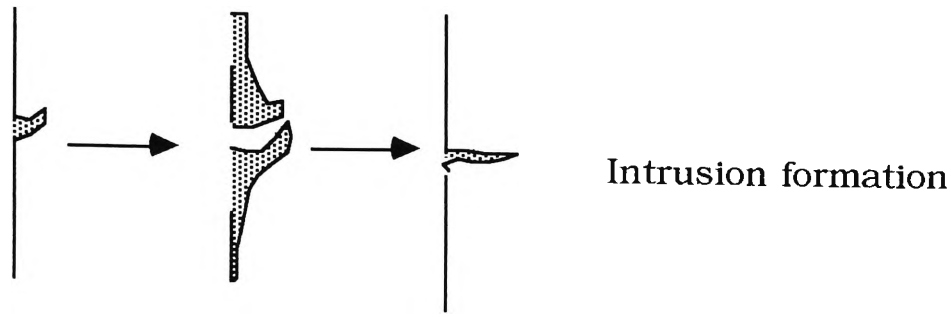
Intrusion formation

Stage IV: Enhanced rate of oxidation and formation of intrusion.
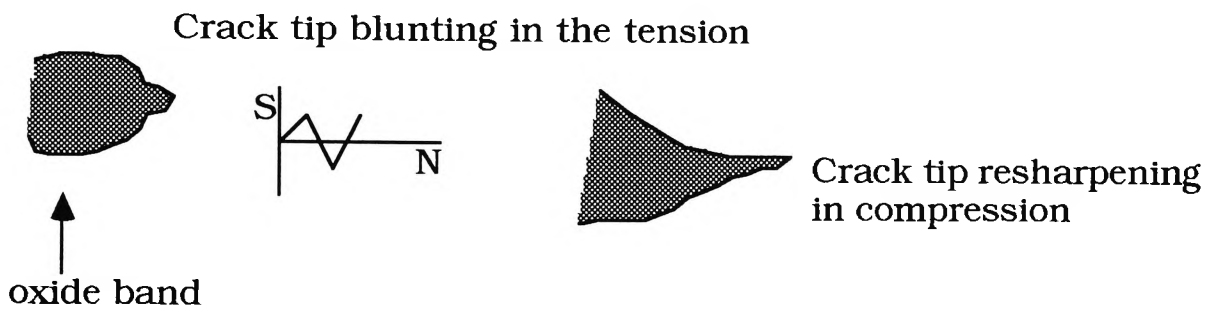
Crack tip blunting in the tension

oxide band

Crack tip resharpening in compression

(a)
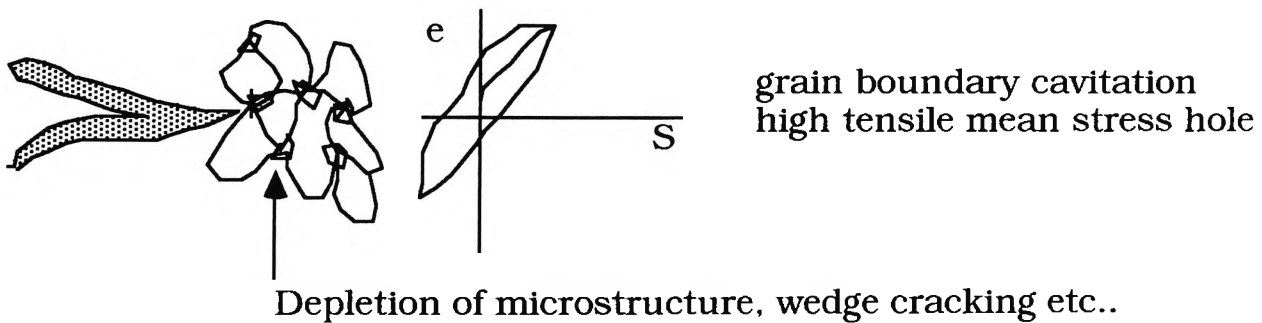
grain boundary cavitation
high tensile mean stress hole

Depletion of microstructure, wedge cracking etc..

(b)

Stage V: Evolution of oxidation damage with creep-fatigue reduces life.

Fig. 7.3. Various stages of a five stage damage development model.

microns to several hundred microns (macro-crack) as shown in Fig. 7.1 (a-d). Multiple intrusions may form depending upon local material stress/strain conditions and surface irregularities that were present on the specimens.

'Stage V': fatigue damage by transgranular crack growth was accelerated, as oxides formed and ruptured that resulted in spikes or cracks. The cracks so developed, filled with oxides and resharpened the crack tip in every compression half cycle. In the case of IMI 318 (96) and IMI 829 (17, 66) the compression hold times were more deleterious under HTLCF than dwell in the opposite (tension) direction are contributed simultaneously to the formation of oxides and crack tip resharpening. Such behaviour, at three strain levels with several compressive dwell periods is described in Fig.(a) of Stage V. For some alloys, a hold in the peak tensile strain direction resulted in the generation of cavities at grain boundary triple points by grain boundary sliding. Cavitation for a low alloy 1Cr-Mo-V (32) steel batch 4 (see Chapter 4) and IMI 829 (93) were observed and documented in Fig. (a).

The MAR M 002, experienced grain boundary sliding and intergranular crack propagation under HTLCF in a temperature range of 850-1000°C (26). Depletion of γ' resulted in wedge type of cracking. Depletion of γ' was observed in this investigation along the crack face and internal matrix that dominated the growth of damage in Fig. (b) of 'Stage V'.

The development of "oxide banding" and multiple intrusions along the specimen surface, described in damage model (Fig. 7.3), was validated with fracture surface examinations at low magnifications for IMI 829 specimens. Distinct multiple crack sites and sites of oxidation spikes are shown in Fig. 7.4 (a and b, pointed by arrows).

7.4. REVIEW OF EMPIRICAL OXIDATION LIFE PREDICTION MODEL

A review of an empirical life prediction method was conducted for a MAR M derivative alloy MAR M 509 which is used as a material for gas turbine vanes. In MAR M 509, Rauchet and Remy (14) observed transgranular crack propagation, and oxidation attack was external as
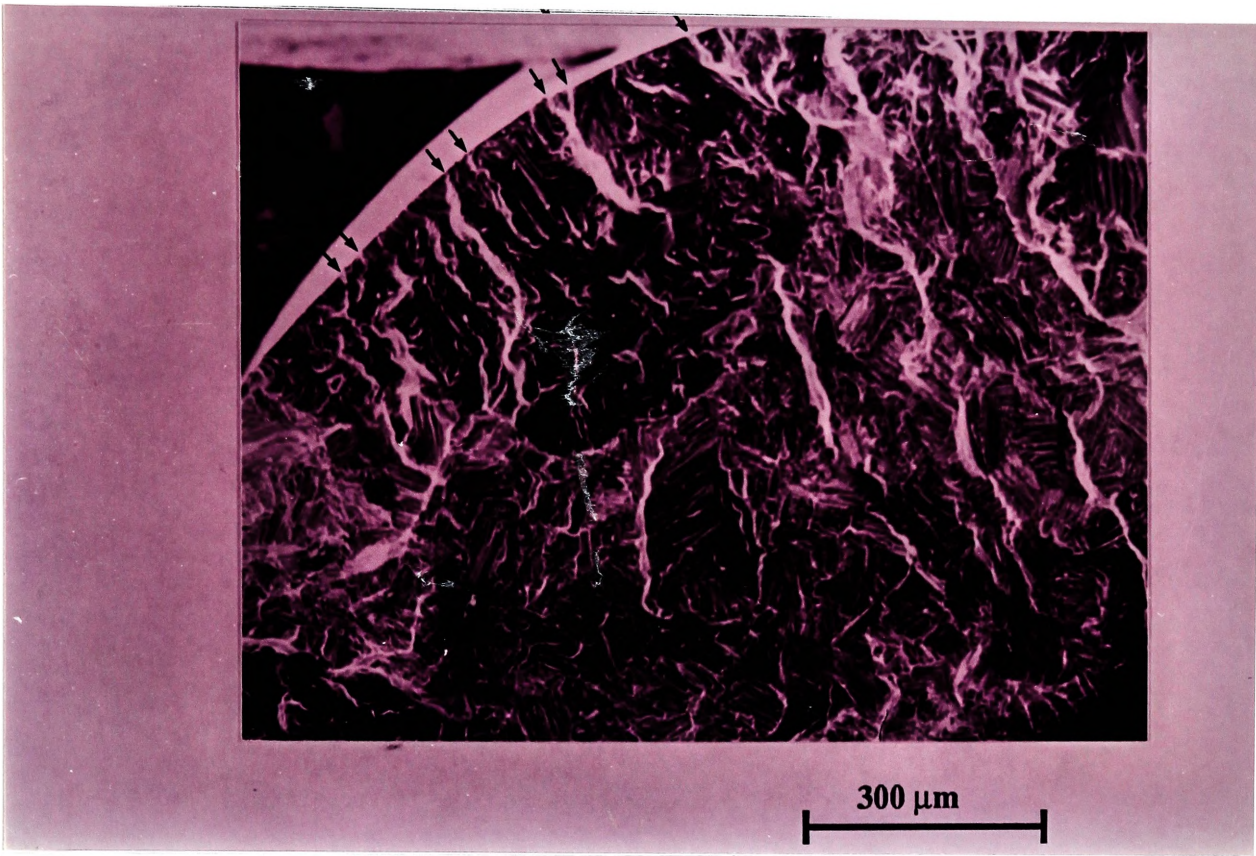
Fig. 7.4 (a). Fracture surface showing multiple crack sites in IMI 829.
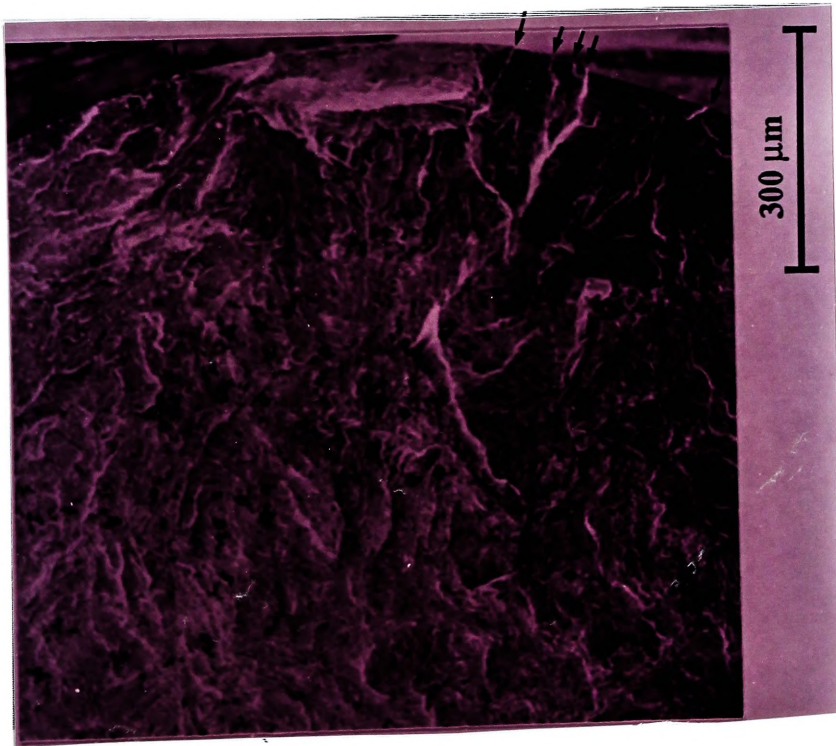
Fig. 7.4 (b). Fracture surface showing multiple crack sites in IMI 829.

well as along the internal matrix in the γ' carbides. The kinetics of matrix oxidation was expressed by a parabolic equation which was assumed to correlate the growth of oxide scale thickness (14, 45, 97) in the following form:

$$h = \sqrt{(D^\circ . t)}$$

$$h = \sqrt{D^*} \exp(-Q/RT) . t \tag{7.1}$$

where, D^* is the diffusion coefficient, R is the universal gas constant, T is absolute temperature (K) and h is the thickness of the oxide layer after time t. The diffusion coefficient was related in the following form:

$$D^* = D_0^* \ e^{(-Q/RT)} \tag{7.2}$$

where D_0^* is the diffusion constant and other symbols have their usual meanings. The crack growth equation was expressed empirically, as follows (14),

$$da / dN = \quad 0.51 \, \Delta\varepsilon_p \, [\, 1/ \, (\text{Cos} \, (\pi/2. \, \sigma/T) - 1]. \, a + (1-f^*_c) \, \alpha^\circ_M \, (1+K_M\Delta\varepsilon_p/2)\sqrt{t_1}$$

$$+ f^*_c \, \alpha_c^\circ \exp(b\sigma) \, t_1^{1/4}. \tag{7.3}$$

where, σ is the maximum cyclic tensile stress, T is the tensile fracture stress, a is the crack size at initiation, f^*_c is the effective fraction of carbides on the crack path, α_M° is the diffusion constant, K_M and b are temperature dependent parameters and t is the duration of the test. This equation was assessed with MAR M 509 tested at 900°C where prediction was found in a factor of ±x2 the observed life. A number of terms used in the equation 7.3 were determined empirically or assumed and applicability of this method was assessed with creep-fatigue data on MAR M 002.

Although there are several empirical models, their applicability to a range of data and materials is not yet determined. Some models (14) assumed linear summation of the damages in terms of crack growth by fatigue, and oxidation, whereas others (45) assumed the growth of damage by a chain rule, which multiplied damage fractions. From study of these models it is evident that no consensus exists about whether a linear summation or multiplication of damage fractions should be used in life prediction. Also, assessment of a phenomenological life prediction method, reviewed in Chapter 6 requires a bank of creep and fatigue data, such

an expanded data bank was not available for MAR M 509 and also for MAR M 002. Hence, a new model was developed from the available data and material parameters for the creep-fatigue life prediction for MAR M 002.

7.5. DEVELOPMENT OF A NEW EMPIRICAL OXIDATION MODEL FOR MAR M 002

A limited number of creep-fatigue tests were carried out on MAR M 002 (18) at 750°C, 850°C and 1000°C. The life prediction methods discussed in Chapter 6 required some hold time data in addition to high temperature fatigue and creep data. Methods such as damage summation and strain range partitioning required more information on creep behaviour of the materials to determine the accumulation of inelastic strains under hold times. These details were unknown for both IMI 829 and MAR M 002. Creep strain components for the tests conducted for IMI 829 (17, 66) and MAR M 002 (18, 26) had not been identified. The data were correlated in terms of either total or plastic strain ranges and life by separating total in plastic and elastic strain components. As a result, no phenomenological method was applicable to assess the life prediction for MAR M 002.

The role of oxidation is not yet understood in the creep-fatigue behaviour and life prediction for high temperature materials. Oxidation damage was documented in this investigation in five stages that were identified in the damage model developed in section 7.3. Only empirical models have been found to account for the effects of oxidation in creep-fatigue, since such models, did not require consensus on various laws and material stress-strain relationships, research workers used both the extremes of a linear summation and chain rule in developing damage equations. Hence an attempt was made to develop a new empirical model for creep-fatigue life prediction when oxidation was found to influence life for MAR M 002.

Diffusion constants and activation energy were determined from Arrhenius relationships from tests conducted at 750°C, 850°C and 1000°C. Extensive oxidation in the

matrix, along crack faces and depleted γ' phases were observed for tests conducted at 850°C and 1000°C. Oxide scale formation due to high temperature exposure in the case of metallic materials was modelled in terms of linear, parabolic and cubic growth rates. Growth of the surface oxide layer was assumed to be described by a parabolic law (14, 45, 95). The models (14, 45, 97) required several parameters which were not available for MAR M 002. Hence an alternate empirical approach was developed using the oxide scale growth together with creep ductility and fatigue cycle time concepts.

A parabolic growth equation was assumed to describe the thickness of oxide layer, represented by the equation below

$$h = \sqrt{(D^*. e^{(-Q/RT)}.t)} \qquad (7.4)$$

where h is the thickness of oxide layer /sec, D^* is the diffusion coefficient for the lattice diffusion, Q is the activation energy, R is universal gas constant, T is test temperature (K) and t is the test duration. Oxide scale formation and its growth rate had not been determined previously (17, 18). Hence, the parameters D^* and Q of equation 7.4 were assumed from the creep data for MAR M 002 (18).

Oxidation was found to occur in multiple steps discussed in damage development model described in section 7.3. At high temperature damage developed by oxidation, which depleted γ' carbides in superalloys and produced multiple cracks for IMI 829. Since γ' improves the strength and fatigue and creep resistance of superalloys, matrix oxidation resulting into γ' depletion was associated with a decrease in material strength and high temperature creep and fatigue resistance. Since previous models (14, 45, 97) assumed only that the external oxidation and oxide growth, role of internal oxidation such as γ' depletion was not accounted. In the new model, equivalent growth of external and internal oxides was assumed twice that of equation 7.1. Also both the creep and the oxidation are diffusion controlled phenomena, where thermal activation determines the damage under both creep and oxidation. The contribution of oxidation under fatigue and creep enhanced the crack growth rate under transgranular or intergranular mode (45).

Following assumptions were made to develop the new empirical model.

1. A chain rule was assumed to govern the final damage by creep-fatigue and oxidation:

$$dh/dN = dh/dt \cdot dt/da \cdot da/dN \tag{7.5}$$

where h and t were time dependent damages and represent oxidation and creep respectively. However, da/dN was cyclic crack growth in fatigue.

2. It was also assumed that oxidation accelerated crack growth under creep-fatigue to a "critical" length and not until failure. Under strain control testing a failure criterion of 10% load decrease was assumed life to crack formation of the order of 10% of gauge diameter in elastic-plastic modelling (80), which was strain range and temperature dependent. A well defined crack, or a dominating crack, grows under creep-fatigue and oxidation to a "critical" length then the crack growth process is governed by local stress/strain response at the crack tip. The effect of oxidation in accelerating the crack growth stops when cycle time is shorter than the time to form a new layer of oxide scale thereby, crack growth occurs by creep-fatigue conditions only. Up to a critical crack length, 10% of the specimen gauge diameter, was assumed that the crack growth occurs under creep-fatigue and oxidation mechanisms. Hence, life under three mechanisms namely; creep-fatigue and oxidation was assumed crack propagation to 10% of gauge diameter only.

3. Growth of crack to a "critical length" is described by equation 7.6:

$$Nf = [D^* \cdot af / \{(2.(h)^n \log(1.1 - t_h))\}^\alpha] \cdot \{D_c\}^\alpha \cdot (\Delta\varepsilon_{in} / \dot{\varepsilon})^{-1} / \alpha\} \tag{7.6}$$

where D^* is diffusion coefficient, af is crack size at failure (10% of gauge diameter), t_h is time of hold (hr), t is the test duration under continuous fatigue condition, which was 0.9, 0.25 and 0.28 hours at 750, 850 and 1000°C respectively, D_c is the creep ductility, $\Delta\varepsilon_{in}$ is the inelastic strain range and $\dot{\varepsilon}$ is the strain rate. The exponent α in the equation 7.6 was determined from appropriate data fitting and was test temperature dependent increasing with increase in temperature. The exponent α was expressed empirically with homologus temperature, as follows;

$$\alpha = \log\{1.49\,(\exp T_h\,)\,\}$$ (7.7)

where T_h is the homologus temperature that ranged from 0.41 to 0.46 for the test temperature range of 750°C to 1000°C.

4. Assumed material parameters for the life prediction equation 7.6 were tabulated in Table 7.3.

5. Thickness of the oxide layer h was determined by equation 7.3. Exponent n was determined from following:

$$n = 1 + 1.3\,\alpha$$ (7.8)

6. The LCF life was integrated between the limits of crack growth from a_o (no damage) to af (critical crack size). The initial crack size was assumed to be zero and the final crack size 0.25 mm depending upon the specimen diameter. For every creep-fatigue test, inelastic strain components were specified and hold times were known. Exponents α and n were determined using equations 7.6 and 7.7

Table. 7.3. Constants in the life prediction model.

Constants	Temperature	Values	Reference No.
For MAR M 002			
$D°$	750,850 and 1000°C	16000	45
$D*$		1.9×10^{-4}	18
Q		283kj/mol	18
α	750°C	0.41	
α	850°C	0.43	
α	1000°C	0.46	
R		0.00831 kj/°c/mol,	
D_c	750,850and 1000°C	6, 6.3 and 4.6	18
af		0.25mm	

Other terms of the equation were specified in Table 7.3. The crack growth equation developed herein determines the cyclic life under the action of creep-fatigue and oxidation and determines the life when the crack reaches critical i.e., 10% of gauge diameter.

7.6. APPLICABILITY OF NEW METHOD FOR MAR M 002

Using the material parameters from Tables 7.3, life prediction equation 7.6 was assessed with creep-fatigue data for MAR M 002 presented in Table 7.2. The predicted and experimental lives for MAR M 002 were tabulated in Table 7.4 for 750°C, 850°C and 1000°C. The continuous fatigue tests conducted at three temperatures were analysed with the equation 7.6 where the predicted life by the new method was in a factor of $\pm$ x2 for 70% of test data points. For other hold time data, the life prediction was higher than the continuous fatigue data where 73% of test data points were predicted in a factor of $\pm$ x2. Only one test was conducted for balanced, tension and compression hold cycles hence no comparison of the data is possible. The analyses performed for the life prediction are presented in Appendix I Tables A1-A3..

Table. 7.4. Life prediction of MAR M 002 under HTLCF by Oxidation model.

NICKEL BASED SUPERALLOY MAR M 002					
Strain range %		Hold time	Cycles to	Predicted	Temp
inelastic	Total	(hr.)	failure	lives	(°C)
0.076	0.896	0/0	352	431	750
0.048	0.772		1099	682	
0.032	0.601		8490	1023	
0.178	0.946		94	294	850
0.094	0.799		549	557	
0.055	0.587		2590	952	
0.411	0.808		127	125	1000
0.256	0.606		160	202	
0.117	0.408		835	442	

Summary of test results for unaged conditions.					
0.076	0.896		352	431	750
0.094	0.900	0 / 0.0833	133	276	
0.115	0.906	0.0833 / 0	330	584	
0.178	0.946		94	294	850
0.219	0.897	0 / 0.0833	28	186	
0.133	0.664	0/0.0833	356	307	
0.264	0.888	0.0833 / 0	290	423	
0.410	0.921	.083/.083	49	127	
0.411	0.808		127	125	1000
0.541	0.816	0/0.083	161	73	
0.465	0.819	0.083/0	127	252	
Summary of test results for aged conditions.					
0.095	0.706		15*	551	850
0.029	0.506		417*	1806	
0.331	0.922	0/0.0833	2	123	
0.111	0.514	0/0.0833	39*	1008	
0.40	0.81		68	129	1000
0.18	0.52		952	287	
0.059	0.26		>5420	877	
0.38	0.74	0/0.0833	38	104	
0.41	0.73	0.083/0	65	286	

(* 10% load drop.)

7.7. SUMMARY

The damage mechanisms under creep-fatigue of titanium and superalloys were observed to be by oxidation which occurred after a threshold temperature was exceeded. A threshold temperature for low alloy steel was lower than titanium and superalloys. In the case of low alloy steels the damage was found to be dominated by either fatigue or creep mechanisms whereas, in the case of the titanium alloy and superalloy, oxidation accelerated the fatigue or creep crack growth at the initial stages up to a critical crack size. Beyond that critical crack

size it is speculated that the mechanisms of damage growth under creep-fatigue for the titanium alloy and superalloy will be similar to that for low alloy steels. A model was developed to describe the damage evolution under high temperature low cycle fatigue where difference by which damage in fatigue, creep and oxidation developed were identified.

An empirical life prediction model was developed which combined crack growth by fatigue, creep and oxidation below a critical size. Since limited data were available comparison of the new method with other standard life prediction models was not possible.

8. DIERCKS EQUATION : MODIFICATION AND APPLICABILITY

Creep-fatigue data for low alloy steels were compiled in Chapter 4 and trends in that behaviour were identified in Chapter 5. Trends in the methods of life prediction using the compiled data were examined in Chapter 6. Creep-fatigue behaviour and life prediction for a titanium alloy IMI 829 and a superalloy MAR M 002 were discussed in Chapter 7. A new model was developed to describe the damage under creep-fatigue for IMI 829 and MAR M 002 and a new life prediction method was developed for MAR M 002 as set out in Chapter 7. Diercks equation, which is a multivariate creep-fatigue life extrapolation equation for stainless steel SS 304, was modified and extended to predict creep-fatigue life for low alloy steels in this Chapter. The applicability of the modified Diercks equation for life prediction was assessed in Chapter 8 using creep-fatigue data compiled in Chapter 4 for low alloy steels. As the Diercks equation is a statistical method derived from a data bank for SS 304 in terms of a multivariate equation, extension of this equation for the life prediction of low alloy steels does not require creep-fatigue tests and material parameters determined therefrom, therefore, use of this method may be made in generating creep-fatigue response curves for low alloy steels.

8.1. INTRODUCTION

Diercks equation (12), and other statistical methods, were widely explored (98-101) as an alternate tool to phenomenological methods for the creep-fatigue life prediction of low alloy steels and other materials. There are many phenomenological methods of life prediction where no one method is better than other methods identified in Chapter 6. Hence, alternate to phenomenological methods are explored in the creep-fatigue life prediction of high temperature materials. Historically, Diercks and Raskey (12), in the Argonne National Laboratory, compiled a bank of creep-fatigue data for stainless steel of type SS 304. They (12) obtained a best fit multi-variate equation, known as the Diercks equation for the data. Therefore, this equation contained several test parameters under which the data were

compiled and fitted with a multi-variate equation. The American Society of Mechanical Engineers (5) recommended this equation for the construction of fatigue diagrams for SS 304.

8.2. DIERCKS EQUATION

The multi-variate best fit Diercks equation, has been expressed (12) by regression functions in strain range, strain rate, temperature, and hold time parameters for creep-fatigue life extrapolation of SS 304, as follows:

$(\log N_f)^{-1/2}$= 1.20551064 + 0.66002143 S + 0.18040042 S^2 - 0.00814329 S^4

$$+ 0.00025308\ RS^4 + 0.00021832\ TS^4 - 0.00054660\ RT^2 - 0.005567\ RH^2 -$$

$$0.00293919HR^2 + 0.0119714HT - 0.00051639\ H^2T^2. \qquad (8.1)$$

where, S is a strain range parameter (S= $\Delta\varepsilon_t$ /100), R is a strain rate parameter R = (log $\dot\varepsilon$), T is a temperature parameter (T= T_c/100), H is a hold time parameter, H= log(1+t_h), $\Delta\varepsilon_t$ is the percentage total strain range, $\dot\varepsilon$ is the strain rate, T_c is test temperature for SS 304 and t_h is the duration of hold time in hours.

Modifications were made to the equation by Kitagawa et al (13) by introducing a fatigue (α) and a temperature correction factor (T_a) such that the life predicted for SS 304 was for a low alloy steel. The fatigue correction factor (α) or "cycle ratio" was observed to be temperature, strain range and strain rate dependent where it varied from 1 to 5 for high to low strain ranges under the condition that the other test parameters remained constant. The "cycle ratio" (α) is a ratio of life for SS 304 and a low alloy steel under same test conditions and requires the fatigue data for both the materials.

α = N_f (of SS 304) / N_f (of low alloy steel) under same conditions.

$[\log (\alpha\ Nf)]^{-1/2}$ = C (right hand side of equation 8.1) $\qquad (8.2)$

Also, the modifications proposed in (13) required relative material properties for SS 304 and a low alloy steel, as evident in equation 8.2, under the same test conditions to establish the fatigue correction factor. The temperature correction factor required the iso-stress creep

rupture properties, which is the value of stress at which same creep rupture life for SS 304 and the low alloy steel occur, when the temperature changed. Kitagawa et al (13), found that the iso-stress creep rupture properties of low alloy steels ranged from 50 to 100°C lower than the creep rupture properties of SS 304 at the same stresses . With the introduction of the temperature correction factor in equation 8.2, creep-fatigue life for low alloy steels did not change significantly when life prediction was carried out with equation 8.2. Hence, the temperature correction factor was assumed to be the same from (13) with the assumption that iso-stress creep rupture behaviour for low alloy steels was 100°C lower than SS 304. A limited number of creep-fatigue data for 2.25Cr-Mo and 9Cr-1Mo were analyzed in (13) where the prediction was found in a factor of $\pm$ x2.

The material data for SS 304 and low alloy steels are quite scarce, hence it was very difficult to establish the fatigue and temperature correction factors. Therefore, a simpler modification was needed to make this equation applicable for a wide range of conditions and low alloy steels. A cycle time factor and a material dependent equivalent strain rate term were introduced to modify Diercks equation. These were determined for every low alloy steel using the data fitting techniques and by trial and error methods by fitting a selected set of data. Later, these terms were kept constant for each low alloy steel and life assessment was carried out. The proposed modifications were conducted to generalize the equation due mainly to the lack of strain rates and other test details in the published literature.

8.3. MODIFICATION OF DIERCKS EQUATION

The Diercks equation (12) is modified in this section due mainly to the complexities associated with the modifications proposed by Kitagawa et al (13). The two parameters, for example, fatigue and temperature correction factors required a bank of data under a range of test conditions to establish them. Hence, a simpler modification was needed to extend the applicability of Diercks equation in the life prediction of low alloy steels. A simpler modification undertaken in this investigation is described below.

8.3.1. Introduction of a Cycle Time (τ) Factor

Owing to the limitations and the advantages of Diercks equation explained in section 8.2, a modification was made to apply this method where details of relative fatigue and iso-stress creep rupture properties were not available. A cycle time parameter (τ), which is the ratio of total strain parameter (S= $\Delta\varepsilon_t/100$), to strain rate (% / sec) was introduced. The equation in a modified form is:

$$[\log(\tau\, N_f)^{-1/2} = 1.20551064 + 0.66002143\, S + 0.18040042\, S^2 - 0.00814329\, S^4$$
$$+ 0.00025308\, RS^4 + 0.00021832\, TS^4 - 0.00054660\, RT^2 - 0.005567\, RH^2 -$$
$$0.00293919HR^2 + 0.0119714HT - 0.00051639\, H^2T^2. \tag{8.3}$$

Under creep-fatigue, life of various low alloy steels by equation 8.3 was found to be the same, provided that the same strain range, temperature and hold time the strain rate parameter was constant. Therefore, to apply Diercks equation in the creep-fatigue life prediction for low alloy steels must contain a material parameter for every low alloy steel being assessed with. Hence, to apply this equation 8.3, for low alloy steels, a material dependent equivalent strain rate ($\dot\varepsilon_e$), was introduced.

8.3.2. Material Dependent Equivalent Strain Rate ($\dot\varepsilon_e$)

The material dependent equivalent strain rate was determined by trial and error as follows.

1) A total strain and life extrapolation equation was obtained by fitting a few creep-fatigue data points with different $\dot\varepsilon$, hold times and temperatures in terms of:

$$\Delta\varepsilon_t = A\,(N_f)^{-\beta} \tag{8.4}$$

2) The parameters (A and -β) of the total strain and life relationship were determined using the best fit equation 8.4, to generate a response curve for an average behaviour.

3) This equation was extrapolated at several strain levels.

4) Equation 8.3 was used with assumed values of material dependent equivalent strain rates by trial and error method probabilistically. It ranged from 0.05 to 0.5 for six low alloy steels investigated in this research.

5) The value of material dependent equivalent strain rate ($\dot{\varepsilon}_e$), was selected when a good degree of fit between the extrapolated life and that predicted by equation 8.3 was obtained. Choices may be made between the most conservative and least conservative responses.

Figure 8.1 describes the fit between the extrapolated behaviour with the life predicted by equation 8.3, with different values of material dependent equivalent strain rate ($\dot{\varepsilon}_e$). Further derivatives of the material dependent equivalent strain rate should be derived depending upon the individual material condition, composition, and the form of the materials by the method described in section 8.3.2.

Material dependent equivalent strain rate varied from data to data as the parameters of the extrapolated equation changed with the creep-fatigue test types. For the six low alloy steels studied in this investigation, the material dependent equivalent strain rate ranged from 0.1 to 0.5. However, one value of the material dependent equivalent strain rate may be very conservative for one type of creep-fatigue data with a particular hold direction and may over predict for the other holds. Hence, the material dependent strain rate should be determined by appropriate data fitting. The material parameters were kept constant for all combinations of hold times and strain ranges for six low alloy steels tabulated in Table 8.1.

Table 8.1. Material parameters of modified Diercks equation.

Material	Material dependent term or equivalent strain rate.	Temperature difference in °C from SS 304.
0.5Cr-Mo-V	0.1	100
1Cr-Mo-V	0.1	100
1.25Cr-Mo	0.25	100
2.25Cr-Mo	0.5	100
2.25Cr-Mo-V	0.5	100
9Cr-Mo	0.5	100
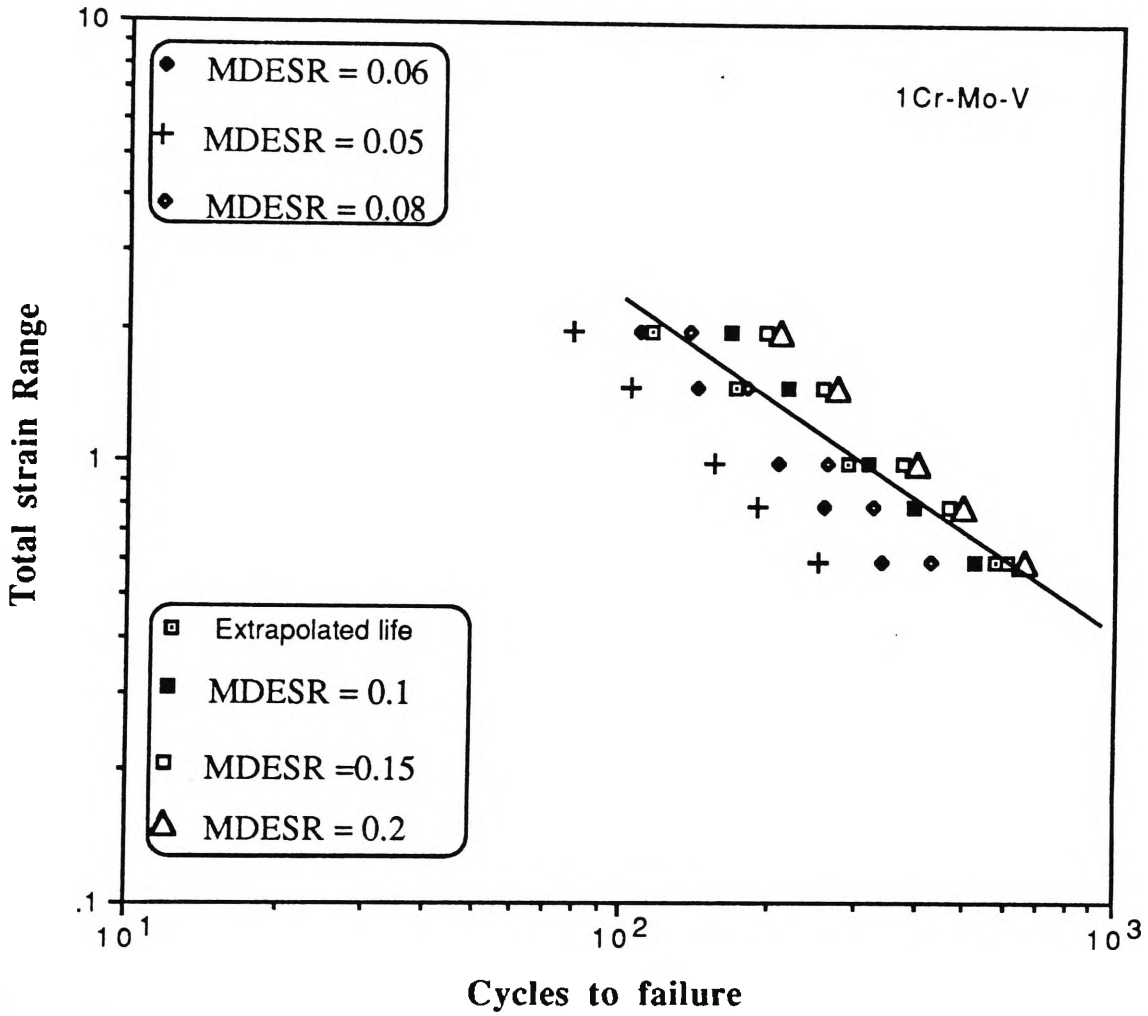
Fig. 8.1. Determination of material dependent equivalent strain rate (MDESR) for 1Cr-Mo-V.

8.3.3. Limitations of Modified Diercks Equation

A few limitations of the modified method are:

1 equations (1-3) only account for hold times in tension,

2 equations (1-3) apply only below a life of 10000 cycles,

3 modified equation 8.3 applies when plastic strain greater than elastic strain range, and

4 the effect of strain rate and waveforms are accounted in tension.

8.4. APPLICABILITY OF MODIFIED DIERCKS EQUATION

The life prediction equation 8.3 was assessed with all the creep-fatigue data compiled in Chapter 4 and the analysis was carried out for every data point presented in Appendix I. In some cases, for example, combined cycles, were beyond the scope of this equation which predicted the same lives under same strain range and hold times with different combined cycles. The effects of combined cycles were very complex where it either resulted in improving or deteriorating the life which was difficult to model and such creep-fatigue data were not assessed with other methods of life prediction discussed in Chapter 6. The comparison of life predicted by the modified Diercks equation with the experimentally determined lives for all the compiled data are tabulated in Tables A4 - A19 in Appendix I.

8.4.1. Life Prediction by Modified Diercks Equation for 0.5Cr-Mo-V Steel

8.4.1.1. Batch 1: Limited data were available for this low alloy steel where only 6% of the test data points were predicted outside the factor of $\pm$ x2. The remaining 94% of test data points were predicted in a factor of 2. From 30 min. to 16 hour tensile hold times were assessed and shown in Fig. 8.2. Details of predicted and actual lives are tabulated in Table A4 in Appendix I.
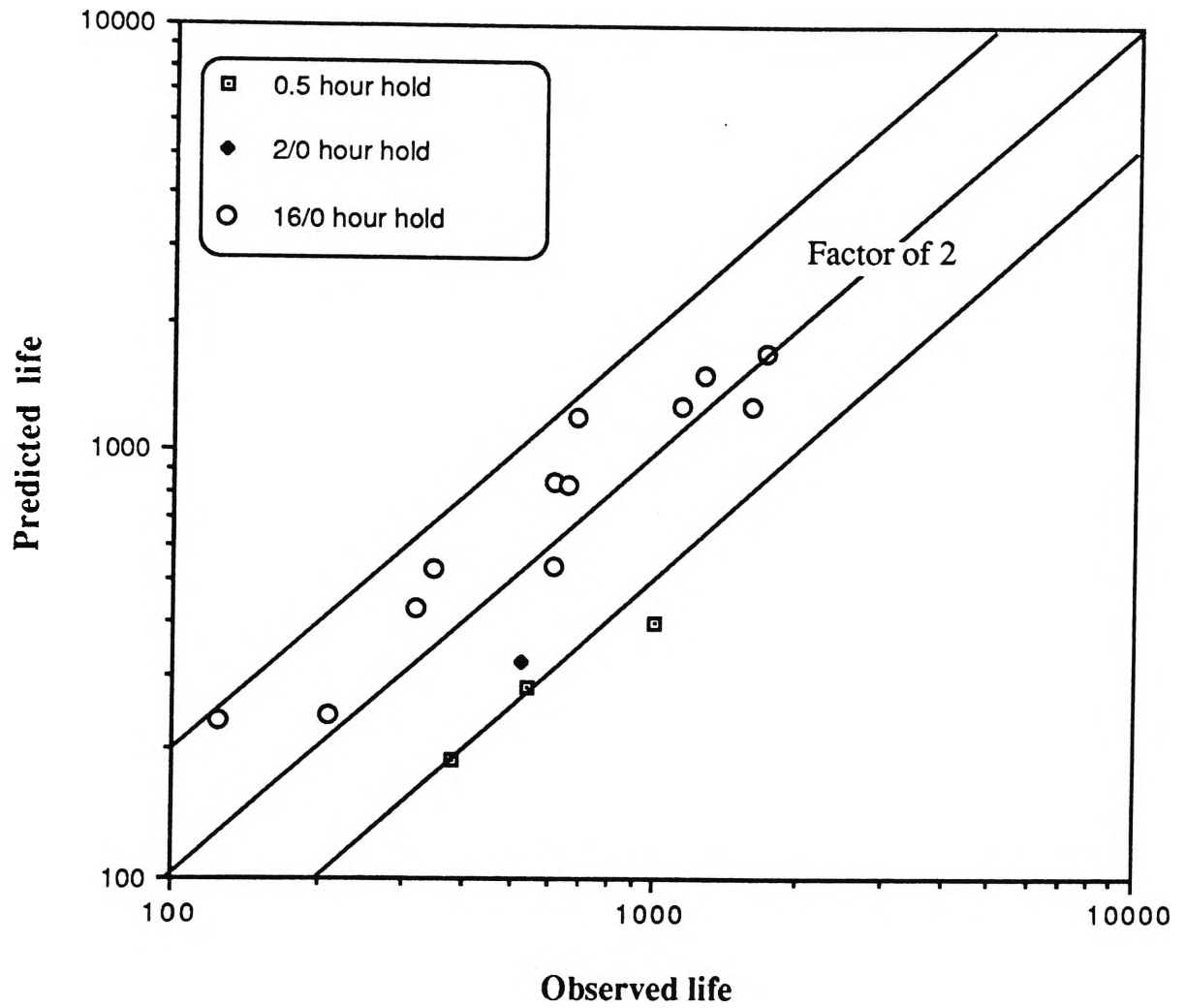
Fig. 8.2. Life Prediction of 0.5Cr-Mo-V "Batch"1 by Modified Dierck's Equation.

8.4.2. Life Prediction by Modified Diercks Equation for 1Cr-Mo-V Steel

8.4.2.1. Batch 1 and 2: Comprised interspersion fatigue-creep tests with 23 and 47 hours tensile hold times for the 1Cr-Mo-V steels. The effect of combined cycles on the creep-fatigue behaviour were noted in Chapter 5. There were beneficial as well as damaging effects of combined cycles, that were like other methods, unaccounted by this model. Predicted life was the same for the same strain range and the same hold time but with different combined cycles. The details of the life predicted by modified Diercks equation for a range of data points are presented in Table A5 in Appendix I.

8.4.2.2. Batch 3: When assessed, 70% of test data points were predicted in a factor of $\pm$ x 2, and remaining 30% of data were in a factor from 3 to 11, shown in Fig. 8.3. The discrepancy exists in the very nature of these data (11).

8.4.2.3. Batch 4: A large number of test combinations were employed for this "batch". The prediction by the modified Diercks equation was found conservative within a factor of $\pm$ x2, shown in Fig. 8.4. The beneficial effect caused by an unbalanced hold (16/0.003 hrs.), enhanced life by 3 times than from only 16 hours tensile hold cycle such effects were not accounted by any other method. However, life predicted for a 16 hrs. tensile dwell cycle was in a factor of $\pm$ x2.

8.4.2.4. Batch 5: Hold time sequences of 30 min. to 16 hours were assessed with the modified Diercks equation. At lower strain ranges (0.5 to 0.6%), with hold times of 30 min. and 16 hours, the life predicted by modified Diercks equation was very conservative. 75% of the test data points were predicted in a factor of $\pm$ x2 as shown in Fig. 8.5.
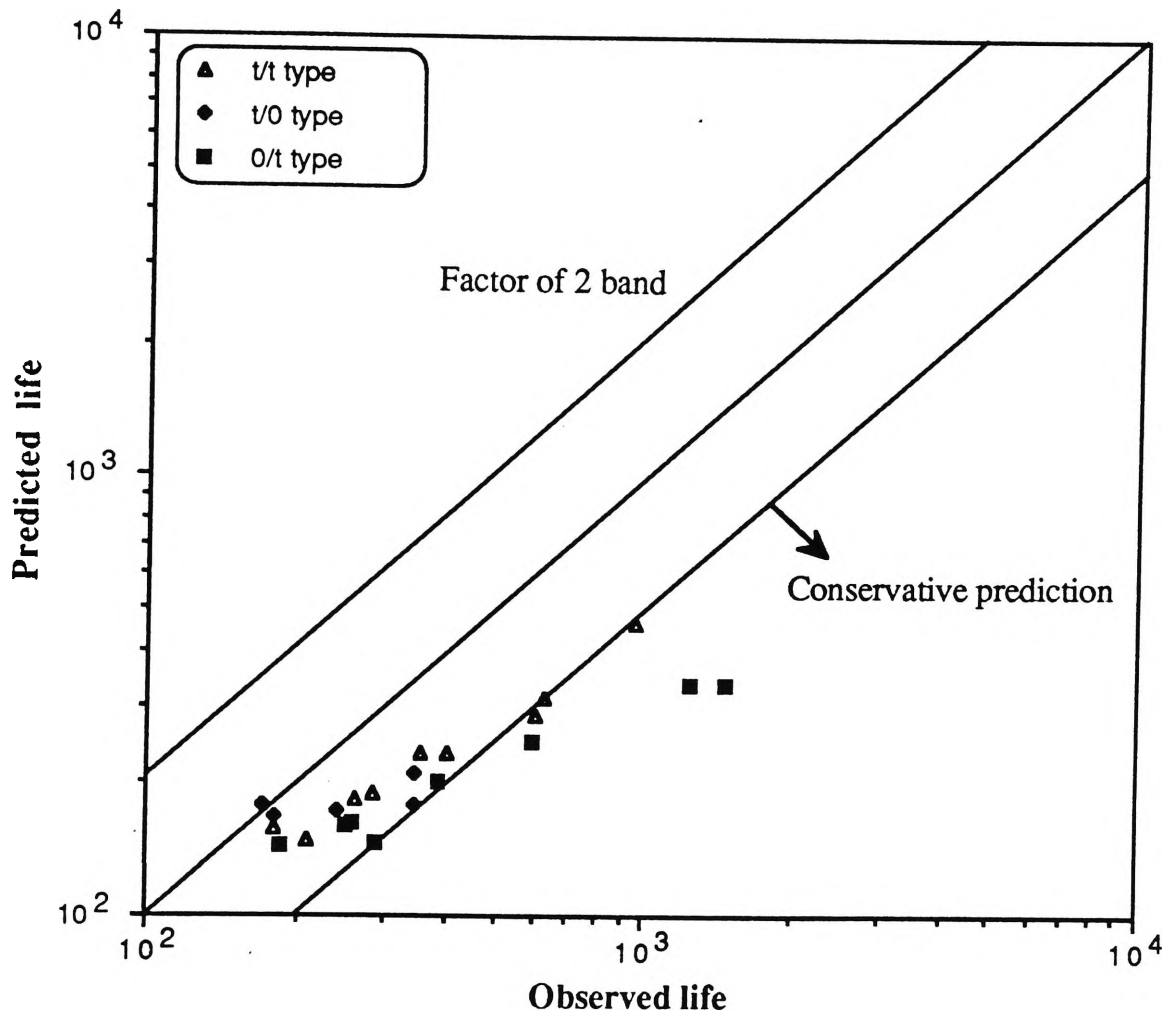
Fig. 8.3. Life prediction of 1Cr-Mo-V "Batch" 3 by Modified Diercks Equation.

Fig. 8.4. Life prediction of 1Cr-Mo-V "Batch" 4 by Modified Diercks Equation.
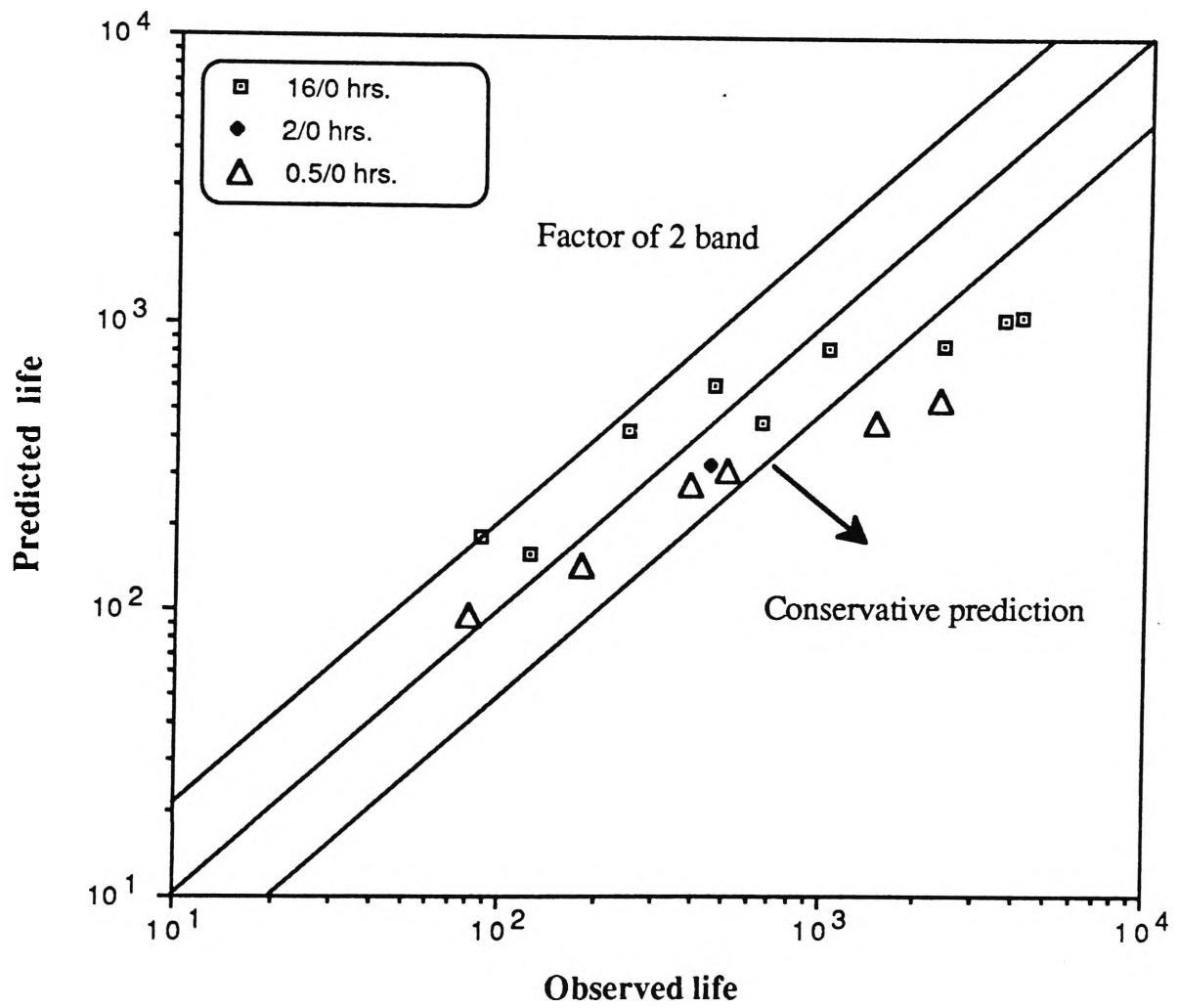
Fig. 8.5. Life prediction of 1Cr-Mo-V "Batch" 5 by Modified Diercks Equation.

8.4.3. Life Prediction by Modified Diercks Equation for 1.25Cr-Mo Steel

8.4.3.1. Batch 1: Pure fatigue and creep-fatigue combinations were analysed with the modified Diercks equation. At least 66% of the test data points were predicted in a factor of ± x2 and the remaining 33% were predicted in a factor of 4 as shown in Fig. 8.6. The discrepancy in the predicted life may be due to the definition of failure criterion which was different for every test, where cycles to failure varied from 20, 33 and 40% decrease in load levels.

8.4.3.2. Batch 2: As high as 90% of the test data points were predicted in a factor of ± x2. In the case of 30 min. hold cycle at 2.03% total strain range the life predicted by the modified Diercks equation was in a factor of 2.06. All creep-fatigue data for "batch 2" were predicted in a factor of ± x2 are shown in Fig. 8.7.

8.4.4. Life Prediction by Modified Diercks Equation for 2.25Cr-Mo Steel

8.4.4.1. Batch 1 and 2: Data compiled in batch 1 and 2 contained interspersion, creep and fatigue type of tests that involved combined cycles. It was pointed out earlier that for a 1Cr-Mo-V steel "batch 1 and 2", combined cycles associated a healing or detrimental effect that can not be accounted for in the models. The modified Diercks equation was assessed with the data where predicted and actual lives are tabulated in Table A12 in Appendix I.

8.4.4.2. Batch 3 : When assessed, 67.5% of the test data points were predicted in a factor of ± x2 and remaining 32.5% were predicted in a factor of ± x3 shown in Fig. 8.8. It may be seen from the data that 5 minutes tensile and compressive hold times were not causing any damage at all, however, life prediction was in a factor of ± x2.

8.4.4.3. Batch 4: When assessed below a life range of 10^4 cycles, for balanced hold cycles only, the life was predicted in a factor of ± x2 as shown in Fig. 8.9. For other data
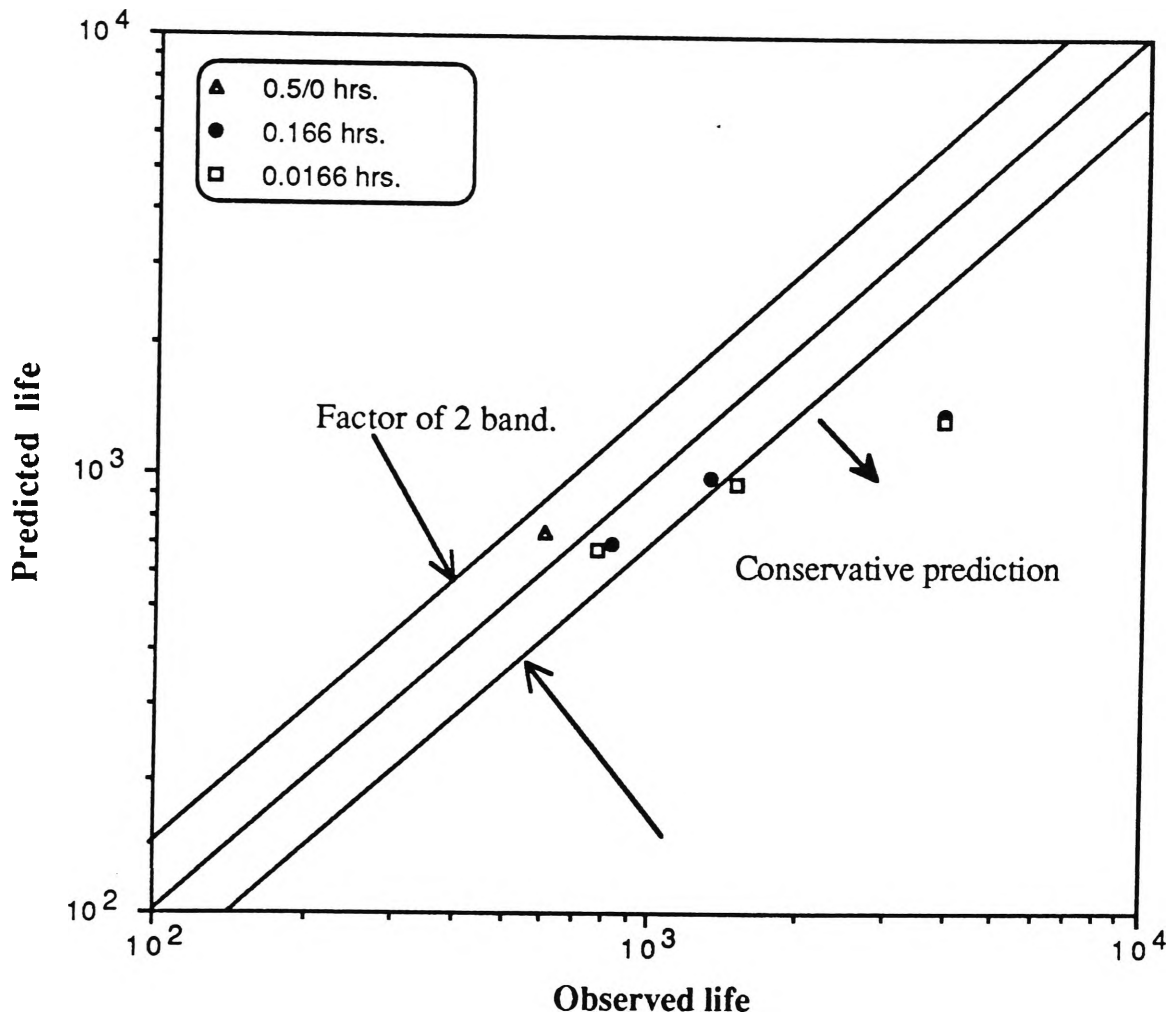
Fig. 8.6. Life prediction of 1.25Cr-Mo "Batch" 1 by Modified Diercks Equation.
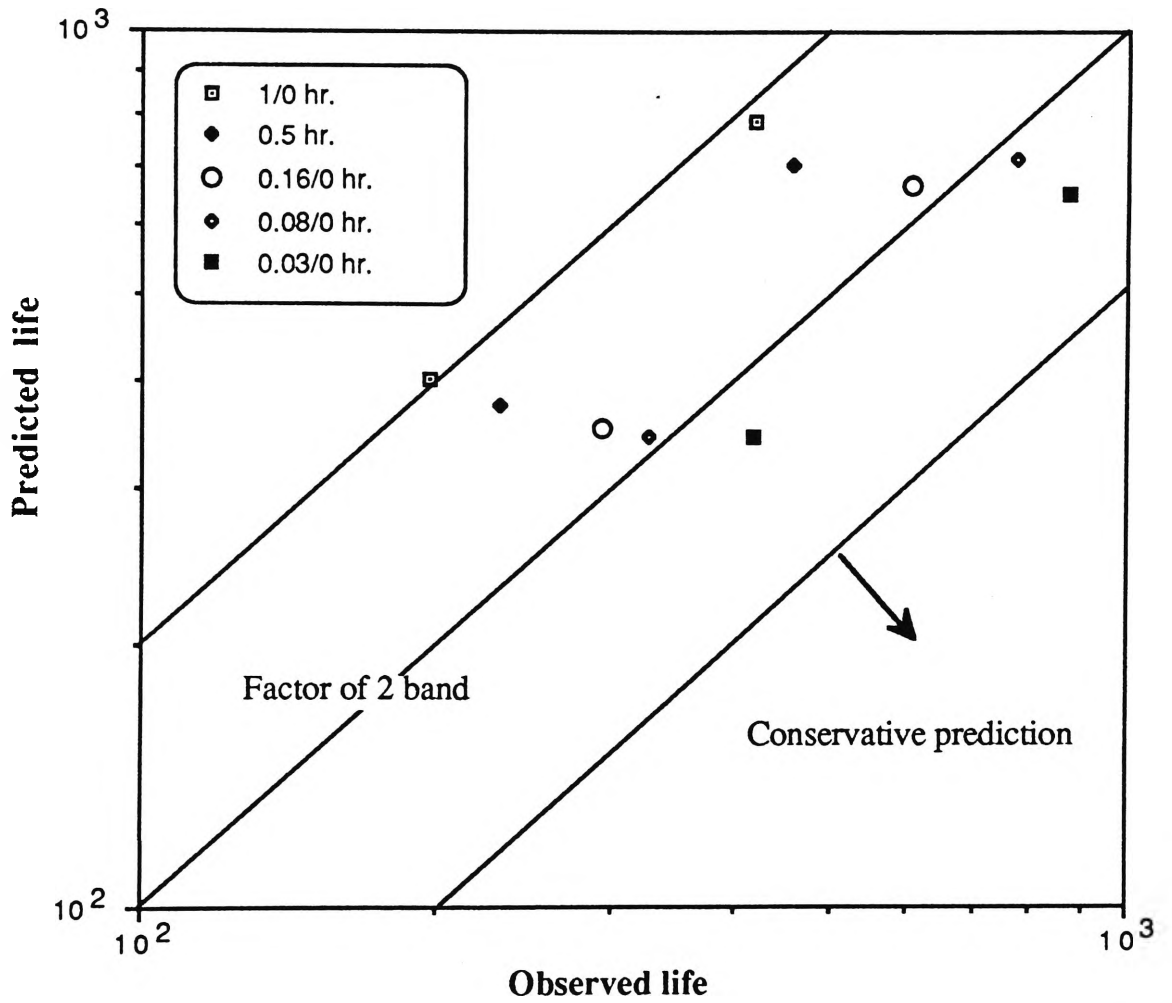
Fig. 8.7. Life prediction of 1.25Cr-Mo "Batch" 2 by Modified Diercks Equation.
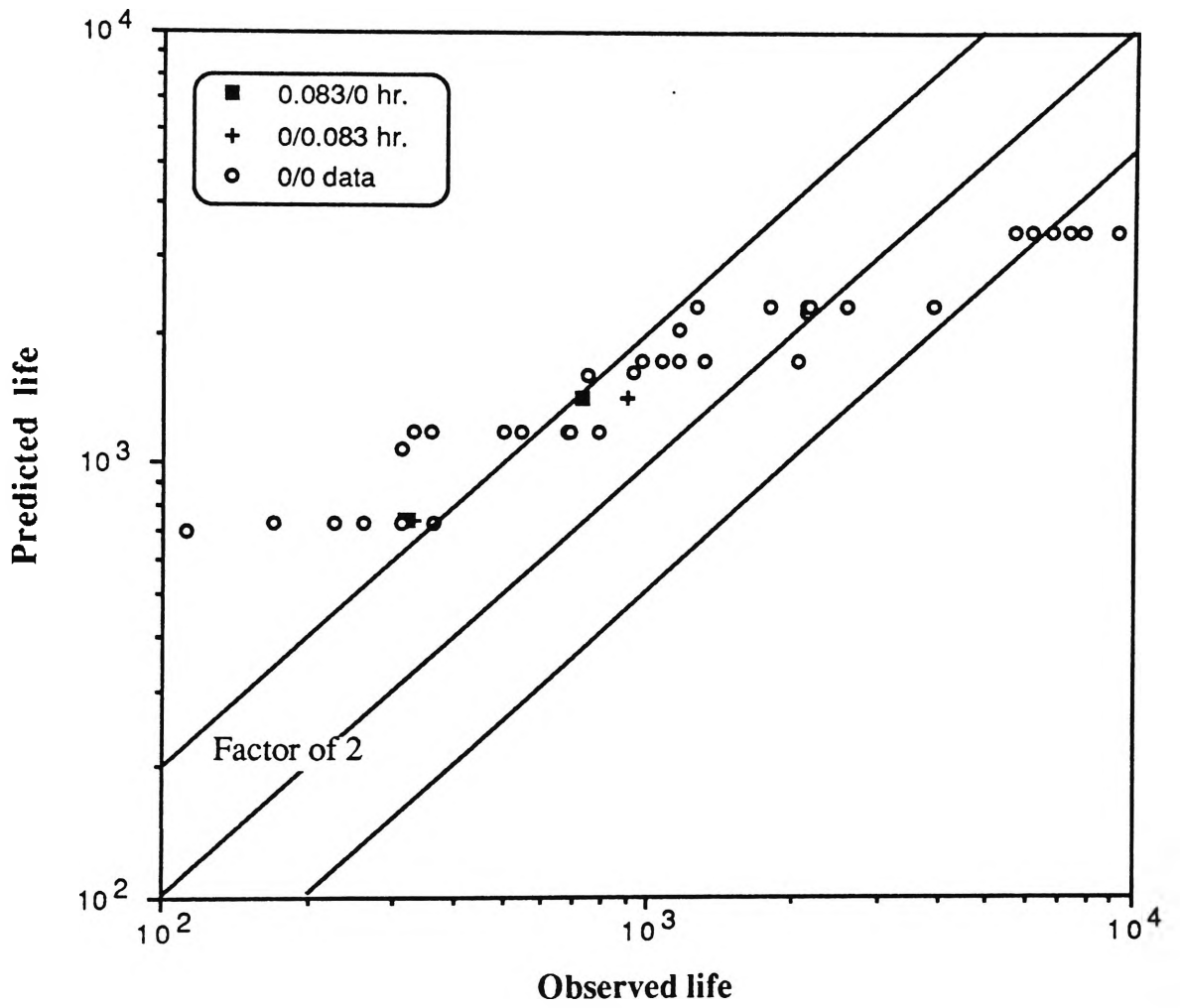
Fig. 8.8. Life prediction of 2.25Cr-Mo "Batch" 3 by Modified Diercks Equation.
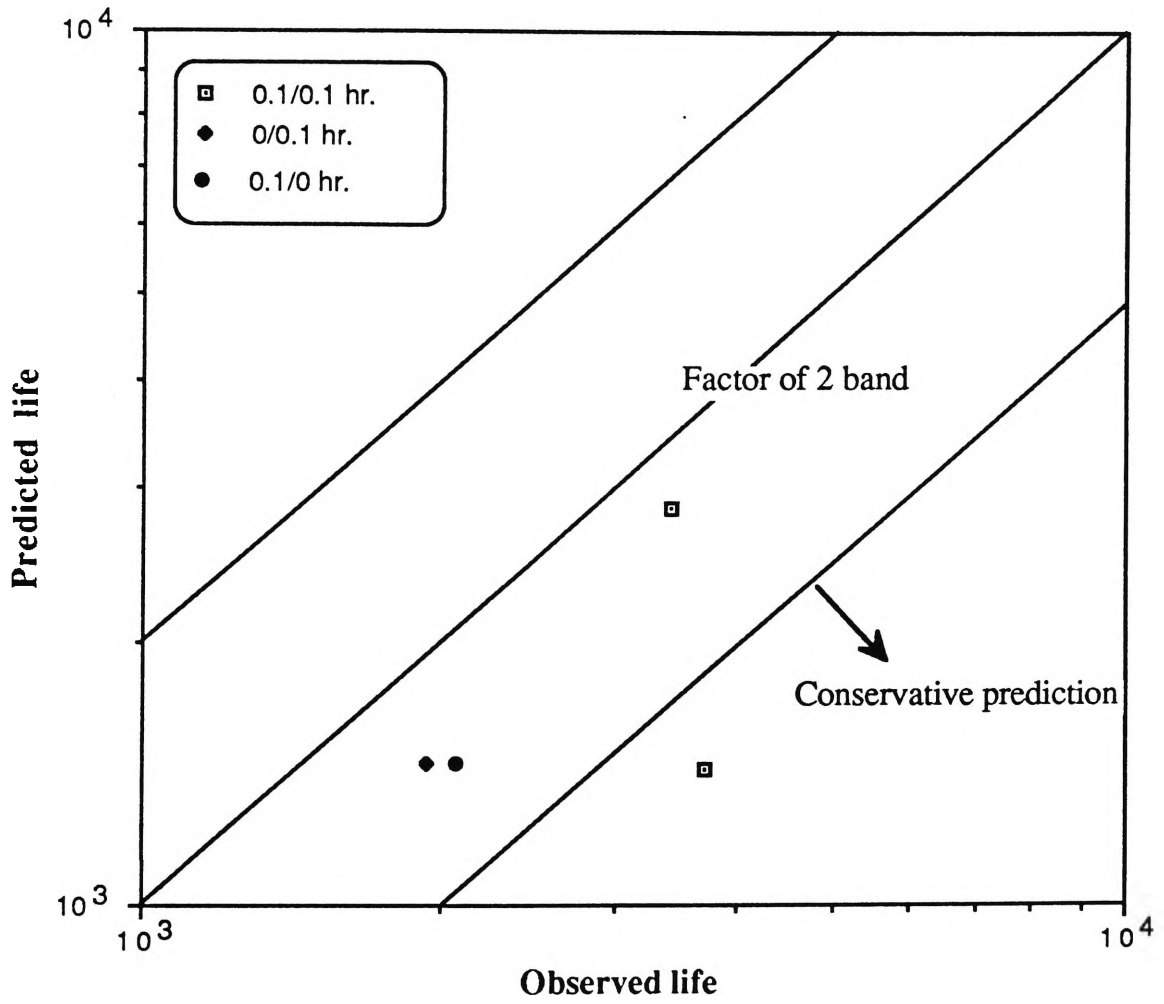
Fig. 8.9. Life prediction of 2.25Cr-Mo "Batch" 4 by Modified Diercks Equation.

the life range was much higher than 10^4 cycles for which the modified Diercks equation is not applicable.

8.4.4.4. Batch 5: The life prediction was in a factor of $\pm$ x2 for 100% of the test data points. The modified Diercks equation was found better than damage summation and comparable to strain range partitioning techniques, shown in Fig. 8.10.

8.4.4.5. Batch 6: Data were analyzed by the modified Diercks equation. The life prediction for 88 % of test data points were in a factor of $\pm$ x2 and remaining 12% of the test data points which involved error in the part of testing where life of 1.2% total strain range and same hold time, was 3/4 of the life at 4.30 % total strain range. The remaining 8% of test data points, were predicted in a factor of 2.2, shown in Fig. 8.11.

8.4.4.6. Batch 7: For 91% of the test data points the prediction was in a factor of $\pm$ x2. Remaining 9% of the test data points were predicted in a factor of 3. The capability of the modified Diercks equation was tested at high strain rate of 1.48% /sec and the prediction was found in a factor of 2 as shown in Fig. 8.12.

8.4.4.7. Batch 8: Information on the creep-fatigue behaviour and life prediction by other methods discussed in Chapter 6 were not available for the 2.25Cr-Mo-V steel. When assessed with the modified Diercks equation, 64% of the test data points were predicted in a factor of $\pm$ x2 and remaining 36% of the test data points were predicted in a factor of 4 to 5, as shown in Fig. 8.13. The discrepancies, where 36% of test data points were in a much larger error band of 4 to 5, was due to the assumption that the 2.25Cr-Mo-V steel was similar to the 2.25Cr-Mo steel, and that the tests involved only continuous fatigue cycling. The modified Diercks equation is applicable only under creep-fatigue conditions with hold times and such data were not reported for the 2.25Cr-Mo-V steel.
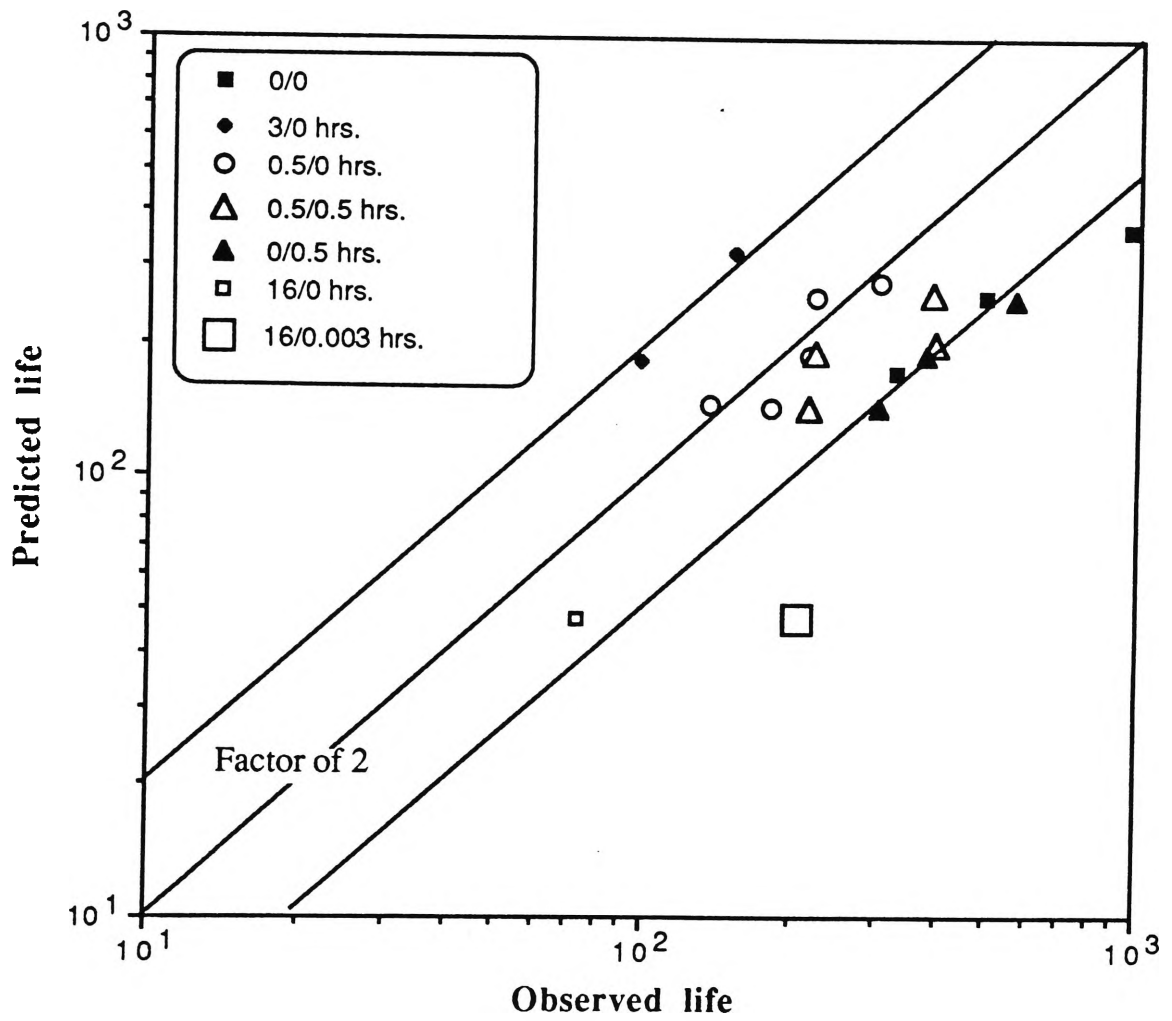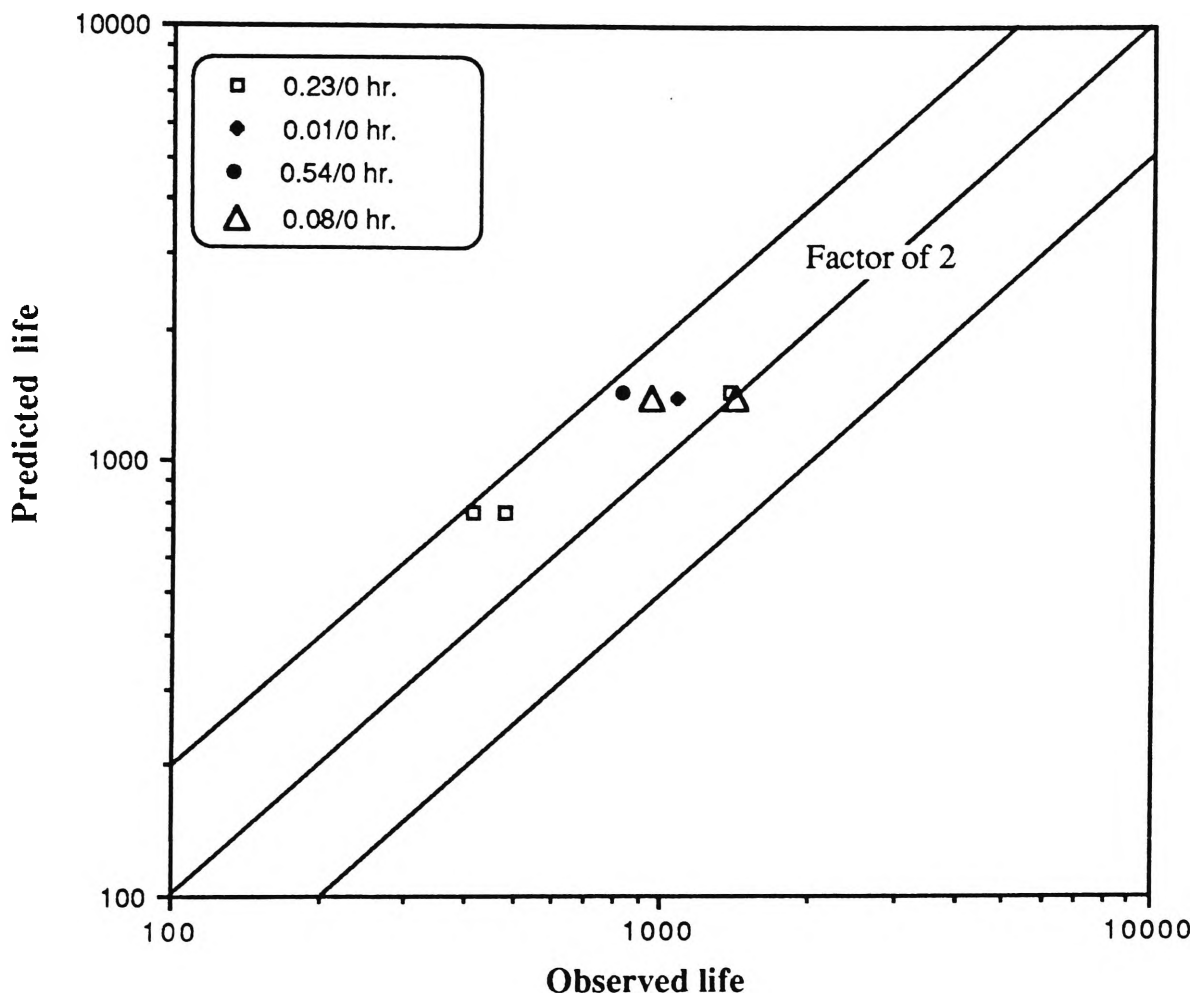
Fig. 8.10. Life prediction of 2.25Cr-Mo "Batch" 5 by Modified Diercks Equation.
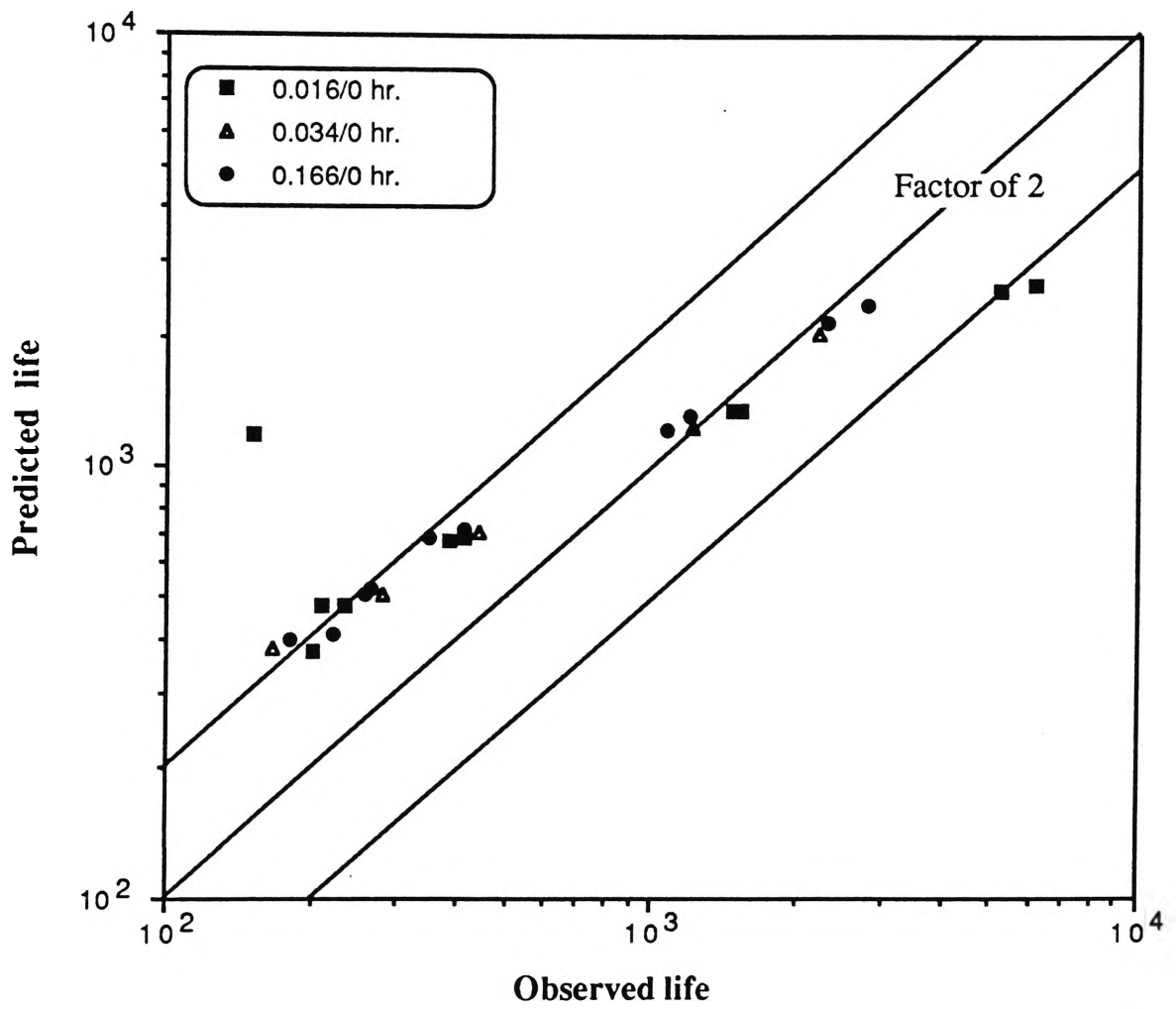
Fig. 8.11. Life prediction of 2.25Cr-Mo "Batch" 6 by Modified Diercks Equation.
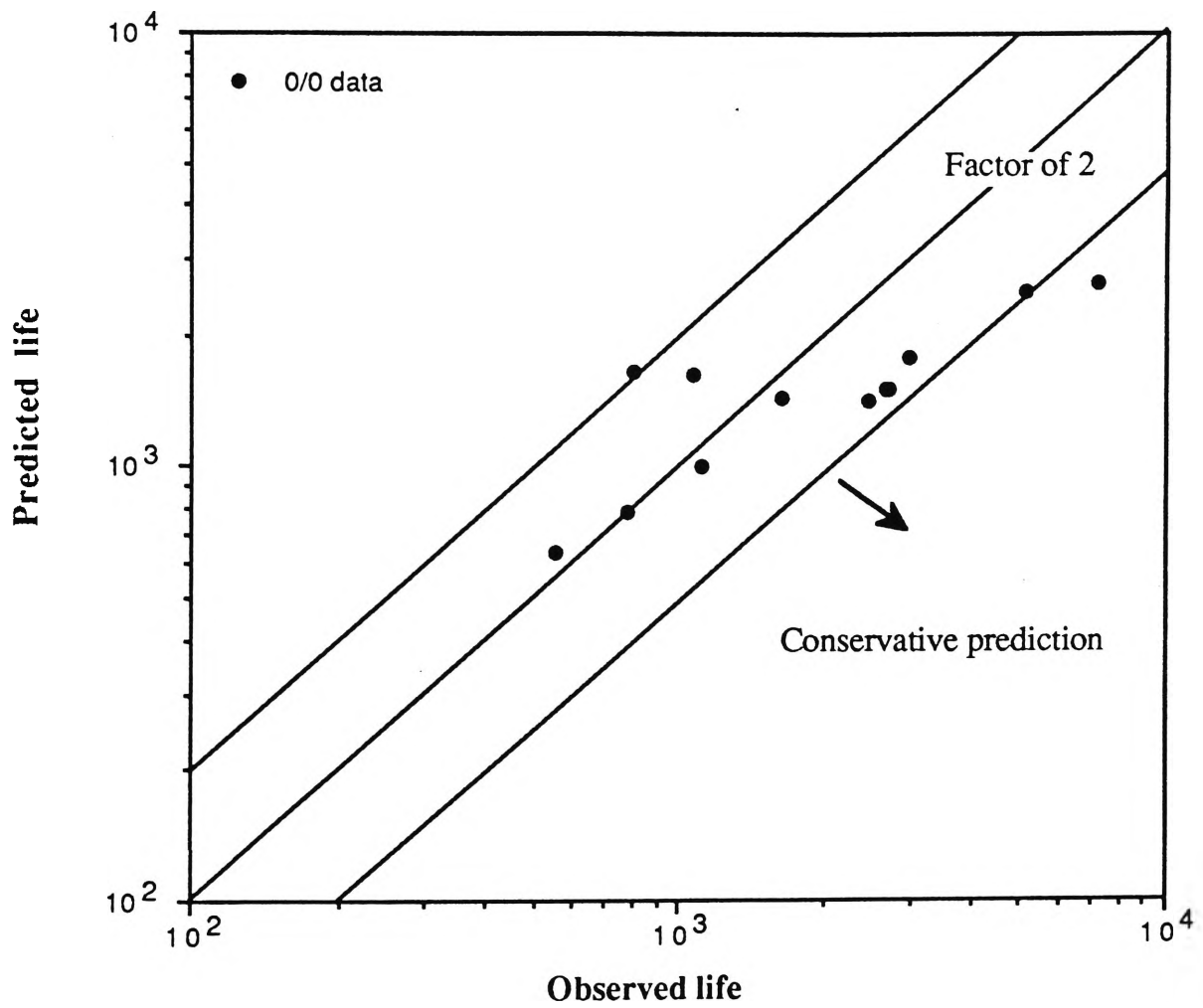
Fig. 8.12. Life prediction of 2.25Cr-Mo "Batch" 7 by Modified Diercks Equation.
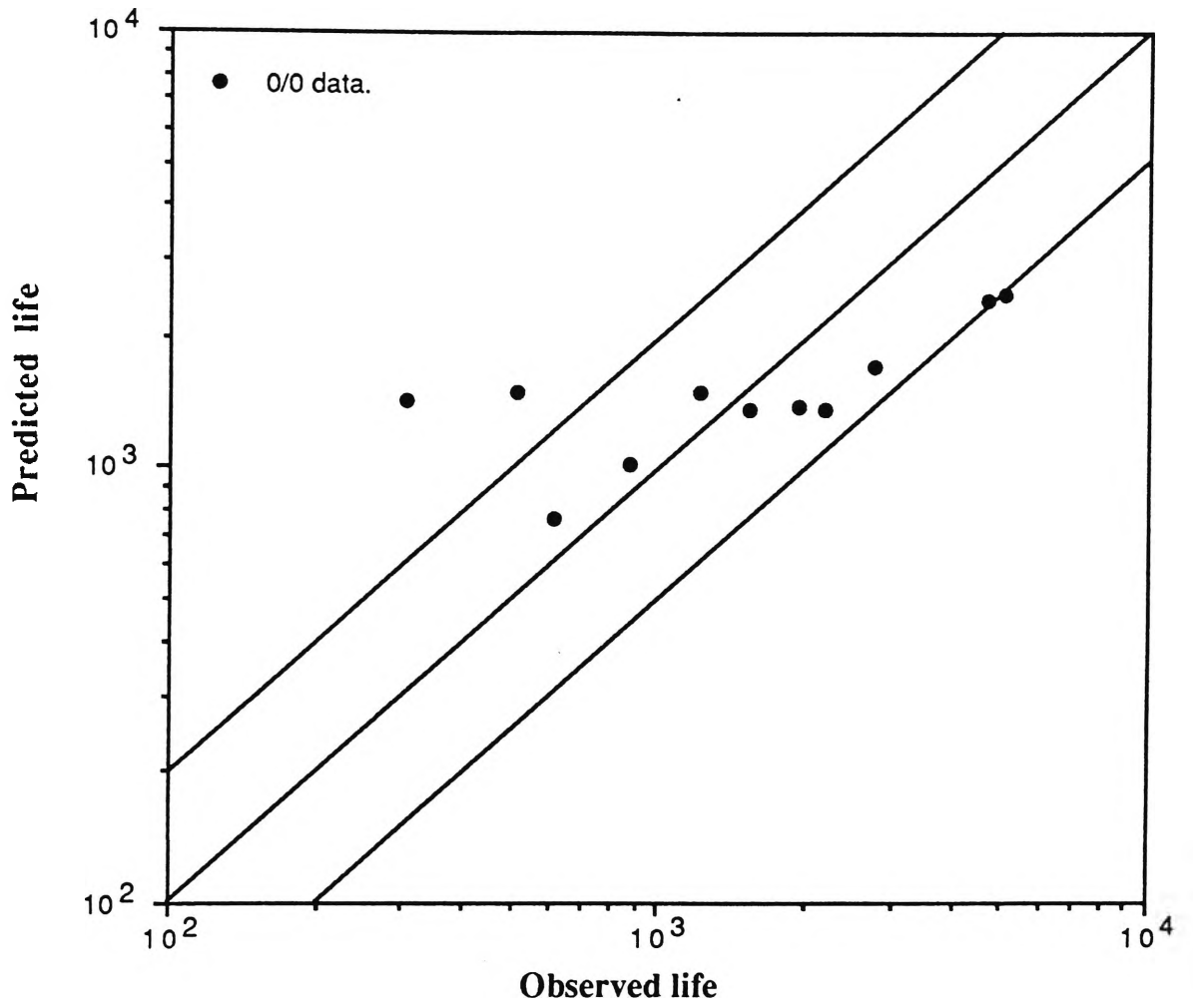
Fig. 8.13. Life prediction of 2.25Cr-Mo "Batch" 8 by Modified Diercks Equation.

8.4.5. Life Prediction by Modified Diercks Equation of 9Cr-1Mo Steel

8.4.5.1. Batch 1: HTLCF data for 9Cr-1Mo steel reported in batch 1 were analysed by equation 8.3 which is applicable below 10^4 cycles. At least 90% of the test data points were predicted in a factor of $\pm$ x2, as shown in Fig. 8.14.

8.4.5.2. Batch 2: The modified Diercks equation was assessed with the creep-fatigue data for the 9Cr-1Mo steel. At a strain of 0.5%, with 15 minutes tensile hold, the prediction by the modified Diercks equation was not good. However, as the hold time and temperature increased, the prediction was found to improve and for 70% of the test data points the prediction was in a factor of $\pm$ x2 as shown in Fig. 8.15.

8.5. PREDICTION CAPABILITY AND LIMITATIONS OF MODIFIED DIERCKS EQUATION

The success of a life prediction method depends upon the spread of the band in which the observed and predicted data are distributed. In creep-fatigue life prediction, the acceptable band is $\pm$ x2 since a high statistical confidence (95%) is maintained with such a factor. Creep-fatigue life prediction methods do not predict 100% of the test data points in a factor of $\pm$ x2 as pointed out in Chapter 6. Comparison of prediction capability for damage summation technique (DST), strain range partitioning (SRP) technique and R-5 with modified Diercks equation (MDE) is provided in Tables 8.2 and 8.3. The percentage of test data points predicted in a factor of $\pm$ x2 by three methods for the same data are tabulated below.

Table 8.2. Comparison of the modified Diercks equation with other methods.

| Material	Batch no	Temperature	Heat Treatment	Prediction by DST	Prediction by SRP	Prediction by MDE
1Cr-Mo-V	4	565°C	N&T	57%	85%	100%
	3	600°C	N&T	70%	100%	67.5%
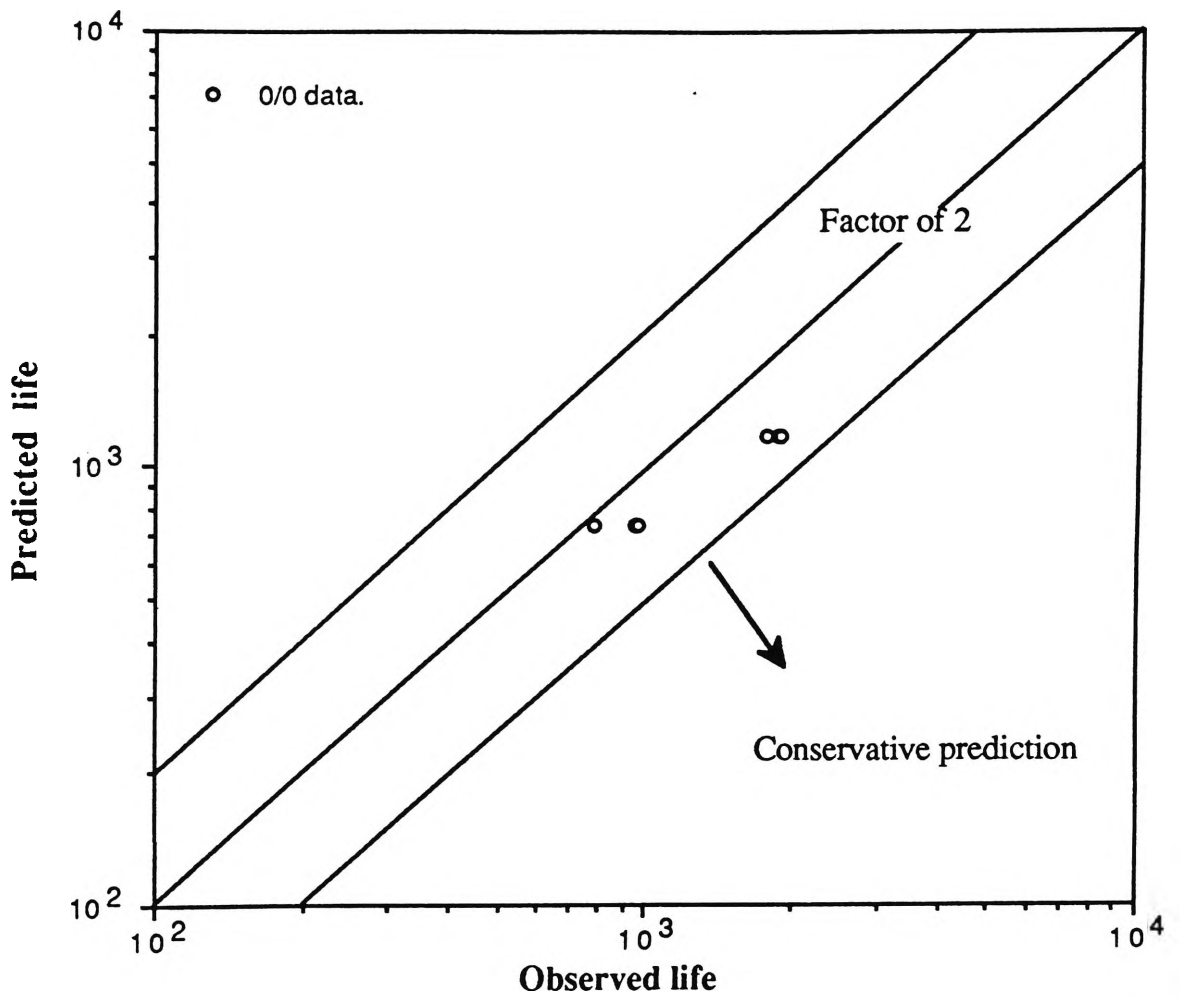
Fig. 8.14. Life prediction of 9Cr-1Mo "Batch 1" by Modified Diercks Equation.
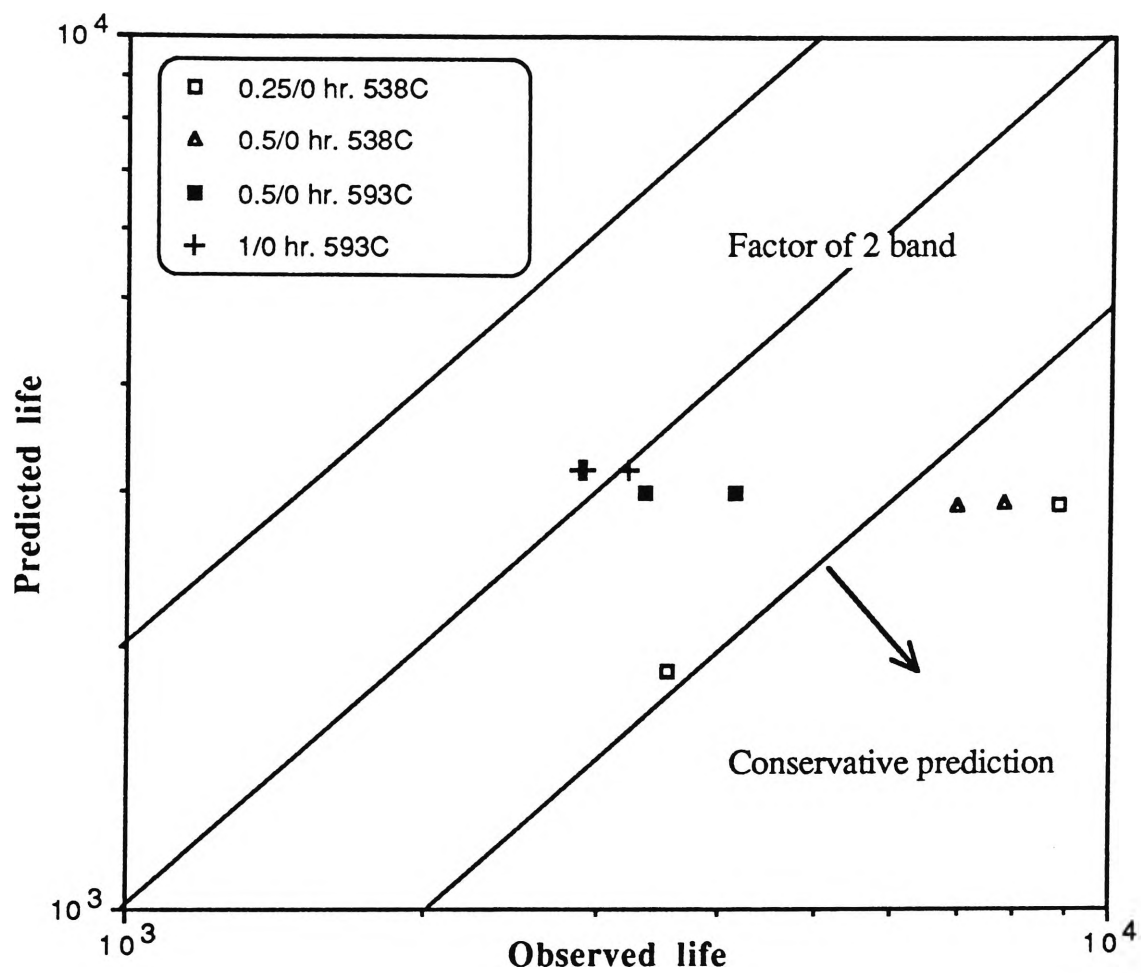
Fig. 8.15. Life prediction of 9Cr-1Mo "Batch" 2 by Modified Diercks Equation.

	5	600°C	N&T	0%	100%	100%

Table 8.2. Comparison of prediction capabilities of R-5 and MDE.

Material	Batch no	Temperature °C	Heat Treatment	Prediction by R-5	Prediction by MDE
0.5Cr-Mo-V	1	550	N&T	68%	94%
1Cr-Mo-V	5	550	N&T	50%	68%

At least, 67.5% of test data points were predicted in a factor of $\pm$ x2 by the modified Diercks equation. It is a simpler method, and does not require creep-fatigue tests and predicted comparable lives that of strain range partitioning and damage summation techniques.

Only batch 4 of 1Cr-Mo-V was tested for different hold times in tension and compression and this set of data is ideal for assessment of the capability of a method. When this data set was assessed with all the popular methods of life prediction described in Chapter 6, it was found that no method was adequate (15). However, all the test data points were predicted in a factor of $\pm$ x2 by modified Diercks equation and it is a better approach.

The modified Diercks equation, like other methods of life prediction, has some limitations since it considers both the tension and compression holds equally damaging and does not account for dwell sensitivity effects. In equation 8.1, a hold time parameter accounted for the time of hold which was log (1+ hold time), in which only tensile hold times can be analysed, as the logarithm of a negative quantity becomes infinite.

Also, in equation 8.3 prediction of hold times data was possible only with tensile hold. The modified Diercks equation was inadequate when the test parameters in tension and compression directions changed. Hence balanced dwell cycles were analysed accounting for

the hold times only in tension. Healing effects that resulted from combined cycles or unbalanced holds were not accounted for in the methods of life prediction discussed in Chapter 6. Such data were under-predicted by all the methods discussed in Chapter 6.

Amidst these demerits, the modified Diercks equation was assessed with a bank of data and the life predicted by this method was reasonable, carried out in this section. It did not require the material parameters determined from complex creep-fatigue tests and the modifications made are probabilistically for a cycle time and a material dependent parameter.

8.6. SUMMARY

The following were concluded:

(1) The modification of Diercks equation proposed in this research did not require any relative material properties as required by other modifications. A cycle time parameter, which was a ratio of strain range parameter with material dependent equivalent strain rate was introduced in this modification.

(2) Material dependent equivalent strain rate was determined from data fitting. For simplicity, by statistically fitting a set of creep-fatigue data for each low alloy steel, its value was kept constant for that particular steel in this investigation.

(3) The modified Diercks equation can be applied to any creep-fatigue data with a length of hold time within a life range below 10^4 cycles. However, compressive dwells together with balanced and unbalanced cycles were treated to be as tensile dwells.

(4) The reliability of the modified Diercks equation was compared with other methods of life prediction and was found better than the other methods.

(5) An approximate creep-fatigue response for low alloy steels can be derived with the modified Diercks equation.

9. RELIABILITY ANALYSIS

A multivariate Diercks equation was modified and it was assessed in Chapter 8 with the creep-fatigue data compiled in Chapter 4. Creep-fatigue life prediction carried out for low alloy steels is analysed in this Chapter for statistical reliability. A reliability analysis determines whether or not a method, such as modified Diercks equation, be extended in the creep-fatigue life prediction of low alloy steels.

9.1. RELIABILITY ANALYSIS:

The standard error (SE) of estimate has been used to evaluate the accuracy of a life prediction method (102) statistically and it was expressed in terms of equation 9.1

$$SE = \sqrt{\Sigma} \text{ (observed life - predicted life)}^2 \text{ / Num} \qquad (9.1)$$

In fatigue design, cyclic lives are expressed in logarithmic terms. Hence, equation 9.1 can be represented in logarithmic form in equation 9.2.

$$SE = \sqrt{\Sigma} (\log(\text{Nobserved}) - \log(\text{Npredicted})^2) \text{ / Num} \qquad (9.2)$$

where $N_{observed}$ and $N_{predicted}$ are observed and predicted lives respectively and Num refers to the number of tests in a batch.

Equation 9.2 can be further simplified:

$$SE = \sqrt{\Sigma} (\log(\text{Nobs/Nprd. }))^2 \text{ / Num} \qquad (9.3)$$

To better understand the magnitude of scatter in life prediction, Saltsman and Halford (47) proposed SE be represented in terms of "equivalent factor on life" (EF) which is defined by the antilogarithm of SE.

The data compiled in Chapter 4 were assessed with modified Diercks equation in Chapter 8 and predicted and observed lives were tabulated in Appendix I which were used to determine SE and EF for all the batches of the data. The life prediction analysis performed for the data is tabulated in Tables A4 - A19 in Appendix I. The SE and EF of various low alloy steel batches are set out in Table 9.1.

Table 9.1. Reliability of modified Diercks equation represented by SE and EF.

Material	Temp.	Batch	% tests in a factor of			SE	EF
	°C		2	3	4		
1Cr-Mo-V(N&T)	540	1	85	15		0.055	1.135
1Cr-Mo-V(N&T)	485	1	75	25		0.065	1.16
1Cr-Mo-V(N&T)	538	2	50	50		0.1457	1.39
1Cr-Mo-V(N&T)	483	2	50		50	0.081	1.205
1Cr-Mo-V(N&T)	550	3	94	6		0.012	1.02
1Cr-Mo-V(N&T)	565	4	100			0.008	1.01
1.25Cr-Mo (A/R)	550	1	67	33		0.102	1.26
1.25Cr-Mo(N&T)	600	2	100			0.021	1.05
2.25Cr-Mo (A)	540	1	60	20	20/5	0.234	1.71
2.25Cr-Mo(N&T)	540	1	67		33/5	0.058	1.14
2.25Cr-Mo(Q&T)	485	1	67		33	0.0256	1.06
2.25Cr-Mo (A)	538	2	100			0.0435	1.1
2.25Cr-Mo(N&T)	538	2	67	33		0.0136	1.03
2.25Cr-Mo(Q&T)	483	2	33	67		0.1692	1.47
2.25Cr-Mo(N&T)	600	3	67	33		0.005	1.01
2.25Cr-Mo(N&T)	502	4	100			0.0636	1.157
2.25Cr-Mo(N&T)	600	5	100			0.064	1.15
2.25Cr-Mo(N&T)	550	6	88	12		0.0059	1.013
2.25Cr-Mo(N&T)	593	7	91	9		0.055	1.135
2.25Cr-Mo-V	593	8	63.6	18	18	0.0282	1.06
9Cr-1Mo (N&T)	550	1	90	10		0.0589	1.145
9Cr-1Mo (N&T)	593	2	70	30		0.0625	1.154

The SE, standard error and the EF, equivalent factor on life were determined statistically, when the percentage of test data points were predicted in a factor of 2, 3 and 4 were presented in Table 9.1, however, when the factor exceeded 4 it was expressed by percentage test data points / range of factor.

From the above analysis it is evident that SE and EF are below a factor of 2 for all batches of data. These values are determined statistically and help in proposing the applicability of modified Diercks equation as a better method of life prediction under creep-fatigue for low alloy steels.

9.2. SUMMARY:

In summary, the following conclusion was drawn:

(1)   The reliability of Diercks equation, modified in this investigation, was found

       better than other methods of life prediction.

10. CONCLUSIONS AND RECOMMENDATIONS

The objectives of the present research "creep-fatigue behaviour and life prediction" were as follows; 1) compile a data bank for low alloy steels and identify the unspecified details in the data, 2) determine the trends in the behaviour for low alloy steels, 3) document the damage mechanisms for titanium alloy IMI 829 and a superalloy MAR M 002, 4) review phenomenological life prediction methods and examine their capability with the compiled data, 5) modify Diercks equation and assess its applicability with low alloy steels, and 6) develop a new life prediction method accounting for the oxidation for the life prediction of MAR M 002. The following conclusions were drawn from this investigation:

(1) The trends identified in the creep-fatigue behaviour were:

    (a) creep-fatigue behaviour of low alloy steels depended upon the heat treatment condition and performance for a 2.25Cr-Mo steel under annealed condition was better than normalized and tempered and quenched and tempered condition,

    (b) creep-fatigue life, in general, depended upon composition and improved with increase in the chromium content, and

    (c) alloying elements such as vanadium in a 2.25Cr-Mo steel caused a decrease in the life.

(2) The trends in life prediction using phenomenological methods were:

    (a) no method, such as the damage summation approach, the frequency modified approach, the strain range partitioning technique, the damage parameter approach, the damage rate approach, the hysteresis energy approach and the assessment procedure R-5 was found better than other method,

    (b) prediction capability of various methods depended upon the material conditions such as heat treatment and test temperature employed, and with the increase in temperature, the prediction capability deteriorated, and

(c) the damage summation approach was more suitable at lower temperatures (for example 485°C) whereas, the strain range partitioning techniques was more applicable at higher temperatures (for example 600-700°C) for annealed condition.

(3) A statistical method known as the Diercks equation, was modified and simplified to extend it to the creep-fatigue life prediction for low alloy steels.

(4) Applicability of modified Diercks equation was assessed using the compiled creep-fatigue data bank and it was found to be better than other methods.

(5) The damage features for a titanium alloy IMI 829 and a superalloy MAR M 002, both tested under high temperature low cycle fatigue, contained oxidation. Oxide banding was found to dominate in both materials and to cause intrusions and multiple cracking in both the materials. In the case of MAR M 002, wedge type cracking and γ' depletion were observed. Damage features were documented and described by a five stage model.

(6) A new empirical life prediction method was developed for the HTLCF life prediction for MAR M 002 and assessed with available data. The new method predicted life within one half to two times the experimental life or in a factor of $\pm$ x2 for most HTLCF data.

A list of seven publications resulted from this research is presented at the beginning of this thesis which demonstrates this area of research in the developmental stage. There is a need to develop a consensus on several aspects of test and material parameters in the high temperature low cycle fatigue testing. A standardised code of practise is needed with clear definitions for parameters such as failure criteria, strain rates, extensometry, specimen design and temperature and other controls. Wide variability exists in creep-fatigue data from the same laboratory in test to test and data from different laboratories, these must be identified and accounted in life prediction. The life prediction methods modified and developed in this investigation need further work before their use be recommended.

REFERENCES

(1)   Krempl, E. and Wundt, B. M. (1971) ASTM STP 489 p. 1.

(2)   Gangadharan, A. C., Pai, D. H. and Berman, I. (1973) I, Mech. Eng. Paper No. 215.

(3)   Cowles, B. A., Sims, D. L., Warren, J. R. and Miner, R.V. Jr. (1980) Trans. ASME J. Eng. Mater. Tech. 102 p. 356.

(4)   Cowles, B. A., Sims, D. L. and Warren, J. R. (1978) NASA Report No. CR 159409.

(5)   American Society of Mechanical Engineers (1974) Code case N-47 ASME Boiler and pressure vessel code.

(6)   Coffin, L. F. (1976) International symposium on creep-fatigue interactions, Ed. Curran, K. M., MPC 3, ASME NY p. 349.

(7)   Manson, S. S., Halford, G. R. and Hirschberg, M. H. (1971) NASA report TMX 67838.

(8)   Chrzanowski, N. (1976) Int. J. Mech. Science, 18 p. 69.

(9)   Majumdar, S. and Maiya, P. S. (1978) ASME/CSME Pressure vessel and piping conference, PVP PB 028.

(10)   Ostergren, W. J. (1976) J. of Testing and Evaluation, no. (4) p. 327.

(11)   Goodall, I. W. and Thomas, D. L. (1990) "An assessment procedure for high temperature response of structures" R-5, Nuclear Electric Plc., U.K..

(12)   Diercks, D. R. and Raskey, D. T. (1976) in ASME Annual winter meeting, p. 33.

(13)   Kitagawa, M., Nonaka, I. and Sonoya, K. in Fatigue-90 conference, 3, p. 1537.

(14)   Reuchet, J. and Remy, L. (1983) Met. Trans. 14A. p.141.

(15)   Priest, R. H. and Ellison, E. G. (1982) Resc. Mechanica Vol. 4.p.127.

(16)   Inoue, T., Igari, T., Okazaki, M. and Tokimasa, K. (1989) Nucl. Engrg. Des. 114, pp.311-21.

(17)   Plumbridge, W. J. and Stanley, M. (1986).Int. J. fatigue. 8,(4) p.209.

(18)   **Ellison, E. G., Plumbridge, W. J. and Dean, M. S.** (1984) Research Project No. 327, University of Bristol, Department of Mechanical Engineering.

(19)   **McMahon, C. J. and Coffin, L. F.** (1970) Met. Trans. 1A, p. 3443.

(20)   **Coffin, L. F.** (1972) Met. Trans. 3A, p. 1777.

(21)   **ASM (1978).** Metals Handbook, Vol. 1.

(22)   **Wöhler, A.** (1958) Z. Bauw, 8 pp. 642 and also in v. 10, (1860) p. 583.

(23)   **Goodman, J.** (1930) Mechanics Applied to Engineering, vol. 1, Ed., Longmans Green, London.

(24)   **Basquin, D. H.** (1910), Proc. ASTM 10 Part 11 p 625.

(25)   **Skelton, R. P.** (1985) High Temp. Technol. 3, p. 179.

(26)   **Plumbridge, W. J. and Ellison, E. G.** (1991) Fat. Frac. Engng. Mater. Struct. 14, 7, p. 721.

(27)   **Ashada, Y. and Mitsuhashi, S., (1980)** in 4th Int. Conf. Pressure Vessel Tech. 1, I Mech. Engrs, Paper C 48/80 p 321.

(28)   **Wareing, J.** (1977). Met. Trans.8A, p.711.

(29)   **Ellis, J. R., Jakub, M. T., Jaske, C. E. and Utah, D. A.** (1975) in Structural Materials for service at elevated temperature in nuclear power generation, ed. Schaefer, A.O. NY ASME MPC-1, p. 213.

(30).   **Ellison, E. G.** (1992). University of Bristol, Private Communications.

(31)   **Swindeman, R. W., Farrell, K. and Conway, J. B.** (1983) Thermal and Environmental Effects in fatigue, research design interface, N.Y. ASME PVP 71, p.121.

(32)   **Plumbridge, W. J., Priest, R. H. and Ellison, E. G.** (1979) Proc. Int. Conf. on Mech.Behaviour of Materials Cambridge.p.129.

(33)   **Brinkman, C. R.** (1985) International Metals Reviews 30, (5) p.235.

(34)   **Coffin, L. F.** (1974) Met. Trans. 5A p. 1053.

(35)   Brinkman, C. R., Strizak, J. P., Booker, M. K. and Jaske, C. E. (1976) J. Nucl. Mater. 62 (2/3) p.181.

(36)   Plumbridge, W. J. and Ellison, E. G. (1990) Private Communications.

(37)   Wareing, J., Tomkins, B., and Sumner, G. (1973) in Fatigue at elevated Temperature, ASTM STP 520 p. 123.

(38)   Jaske, C. E., Leis, B. N. and Pugh, C. E. (1975) ASME MPC -1, p. 191.

(39)   Manson, S. S. (1965) Exp. Mechanics, 5, no. 7, p. 193.

(40)   Muralidharan, U. and Manson, S. (1988) J. Testing and Evaluation, 16, no.2, p. 124.

(41)   Hales, R. (1980) Fat. Engng. Mater. Struct., 3 p. 339.

(42)   Majumdar, S. (1987).Symposium on Thermal Stress, Material Deformation, and Thermo-Mechanical fatigue - PVP vol. 123. ASME Book no. G00369. p.31.

(43)   Priest, R. H. and Ellison, E. G. (1981) Mat. Sc. and Eng., 49, p. 7.

(44)   Antolovitch, S. D., Domas, P. and Strudel, J. L. (1979). Met. Trans. 10A, p 1859.

(45)   Sehitoglu, H. and Boismier, D. A.(1990). J. Engrg. Mater. & Techn. 112, p. 63.

(46)   Batte, A. D., Thomas, G. and Carlton, R. G. (1982) C.E.G.B. Report GDCD/PET/MD/ 17/82 (CEGB Report FWP 97).

(47)   Saltsman, J. F. and Halford, G.R. (1979) in Methods for Predicting Material life in Fatigue ASME MPC ed., W.J. Ostergren and J.R. Whitehead.

(48)   Curran, R. M. and Wundt, B. M. (1976) in ASME Symposium on Creep-Fatigue Interactions, NY ed., R.M. Curran p.203.

(49)   Hoffelner, W., Melton, K. N. and Wuthrich, C. (1983) Fatigue Fract. Engeg. Mater. & Struct. 6 (1) p. 77.

(50)   Ellison, E. G. and Paterson, A. J. F. (1976) Proc. Instn. Mech. Engrs. 190 I-III parts p. 321.

(51)   Mann, S. D. (1989) M.S. Thesis, Monash University, Department of Materials Engineering.

(52) **Yamaguchi, K., Suzuki, N., Ijima, K., Kanazawa, K. and Nishijima, S.** (1986) Trans. Nat. Research Inst. Metals 28, (2) p.64.

(53) **Inoue, T., Ohno, N., Suzuki, A. and Igari, T.** (1989) Nucl. Engeg. Des. 114 p.295.

(54) **Challenger, K. D. and Vining, P. G.** (1983) Mater. Sci. & Engeg. 58 p. 257.

(55) **Setoguchi, K., Igari, T. and Yamaguchi, M.** (1984) Society of material Science Japan, 33, 370 p. 862.

(56) **Cusolito, R. and Mandorini, V.** (1988) Commission of the European Communities, Boite Postale, 1003, Luxembourg, Report no. EUR No. 8863.

(57) **Teranishi, H. and McEvily, A. J.** (1981) Fifth International Conference on Fracture p. 2439.

(58) **Plumbridge, W. J. and Ellison, E. G.** (1990) Unpublished work carried out for 9Cr-1Mo steel under the European Communities.

(59) **Gieseke, B. G., Brinkman, C. R. and Maziasz, P. J.** (1992) in First International Symposium on Microstructures and Mechanical Properties of Aging Materials.

(60) **Brinkman, C. R.** (1992-93) Private discussions.

(61) **Smith, G. V.** (1973) ASTM Data Series Publication DS 58 Prepared for the Metals Properties Council.

(62) **Jaske, C. E. and Mindlin, H.** (1971) in 2.25Cr-Mo steel in Pressure Vessels and Piping ASME p. 137.

(63) **UKHTMTC/LCF/2/86** UK High Temperature Mechanical Testing Committee Jan 86.

(64) **Narumoto, A.** (1987). Japan -US joint seminar on advanced materials for severe service applications (1986 Tokyo Japan), Ed. by Iida, K and Mc Evily,A.J. p. 219.

(65) **Melton, K. N.** (1982). Mater.Sc. & Engrg. 55. p.21.

(66) **Plumbridge, W. J. and Stanley, M.** (1986) in I. Mech. Eng. Paper No. C250/86, p. 377.

(67)   **Miller, D. A., Priest, R. H. and Ellison, E. G.** (1984) High Temp. Mater. and Processes, 6, (3&4) p. 155.

(68)   **Lloyd, G. J. and Wareing, J.** (1981) Metals Technology 804 p. 297.

(69)   **Miner, M. A.** (1945) Jr. of Applied Mechanics 12 -3 A p. 159.

(70)   **Robinson, E. L.** (1952) Trans. ASME 74, 5 , p.777- 81.

(71)   **Taira, S.** (1962). Creep in structures, Acad. Press, p. 96.

(72)   **Coffin, L. F.,** (1954) Trans. ASME (Series. A) 76, p. 931.

(73)   **Coffin, L. F.** (1976) International symposium on Creep-fatigue interactions, Ed. K.M. Curran, MPC.3, ASME N.Y. p.349.

(74)   **Coffin, L. F.** Fatigue at high temperature and interpretation, Proceedings of Institute of Mechanical Engineers. (1974) 9/74, p.188.

(75)   **Majumdar, S. and Maiya, P. S.** (1978) ASME/CSME pressure vessel and piping conference. PVP. PB 028.

(76)   **Manson, S. S. and Halford, G. R.** (1983) Israel J. of Tech. 21, p. 29.

(77)   **Manson, S. S. and Zab, R.** (1977) ORNL / Sub 3988/1 Case reserve Western University, Ohio .

(78)   **Majumdar, S.and Maiya, P. S.** (1976) ANL report 76/58.

(79)   **Majumdar, S. and Maiya, P. S.**(1979) Proc. of 3rd, Int. Conf. on the mech.behaviour of materials Cambridge 79. 2, p.101.

(80)   **Morrow, J.** (1965) ASTM -STP 378, p. 3.

(81)   **Kachanov, L. M.** (1958) Izv Hkad Nank ssr otd Tekh. Nank No.8. p.26.

(82)   **Chaboche, J. L.** Seminaire internationale sur I' approche Locale de la rupture. Moret -sur loing (1986) (ONERA TP 53).

(83)   **Lemaitre, J. and Plumtree, A.** (1979) ASME EM (101).p.284.

(84)   **Becigo, V. and Ragazzoni, S.** (1990) in 'Fatigue 90' vol. 3. p. 1541.

(85)   **Sonoya, K., Nonaka, I. and Kitagawa, M.** (1991) The Iron and Steel Institute of Japan, 31, (12) p.1424.

(86)   Ellison, E. G. and Walton, D. (1973) I. Mech. Eng. Paper no. C 173.

(87)   Kanazawa, K. and Yoshida, S. (1974) I. Mech. Eng. Paper no. C 226.

(88)   Day, M. F.and Thomas, G. B. (1978) AGARD Conf. Proc. No. 243. paper 10.

(89)   Halford, G. R., Saltsman, J. F. and Hirschberg, M. H. (1977) NASA Tech. Note
       TM 73737.

(90)   Chaboche, J. L., Policella, H. and Kaczmarek, H. (1978) AGARD Conf. Proc.
       No. 243, paper, 4.

(91)   Becigo, V., Fossati, C.and Ragazzoni, S. (1987) Low cycle fatigue ASTM STP
       942.p.1237.

(92)   AGARD CP 343 (1978) Charaterization of low cycle fatigue life by strain range
       partitioning technique.

(93)   Plumbridge, W. J. (1987). Fatigue and Fract. of Engrg. Mater. & Struct.10, (5)
       p 385.

(94)   Oshida, Y. and Liu, H. W. (1988) in Low Cycle Fatigue ASTM STP 942 Ed
       Solomon, Halford, Kaisand and Leis.

(95)   Das, G. and Vahldiek, F. W. (1989) in Corrosion and particle erosion at high
       temperature, TMS-ASM Joint Symposium p. 531.

(96)   Drapier, J. M. and Hirschberg, M. (1979) AGARD AR 130.

(97)   Antolovitch, S. D., Liu, S. and Baur, R. (1981). Met Trans. 12A, p, 473.

(98)   Wada, Y., Kawakami, Y. and Aoto, K. (1987) in Thermal stress, material
       deformation and thermomechanical fatigue, Ed., H. Sehitoglu and S. Y. Zamrik
       PVP vol. 123, p. 37.

(99)   Aoto, K., Wada, Y. and Komine, R. (1987) same as (98) p. 43.

(100) Yamaguchi, K., Kobayashi, K., Ijima, K. and Nishijima, S., ASME J. Eng.
       Mater. and Struc. in press.

(101) Taira. S., Fujino, M. and Ohtani, R. (1979) Fatigue of Engeg. Mater. Struct. 1,
       p. 495.

(102) **Spiegel, M.** (1961) in Schaum's outline of theory and problems of statistics' McGraw Hill Book Co. NY. p. 243.

APPENDIX I

In this section the analyses of life prediction for the MAR M 002 by empirical method developed in Chapter 7 and low alloy steels by the modified Dierck's equation are provided. The first three Tables (A1-A3) list the experimental and predicted lives for MAR M 002 and Tables from A4-A19 describe for low alloy steels predicted by Modified Diercks Equation (MDE).

Life Prediction for MAR M 002 by the new method

The expression for the life prediction equation has the following form:

$$Nf = [D° .af / \{(2.(h)^n \log(1.1- t_h))\}^\alpha].\{D_c\}^\alpha.(\Delta\varepsilon_{in} / \dot{\varepsilon})^{-1} / \alpha\} \qquad \text{(i-1)}$$

where D° is diffusion coefficient for oxidation, af is the final crack size at failure (assumed 10% of gauge diameter), t_h is the time of hold (in hrs.), t is the test duration under 0/0 condition which is 0.9, 0.25 and 0.28 hrs. at 750°C, 850°C and 1000°C respectively , D_c is the creep ductility, $\Delta\varepsilon_{in}$ and $\dot{\varepsilon}$ are inelastic strain range and strain rate respectively. The exponent α in the above equation was calculated by fitting the data, it depended upon the test temperature and increased with increase in temperature. The exponent was expressed empirically with homologus temperature in equation i-2

$$\alpha = \log\{1.49 (\exp T_h) \} \qquad \text{(i-2)}$$

where T_h is the homologus temperature which is a ratio of test temperature with melting temperature in absolute scale. It ranged from 0.28 to 0.4 for the test temperature range of 750°C to 1000°C. The symbols in the equation i-1 were assumed as follows:

'h' is the thickness of the oxide layer determined by assuming a parabolic law, whose growth is represented by the equation:

Various parameters in the equation i-1 were determined as follows;

The thickness of oxide layer $h = \sqrt{(D^*.\ Exp\ (-Q/RT).t)}$ (i-3)

However, the rate of formation of oxide layer is in seconds (/3600). Exponent n was determined from following;

$$n = 1 + 1.3\ \alpha$$ (i-4)

The life prediction was carried out by integrating the crack growth between the limits of initial and final crack growth (a_o to af). The initial crack size was assumed 0 and the af was assumed 0.25 mm. For every creep-fatigue test, inelastic strain components are specified and hold times are presented in Table 7.2. Exponents α and n are determined using equations i-2 and i-4 respectively.

Table. A1. Parameters in the life prediction model equation i-1..

Constants	Temperature	Values	Reference
For MAR M 002			
D°	750,850 and 1000°C	15300	45.
D^*		1.9×10^{-4}	18
Q		283kj/mol	18
α	750°C	0.28	
α	850°C	0.30	
α	1000°C	0.39	
R		0.00831	kj/°c/ mol,
D_c	750, 850and 1000°C	6, 6.3 & 4.6	18
af		0.25mm	for MAR M 002

Table A2. Life prediction for MAR M 002 under unaged condition.

NICKEL BASED SUPERALLOY MAR M 002					
Strain range %		Hold time	Cycles to	Predicted	Temp
inelastic	Total	(hr.)	failure	lives	(°C)
0.076	0.896	0/0	352	431	750
0.048	0.772		1099	682	

0.032	0.601		8490	1023	
0.178	0.946		94	294	850
0.094	0.799		549	557	
0.055	0.587		2590	952	
0.411	0.808		127	125	1000
0.256	0.606		160	202	
0.117	0.408		835	442	
Summary of test results for unaged conditions.					
0.076	0.896		352	431	750
0.094	0.900	0 / 0.0833	133	276	
0.115	0.906	0.0833 / 0	330	584	
0.178	0.946		94	294	850
0.219	0.897	0 / 0.0833	28	186	
0.133	0.664	0/0.0833	356	307	
0.264	0.888	0.0833 / 0	290	423	
0.410	0.921	.083/.083	49	127	
0.411	0.808		127	125	1000
0.541	0.816	0/0.083	161	73	
0.465	0.819	0.083/0	127	252	

Table A3. Life prediction of MAR M 002 under aged condition.

Summary of test results for aged conditions.					
0.095	0.706		15*	551	850
0.029	0.506		417*	1806	
0.331	0.922	0/0.0833	2	123	
0.111	0.514	0/0.0833	39*	1008	
0.40	0.81		68	129	1000
0.18	0.52		952	287	
0.059	0.26		>5420	877	
0.38	0.74	0/0.0833	38	104	
0.41	0.73	0.083/0	65	286	

Life prediction for low alloy steels by the modified Diercks equation

Diercks equation:

$$(\log N_f)^{1/2} = 1.20551064 + 0.66002143\ S + 0.18040042\ S^2 - 0.00814329\ S^4$$

$$+0.00025308\ RS^4 + 0.00021832\ TS^4 - 0.00054660\ RT^2 - 0.005567\ RH^2 -$$

$$0.00293919HR^2 + 0.0119714HT - 0.00051639\ H^2T^2. \qquad (i\text{-}5)$$

where   S is a strain range parameter ($\Delta \varepsilon_t$ / 100)

                 R is a strain rate parameter ($\log \varepsilon$)

                 T is a temperature parameter (T_c / 100)

                 and H is a hold time parameter ($\log (1+t_h)$).

and $\Delta \varepsilon_t$ is the % total strain range, $\dot{\varepsilon}$ is the strain rate, T_c is cycle temperature (°C) for SS

304 and t_h is the duration of hold time in hours.

The Diercks equation is modified in this investigation and presented in a modified form,

(MDE) as follows:

$$[\log (\tau\, Nf)]^{1/2} = C \qquad (i\text{-}6)$$

where, τ is the cycle time and C is a constant under a set of S, T, $\dot{\varepsilon}$ and H, it is the right hand

side of equation in (i-5).

Material dependent equivalent strain rate parameter ($\dot{\varepsilon}$) was

         = 0.1 for 1Cr-Mo-V alloy.

         = 0.25 for 1.25Cr-Mo alloy.

         = 0.5 for 2.25Cr-Mo alloy.

Cycle time parameter = Strain range /($\dot{\varepsilon}$)

Thus for a 23 hrs hold time, at 0.55% strain range and 540°C, the S, T, R, and H parameters

become,

         S= 0.55/100 = 0.0055

         T= Cycle temperature of LAS + 100 / 100 = 6.4.

R= log (0.1) = -1.

H= log (1 +23) = 1.380.

τ = 1 + (0.0055 / 0.1) = 1.055.

Substituting the parameters in the equation (i-5), the C was determined.

Log Nf = 1.735

The cycles to failure (Nf) was calculated from the anti-log of C and was

Nf =   54

In the above manner, the life prediction for all creep-fatigue data were assessed. The predicted and observed lives are tabulated below for the compiled data presented in batches.

Table A4. Predicted and observed lives for 0.5Cr-Mo-V, Batch 1 by (MDE).

Total strain range (%)	Hold time (hours)	Life predicted by R-5	Observed-cycles (Nf)	Predicted life (MDE)
1.51	0.5	252	375	189
1.0	0.5	350	537	281
0.70	0.5	462	998	397
1.02	2.0	322	519	321
0.70	16	289	340	529
0.4	16	576	1590	1297
2.39	16	110	124	234
1.25	16	157	314	427
0.61	16	242	604	854
0.43	16	307	675	1203
0.34	16	358	1249	1517
2.30	16	123	209	242
0.92	16	213	611	573
0.62	16	321	647	841
0.4	16	647	1126	1292
0.3	16	1306	1700	1716

Table A5. Predicted and observed lives for 1Cr-Mo-V, Batch 1 by (MDE).

Total strain range (%)	Hold time (hours)	Test temperature (°C)	Observed-cycles (Nf)	Predicted life (MDE)
0.55	23	540	29	54
1.50	23	"	22	51
1.10	47	"	24	67
1.50	47	"	29	65
1.50	23	"	42	51
0.55	47	"	84	68
1.50	47	"	87	65
1.50	23	"	209	51
1.50	47	"	150	65
0.55	47	485	27	67
0.55	47	485	48	67
1.50	47	"	30	59
1.50	23	"	42	48
1.50	23	"	145	48
0.55	23	"	149	50
0.55	23	"	25	50
1.50	47	"	87	59
0.55	47	"	96	67

Table A6. Predicted and observed lives of 1Cr-Mo-V Batch 2 by (MDE).

Total strain range (%)	Hold time (hours)	Test-temperature (°C)	Observed-cycles (Nf)	Predicted life by MDE
0.55	0	538	5105	4570
1.5	0	"	520	1675
0.55	23	538	130	54
1.5	23	"	68	51
0.55	0	483	8400	4661
1.5	0	"	500	1709
1.5	23	483	49	48

0.55	47	"	96	61
0.55	47	"	149	61
0.55	23	"	161	50

Table A7. Predicted and observed lives of 1Cr-Mo-V Batch 3 by (MDE).

Inelastic strain (%)	Total Strain (%)	Test-temperature (°C)	Observed-cycles (Nf)	Predicted life by MDE
1.27	1.95	550	208	149
0.84	1.5		283	190
0.57	1.2		400	236
1.6	2.14		165	148
2.57	2.7		165	120
2.29	2.54		90	79
0.946	1.6		340	179
1.004	1.67		240	172
1.038	1.72		180	167
2.257	2.5		52	48
0.95	1.62		171	177
0.708	1.35		340	211
1.554	2.22		113	98
2.33	2.54		92	79
1.297	1.98		285	147
1.14	1.81		250	160
2.18	2.33		95	89
0.24	0.83		1460	336
0.24	0.83		1230	336
0.76	1.41		380	202
1.32	2		185	145
1.11	1.78		255	162
0.5	1.13		590	250
0.3	0.9		625	311
0.57	1.2		350	236
1.167	1.84		180	157

1.923	2.4		108	104
0.892	1.55		260	185
0.369	0.98		600	286
0.093	0.6		950	461

Table A8. Predicted and observed lives of 1Cr-Mo-V Batch 4 by (MDE).

Total strain range (%)	Hold time (hours)	Test-temperature (°C)	Observed-cycles (Nf)	Predicted life by MDE
1.5	0	565	327	175
1.0	0	"	490	257
0.7	0	"	960	364
1.96	3		97	186
1.08	3	"	150	327
1.96	0.5	"	135	148
1.08	0.5	"	220	260
1.06	0.5/0.5	"	385	264
1.46	0.5/0.5	"	220	195
2.0	0.5/0.5	"	215	145
1.4	0.5/0.5	"	390	203
1.3	16	"	73	48
1.3	16/0.003	"	208	48
2.0 0.5		"	180	145
1.5 0.5		"	215	190
1.0 0.5		"	300	280
2.0 0/0.5		"	300	145
1.5 0/0.5		"	374	190
1.1 0/0.5		"	560	255

Table A9. Predicted and observed lives for 1Cr-Mo-V, Batch 5 by (MDE).

Total strain range (%)	Hold time (hours)	Life predicted by R-5	Observed-cycles (Nf)	Predicted life by (MDE)
3.02	0.5	139	80	95

2.0	0.5	189	176	145
1.0	0.5	287	382	281
0.9	0.5	305	500	311
0.60	0.5	384	1456	461
0.5	0.5	432	2300	552
1.0	2.0	258	448	328
3.19	16	81	86	181
1.23	16	114	244	434
0.84	16	135	454	626
0.63	16	162	1033	828
0.5	16	210	3557	1038
3.74	16	76	122	158
1.16	16	164	645	459
0.61	16	709	2347	854
0.48	16	1681	4087	1080

Table A10. Predicted and observed lives of 1.25Cr-Mo Batch 1 by (MDE).

Total strain range (%)	Hold time (hours)	Test temperature (°C)	Observed-cycles (N_f)	Predicted life by MDE
0.5	0	550	5284	3167
0.7	0		1667	2262
1.0	0		945	1583
0.5	0.0166		3919	1343
0.7	0.0166		1475	966
1.0	0.0166		769	683
0.5	0.166		3896	1379
0.7	0.166		1311	992
1.0	0.166		820	702
1.0	0.5		601	738

Table A11. Predicted and observed lives of 1.25Cr-Mo Batch 2 by (MDE).

Total strain range (%)	Hold time (hours)	Test temperature (°C)	Observed-cycles (Nf)	Predicted life by MDE
2.01	0	600	560	788
1.52	0	"	760	1029
0.98	0	"	1500	1596
0.62	0	"	6100	2523
0.59	0	"	5800	2651
0.48	0	"	5000	3259
2.04	0.03	"	418	345
1.04	"	"	871	652
2.05	0.08	"	327	346
0.95	"	"	772	718
2.04	0.16	"	292	353
1.04	"	"	605	668
2.03	0.5	"	230	375
1.04	"	"	455	707
2.03	1	"	195	402
0.99	"	"	418	792

Table A12. Predicted and observed lives of 2.25Cr-Mo Batch 1 by (MDE).

Total strain range (%)	Hold time (hours)	Test temperature (°C)	Observed-cycles (Nf)	Predicted life by MDE
0.55	47	540	67	82
1.50	23	"	141	65
2.30	47	"	59	86
2.30	23	"	73	66
1.50	23	"	202	65
1.50	23	"	50	65
0.55	47	"	13	82
2.3	47	"	24	86
2.3	23	"	43	66

0.55	47	"	60	82
1.5	23	"	110	65
0.55	47	485	23	73
1.50	23	"	31	59
2.3	47	"	15	76
2.3	23	"	29	60
0.55	47	"	48	73
1.50	23	"	77	59

Table A13. Predicted and observed lives of 2.25Cr-Mo Batch 2 by (MDE).

Total strain range (%)	Hold time (hours)	Test-temperature (°C)	Observed-cycles (N_f)	Predicted life by MDE
0.55	0	538	3655	1497
1.5	0	"	930	549
2.3	0	"	348	358
0.55	47	"	67	82
0.55	23	"	103	63
1.50	23	"	13	65
0.55	0	538	2990	1497
1.5	0	"	672	549
2.3	0	"	281	358
0.55	47	"	13	82
0.55	23	"	32	63
0.55	47	"	60	82
1.5	23	"	13	65
0.55	0	483	7440	1507
1.50	0	"	474	552
2.3	0	"	265	360
0.55	47	"	23	72
0.55	23	"	90	58
1.50	23	"	77	59

Table A14. Predicted and observed lives of 2.25Cr-Mo Batch 3 by (MDE).

Total strain range (%)	Hold time (hours)	Test-temperature (°C)	Observed-cycles (Nf)	Predicted life by MDE
2.0	-	600	257	730
"	-	"	355	730
1.2	-	"	780	1182
"	-	"	668	1182
0.8	-	"	2008	1747
"	-	"	1294	1747
0.6	-	"	3865	2313
"	-	"	2100	2313
0.4	-	"	7786	3444
"	-	"	6742	3444
"	-	"	6075	3444
2.1	-	"	112	698
1.3	-	"	308	1095
1.2	-	"	350	1182
0.87	-	"	731	1611
0.8	-	"	1048	1747
0.68	-	"	1140	2047
0.6	-	"	2129	2313
0.4	-	"	7346	3444
2.0	-	"	305	730
1.2	-	"	540	1182
"	-	"	678	1182
0.8	-	"	1049	1747
"	-	"	1138	1747
0.62	-	"	2095	2240
0.6	-	"	2560	2313
0.4	-	"	5630	3444
2.0	-	"	224	730
"	-	"	168	730
1.2	-	"	325	1182
"	-	"	496	1182

0.86	-	"	915	1629
0.8	-	"	955	1747
0.6	-	"	1768	2313
"	-	"	1229	2313
0.4	-	"	9227	3444
2.0	0.083	"	312	742
1.0	0.083	"	720	1431
2.0	0/0.083	"	325	742
1.0	0/0.083	"	894	1431

Table A15. Predicted and observed lives of 2.25Cr-Mo Batch 4 by (MDE).

Total strain range (%)	Hold time (hours)	Test-temperature (°C)	Observed-cycles (Nf)	Predicted life by MDE
0.5	0/0.1	502	61111	1682
0.5	0.1	"	20147	1682
0.5	0.1/0.1	"	3420	2845
1.0	-	"	3721	1424
1.0	0/ 0.1	"	1924	1449
1.0	0.1	"	2059	1449

Table A16. Predicted and observed lives of 2.25Cr-Mo Batch 5 by (MDE).

Total strain range (%)	Hold time (hours)	Test-temperature (°C)	Observed-cycles (Nf)	Predicted life by MDE
1.01	0.23	600	1360	1456
1.99	0.22	"	472	765
1.00	0.01	"	1070	1411
1.07	0.54	"	820	1447
1.02	0.08	"	940	1403
1.97	0.22	"	410	772

Table A17. Predicted and observed lives of 2.25Cr-Mo Batch 6 by (MDE).

Total strain range (%)	Hold time (hours)	Test-temperature (°C)	Observed-cycles (Nf)	Predicted life by MDE
3.20	0.016	550	234	482
2.15	"	"	410	689
0.54	"	"	5200	2588
1.05	"	"	1520	1356
4.30	"	"	200	374
3.20	"	"	208	482
2.20	"	"	380	675
1.20	"	"	150	1193
0.52	"	"	6100	2685
1.05	"	"	1450	1356
4.25	0.034	"	165	379
3.00	"	"	280	512
2.10	"	"	440	707
1.15	"	"	1200	1247
0.68	"	"	2200	2072
4.1	0.166	"	180	400
3.0	"	"	265	524
2.2	"	"	345	693
1.2	"	"	1070	1225
0.66	"	"	2300	2185
4.0	"	"	220	408
3.1	"	"	255	509
2.1	"	"	410	724
1.1	"	"	1180	1331
0.60	"	"	2750	2397

Table A18. Predicted and observed lives of 2.25Cr-Mo Batch 7 &8 by (MDE).

Total strain range (%)	Hold time (hours)	Test-temperature (°C)	Observed-cycles (Nf)	Predicted life by MDE
0.523	-	593	7179	2648
0.544	-	"	5100	2548
0.773	-	"	2980	1808
0.84	-	"	799	1668
0.86	-	"	1065	1630
0.92	-	"	2647	1527
0.927	-	"	2699	1516
0.973	-	"	1623	1447
0.993	-	"	2443	1419
1.41	-	"	1109	1015
1.84	-	"	777	790
2.33	-	"	555	635
0.557	-	"	5072	2490
0.571	-	"	4645	2430
0.813	-	"	2734	1722
0.933	-	"	505	1507
0.94	-	"	1201	1496
0.984	-	"	301	1431
1.024	-	"	1904	1377
1.027	n =1.027%/s	"	2159	1374
1.040	=0.042%/s	"	1519	1357
1.40		"	861	1021
1.90		"	605	767

Table A19. Predicted and observed lives for 9Cr-1Mo Batch 1 by (MDE).

Total strain range (%)	Hold time (hours)	Test-temperature (°C)	Observed-cycles (Nf)	Predicted life by MDE
2.0	-	550	780	735
"	-	"	935	735

-	"		947	735
1.2	-	"	1839	1189
"	-	"	1852	1189
"	-	"	1740	1189
0.6	-	"	16960	1400
"	-	"	13000	1400
"	-	"	10300	1400